August 2010

Addressing Computational Complexity of Electromagnetic Systems Using Parameterized Model Order Reduction

Majid Ahmadloo
University of Western Ontario

Supervisor
Dr. Anestis Dounavis
The University of Western Ontario

Graduate Program in Electrical and Computer Engineering

A thesis submitted in partial fulfillment of the requirements for the degree in Doctor of Philosophy

Addressing Computational Complexity of Electromagnetic Systems Using Parameterized Model Order Reduction

(Spine Title: Numerical Reduction Techniques for Electromagnetic Systems)

(Thesis format: Monograph)

by
Majid Ahmadloo

Graduate Program in Engineering Science
Department of Electrical and Computer Engineering

A THESIS SUBMITTED TO THE FACULTY OF GRADUATE STUDIES AND RESEARCH IN PARTIAL FULLFILMENT OF THE REQUIREMENTS FOR THE DEGREE OF DOCTOR OF PHILOSOPHY

THE SCHOOL OF GRDAUATE AND POSTDOCTORAL STUDIES
THE UNIVERSITY OF WESTERN ONTARIO, LONDON, ONTARIO, CANADA

THE UNIVERSITY OF WESTERN ONTARIO
SCHOOL OF GRADUATE AND POSTDOCTORAL STUDIES

CERTIFICATE OF EXAMINATION

Supervisor

Dr. Anestis Dounavis

Supervisory Committee

Examiners

Dr. Kazimierz Adamiak

Dr. Jayshri Sabarinathan

Dr. Anand V. Singh

Dr. Mustapha C. E. Yagoub

The thesis by

Majid Ahmadloo

entitled:

Addressing Computational Complexity of Electromagnetic Systems Using Parameterized Model Order Reduction

is accepted in partial fulfilment of the
requirements for the degree of

Doctor of Philosophy

Date_____

Chair of the Thesis Examination Board

Abstract

As operating frequencies increase, full wave numerical techniques such as the finite element method (FEM) become necessary for the analysis of high-frequency and microwave circuit structures. However, the FEM formulation of microwave circuits often results in very large systems of equations which are computationally expensive to solve. The objective of this thesis is to develop new parameterized model order reduction (MOR) techniques to minimize the computational complexity of microwave circuits. MOR techniques provide a mechanism to generate reduced order models from the detailed description of the original FEM formulation.

The following contributions are made in this thesis:

1. The first project deals with developing a parameterized model order reduction to solve eigenvalue equations of electromagnetic structures that are discretized by using FEM. The proposed algorithm uses a multidimensional subspace method based on modified perturbation theory and singular-value decomposition to perform reduction directly on the finite element eigenvalue equations. This procedure generates parametric reduced order models that are valid over the desired parameter range without the need to redo the reduction when design parameters are changed. This provides significant computational savings when compared to previous eigenvalue MOR techniques, since a new reduced order model is not required each time a design parameter is changed.
2. Implicit moment match techniques such as the Arnoldi algorithm are often used to improve the accuracy of the reduced order model. However, the traditional Arnoldi algorithm is only applicable to first order linear systems and can not directly include

arbitrary functions of frequency due to material and boundary conditions. In this work, an efficient algorithm to create parametric reduced order models of distributed electromagnetic systems that have arbitrary functions of frequency (due to material properties, boundary conditions, and delay elements) and design parameters. The proposed method is based on a multi-order Arnoldi algorithm used to implicitly calculate the moments with respect to frequency and design parameters, as well as the cross-moments. This procedure generates parametric reduced order models that are valid over the desired parameter range without the need to redo the reduction when design parameters are changed and provides more accurate reduced order systems when compared with traditional approaches such as Modified Gram Schmidt.

3. This project develops an efficient technique to calculate sensitivities of microwave structures with respect to network design parameters. The proposed algorithm uses a parametric reduced order model to solve the original network and an adjoint variable method to calculate sensitivities. Important features of the proposed method are 1) that the solution of the original network as well as sensitivities with respect to any parameter is obtained from the solution of the reduced order model, and 2) a new reduced order model is not required each time design parameters are varied.

Acknowledgement

This thesis could not be successful without the invaluable support of my supervisor Dr. Anestis Dounavis of the Department of Electrical and Computer Engineering, University of Western Ontario. I would like to express my gratitude towards him for introducing me to the area of model order reduction and imbibing in me the enthusiasm for research. His motivation, keen acumen in this field of research and friendly disposition has always had a positive effect on my work.

I would also like to extend my thanks towards every faculty member, staff member and friend of the Department of Electrical and Computer Engineering, University of Western Ontario for their support and help at various stages of my thesis work. I would like to specially mention my colleagues Amir Beygi and Ehsan Rasekh and Sourajeet Roy for their invaluable advice.

My final thoughts are with my parents, Abolghasem and Fatemeh. Without their encouragement and endless support, I would not have had the opportunity to complete this study.

Contents

List of Tables

List of Figures

Abbreviations

AWE	Asymptotic Waveform Evaluation.
CFH	Complex Frequency Hopping.
EM	Electromagnetic.
FEM	Finite Element Method.
LU	Lower-upper matrix decomposition.
MGS	Modified Gram Schmidt.
MOR	Model Order Reduction.
ODE	Ordinary Differential Equation.
PDE	Partial Differential Equation.
PEC	Perfect Electric Conductor.
PMC	Perfect Magnetic Conductor.
p.u.l.	Per-unit-length.
RF	Radio Frequency.
SVD	Singular Value Decomposition.
TEM	Transverse electromagnetic.
VLSI	Very Large Scale Integration.

Chapter 1

1. Introduction

1.1. Background and Motivation

The rapid advances of high frequency circuit technology have significantly affected the construction of different types of microwave, millimeter-wave, optical and VLSI devices commonly used in mobile communications, radio links, optical communications, and various other automotive electronics systems. Modern wireless systems involve electrically large electromagnetic (EM) structures such as the waveguides, antennas, microwave circuits, and optical components, which are very complex in both geometry and material properties [1]. Also technological advances in the circuit technology have significantly reduced the feature sizes of high-speed electronic circuits and increased the density of chips. This leads to the need for efficient analysis and design tools for simulating and modeling the behavior of such structures and also performing optimization on the parameters of such devices prior to costly prototype development. Moreover, circuit designers also demand that the simulation techniques be fast and run on relatively small computing platforms, such as standard desktop personal computers [1]. Hence at higher frequencies, integrated and microwave circuits require fast and accurate modeling and simulation techniques for the optimization and design space exploration problems.

The design of electromagnetic devices such as wave-guiding structures, microstrip devices, filters, couplers, junctions and resonators are usually described by Partial

Differential Equations (PDE)s such as the vector wave equation derived by Maxwell's equations and hence full wave techniques are required to accurately characterize these systems [2]-[6]. Numerical methods, such as the Finite Element Method (FEM), have become extensively popular for accurate full wave analysis of microwave waveguide devices [2]-[6]. The key advantages of the FEM are the accuracy, versatility and its ability to handle complex materials (including anisotropic, lossy, non-linear etc) and complicated geometries [2]-[4]. However it relies on the discretization of three dimensional space and thus results in very large systems of equations which are prohibitively expensive to solve. Furthermore, these equations are solved for a wide frequency band and at different design parameters. One way to address computational complexity of FEM is based on Model Order Reduction (MOR) techniques [7]-[19], [28]-[30]. MOR techniques have been developed to efficiently calculate the scattering parameters [11]–[12], [14]-[16], [19] and to perform fast wideband eigenmode analysis of electromagnetic devices [28]–[31]. These algorithms are able to capture the frequency response of large linear networks with low-order rational approximations. The underlying concept of MOR is that distributed networks usually have large number of poles, however, only a small percentage of these poles is dominant. Dominant poles are defined as poles that have significant influence in the behavior of the network. By capturing only the dominant poles, the CPU expense of the simulation can be significantly reduced without compromising accuracy.

MOR techniques provide a mechanism to generate reduced order models from the detailed description of the original FEM network. This is achieved by using moment matching techniques, where the reduced order model matches the moments of the

original system to approximate the response with a low-order transfer function [12], [14]-[17], [19], [21]-[30]. However, these numerical techniques all conserve the original system moments only with respect to frequency. While this provides a significant CPU cost advantage when performing a single frequency sweep, a new reduced order model is required each time a parameter is varied in the structure under study. This results in a significant overhead and reduced efficiency when performing common design steps such as optimization and design space exploration. Parameterized model order reduction techniques have been proposed in the circuit area to address such concerns which produce reduced order models that are functions of frequency or time as well as other design parameters [20]-[26]. However, parameterized MOR techniques have not been developed to solve microwave systems described by FEM equations.

Reduced order models are accurate at the frequency point of expansion and less accurate away from the expansion point. To increase the accuracy of the reduced order model additional moments are required or multiple expansion points can be used [43]. An issue in developing efficient reduced order models is that as the number of moments increases, the moments become ill-conditioned due to the fact that the higher order moments converge to the largest eigenvalue of the system and are almost identical or parallel to each other [43]-[44]. This minimizes the efficiency of the reduced order model. One approach to improve the conditioning of the moment generating process is to use implicit moment matching techniques such as the Arnoldi process [43]-[44]. The traditional Arnoldi algorithm is applicable to first order linear systems that have a linear dependency with respect to frequency. However, distributed microwave systems are described by a second order polynomial matrix and may contain arbitrary functions of

frequency due to material properties and boundary conditions. As a result, traditional Arnoldi algorithms are not directly applicable in calculating the moments of the reduced order system for microwave systems that exhibit arbitrary functions of frequency due to high frequency phenomena such as skin effect.

MOR techniques have also been applied to perform sensitivity analysis of distributed interconnects and microwave systems [80], [89]-[90]. However, these MOR-sensitivity algorithms capture only the frequency moments of the original system. As a result, a new reduced order model is required each time a design parameter is modified, which can significantly increases the overhead of the optimization process.

The next sections describe the objectives and contributions of this thesis.

1.2. Objectives

The objective of this thesis is to develop efficient modeling techniques for the EM structures and high frequency microwave circuit simulation. The proposed methodology uses parameterized MOR techniques to reduce the computational complexity of microwave systems described by the FEM formulation.

The FEM model used for microwave systems is obtained from the vector wave equation for the electric field derived from Maxwell's equation [27]. FEM discretization of the vector wave equation results in a very large system of equations that are inherently time consuming to solve. MOR techniques have been proposed in literature to significantly reduce the CPU time required to simulate these large scale FEM problems [11]–[12], [14]-[16], [19], [28]-[31]. However, the reduced order models do not capture the variance with respect to design parameters since only the frequency moments are

matched. As a result, a new reduced order model is required each time a design parameter is modified which increases the overhead of the optimization process. In this thesis, a methodology is proposed to form parametric reduced order models to perform fast wideband eigenmode analysis of waveguide structures and to efficiently solve the scattering parameters of microwave devices. The resulting reduced order models match the characteristics of the original system in frequency domain as well as the other design parameters within a range of interest.

For the scattering problems, the general form of the resulting FEM equations may contain arbitrary functions of frequency due to material properties and boundary conditions. However, these equations are not directly compatible with the traditional Arnoldi algorithm, which relies on an implicit moment matching technique to obtain numerically well conditioned subspace from the moments of the original system. In this thesis the Arnoldi algorithm is extended to include arbitrary functions of frequency and design parameters. This approach yields more accurate reduced order models for complicated microwave systems that exhibit arbitrary functions of frequency and design parameters due to material properties and boundary conditions.

Microwave designers must make proper trade-offs, often between conflicting design requirements to obtain the best possible performance. Sensitivity analysis provides designers with valuable information in terms of identifying critical components in the design and provides gradient information needed for optimization. To combat the computational burden of performing sensitivity analysis on large EM systems a parameterized MOR technique is presented. Such an approach is significantly more CPU

efficient in optimization since a new reduced model is not required each time a design parameter is modified.

1.3. Contributions

The main contributions of this thesis are:

1. A parameterized model order reduction algorithm is developed to solve eigenvalue equations of electromagnetic systems. The model uses perturbation technique to obtain frequency moments as well as the moments with respect to other design parameters of interest. Next Singular Value Decomposition (SVD) is used to obtain a parameterized reduced order model which can be used to calculate the dispersion curves of the microwave devices. This procedure generates parametric reduced order models that are valid over the desired parameter range without the need to redo the reduction when design parameters are changed.

2. An Arnoldi technique is developed for the reduction of finite element electromagnetic systems to model structures with frequency dependant materials, delay elements and boundary conditions, as traditional MOR techniques using the Arnoldi algorithm are only applicable to first order linear systems and can not directly include arbitrary functions of frequency. The algorithm uses multi-order Arnoldi method to implicitly calculate the moments of the original system with respect to frequency, design parameters and well as cross-moments. Numerical examples will illustrate that this approach yields more accurate parameterized reduced order models when compared to explicit moment match techniques such as Modified Gram Schmidt (MGS).

3. The parameterized MOR technique is developed to perform sensitivity analysis of electromagnetic devices. The proposed algorithm uses a parametric reduced order model to solve the original network and an adjoint variable method to calculate sensitivities. Important features of the developed algorithm are: 1) a new reduced order model is not required each time design parameters are varied, and 2) the solution of the original network as well as sensitivities with respect to any parameter is obtained from the solution of the reduced order model.

1.4. Organization of Thesis

The organization of the thesis is as follows. Chapter 2 begins by reviewing the FEM based full wave analysis of microwave systems. From this discussion, MOR techniques are examined to reduce the computational difficulties of large scale FEM systems. In Chapter 3, a parameterized MOR technique for eigenvalue analysis of electromagnetic structures is presented. The development of a perturbation method and the SVD technique is described to create parametric reduced order models. Numerical examples are presented to demonstrate the efficiency of the proposed eigenvalue analysis algorithm. Chapter 4 describes the details of a multi-order Arnoldi technique for the reduction of finite element electromagnetic systems to include the effect of frequency dependant materials, delay elements and boundary conditions in the reduced order model. This chapter is concluded by presenting some numerical examples to show the efficiency of the algorithm. In Chapter 5, the parameterized MOR technique is developed to calculate the sensitivities of wave-guiding structures and the adjoint variable method

using parameterized MOR is described. A numerical example is presented to illustrate the validity of the algorithm. Chapter 6 presents a summary and suggestions for future works.

Chapter 2

2. Background and Literature Review

2.1. Introduction

The finite-element method (FEM) is one of the most used numerical techniques for the analysis and design of microwave and optical wave guiding structures. While the FEM provides a high degree of versatility and accuracy, it relies on the discretization of 2-D or 3-D space and thus results in very large systems of equations which are computationally expensive to solve. If the solution over a broad frequency spectrum is required, then the analysis must be repeated at many frequency points. This problem is further exacerbated when one considers the typical design process which includes optimization and design space exploration and thus requires repeated simulation of the same problem for different parameter values.

One approach to minimize the computational complexity of FEM is based on model-order reduction (MOR) [20], [28]-[31], [47]-[48]. These techniques provide a mechanism to generate reduced order models from the detailed description of the original FEM network. MOR techniques are able to conserve the moments of the original network and approximate the response with a low-order transfer functions. The goal of this chapter is to review the FEM formulation and MOR techniques that are used to model high speed VLSI interconnects and microwave circuits.

This organization of this chapter is as follows. The finite element formulation for the analysis microwave circuits is described in Section 2.2. This formulation leads to solving

a generalized eigenvalue problem or algebraic set of equations. Section 2.3 reviews MOR techniques that are used to reduce the computational complexity of the FEM formulation.

2.2. Simulation of Microwave Systems

Microwave devices such as antennas, waveguides, filters, couplers, junctions and microstrip devices are usually very complicated in geometrical structure and material properties. These devices are governed by the Maxwell's equations which can be expressed in the form of PDEs. The mathematical difficulties inherent in analytical solution of Maxwell's equation, e.g. geometries with various cross-sections of conventional microwave devices, and the use of anisotropic, nonlinear, and lossy materials, make the analysis of such devices considerably complicated. As the operating frequencies increase, full wave methods which directly solve Maxwell's equation are essential in order to accurately predict high frequency electromagnetic behaviour of microwave devices. The FEM technique has now been a very popular approach for full wave electromagnetic modeling of high frequency microwave devices due to its accuracy, versatility and flexibility. However, the resulting system of equations after the FEM discretization is typically very large and cumbersome to solve. This section briefly reviews the FEM formulation for the microwave systems and MOR techniques to be used to reduce the computational complexities of the FEM analysis.

2.2.1. FEM formulation of Microwave Systems

Considering a general waveguide whose conductors can be lossy and whose dielectrics can be inhomogeneous and anisotropic, the FEM formulation begins with the discretization of the electric field vector wave equation [27]

$$\nabla \times \left([\mu_r]^{-1} \cdot \nabla \times \boldsymbol{E} \right) - k^2 [\tilde{\varepsilon}_r] \cdot \boldsymbol{E} = 0 \tag{2.1}$$

where $k^2 = \omega^2 \varepsilon_0 \mu_0$. The variables ε_0 and μ_0 are the permittivity and permeability of free space; $[\mu_r]$ and $[\tilde{\varepsilon}_r] = [\varepsilon_r] - j[\sigma]/(\omega \varepsilon_0)$ are the relative permittivity and permeability coefficients, respectively; $[\sigma]$ is the conductivity; ω is the angular frequency and $\boldsymbol{E}$ is the electric field vector. For waveguide problems, on the conducting surfaces, the electric field satisfies the Dirichlet boundary condition on perfect electric conductor (PEC) as

$$\hat{n} \times \boldsymbol{E} = 0 \tag{2.2}$$

If symmetry can be used to reduce the size of the original problem then Neumann boundary condition on perfect magnetic conductor (PMC) is applied

$$\hat{n} \times ([\mu_r]^{-1} \cdot (\nabla \times \boldsymbol{E})) = 0 \tag{2.3}$$

By a variational formulation, the functional related to (2.1) and the boundary conditions can be expressed as [27], [30]

$$\begin{aligned} F(\boldsymbol{E}) = \frac{1}{2} \iint_{\Omega} \Big\{ & [\mu_{rz}]^{-1} (\nabla \times \boldsymbol{E}_t) \cdot (\nabla \times \boldsymbol{E}_t) - k_0^2 (\boldsymbol{E}_t \cdot \varepsilon_{rt} \cdot \boldsymbol{E}_t - \varepsilon_{rt} \boldsymbol{E}_z \boldsymbol{E}_z) \\ & + (-\gamma \boldsymbol{E}_t - \nabla_t \boldsymbol{E}_z) \cdot [\mu_{rt}]^{-1} \cdot (\gamma \boldsymbol{E}_t + \nabla_t \boldsymbol{E}_z) \Big\} d\Omega \end{aligned} \tag{2.4}$$

where $\gamma = \alpha + j\beta$ is the complex propagation constant and Ω the cross section of the waveguide. Considering the following transformations $\boldsymbol{e}_t = \gamma \boldsymbol{E}_t$ and $\boldsymbol{e}_z = \gamma \boldsymbol{E}_z$ along with combining the basis functions, the following formulation can be obtained

$$F(\boldsymbol{E}) = \boldsymbol{e}^T \boldsymbol{K} e - \gamma^2 \boldsymbol{e}^T \boldsymbol{M} e \tag{2.5}$$

where

$$\boldsymbol{e}^T \boldsymbol{K} e = \iint_\Omega \left\{ \left[\mu_{rz}\right]^{-1} (\nabla \times \boldsymbol{e}_t) \cdot (\nabla \times \boldsymbol{e}_t) - k_0^2 \boldsymbol{e}_t \cdot \varepsilon_{rt} \cdot \boldsymbol{e}_t \right\} d\Omega$$

$$\boldsymbol{e}^T \boldsymbol{M} e = \iint_\Omega \left\{ (\boldsymbol{e}_t + \nabla_t \boldsymbol{e}_z) \cdot \left[\mu_{rt}\right]^{-1} \cdot (\boldsymbol{e}_t + \nabla_t \boldsymbol{e}_z) - k_0^2 \varepsilon_{rz} \boldsymbol{e}_t \boldsymbol{e}_z \right\} d\Omega$$

where $\boldsymbol{e}$ is a column vector containing nodal and edge variables related to field distribution. Applying Ritz method to (2.5) result in a generalized eigenvalue problem

$$\boldsymbol{K} e = \gamma^2 \boldsymbol{M} e \tag{2.6}$$

Finally the frequency dependant eigen problem of (2.6) can rewritten as

$$(\boldsymbol{A}(k) - \lambda(k)\boldsymbol{B}(k)) \cdot \boldsymbol{E}(k) = 0 \tag{2.7}$$

where $\lambda = \gamma^2$ and $\boldsymbol{E}$ are the eigenvalues and eigenvectors, respectively and k is the wavenumber. The matrices $\boldsymbol{A}$ and $\boldsymbol{B}$ are functions of the wave number k which can be expressed as

$$\begin{aligned} \boldsymbol{A}(k) &= \boldsymbol{A}_0 + k\boldsymbol{A}_1 + k^2 \boldsymbol{A}_2 \\ \boldsymbol{B}(k) &= \boldsymbol{B}_0 + k\boldsymbol{B}_1 + k^2 \boldsymbol{B}_2 \end{aligned} \tag{2.8}$$

To perform modal analysis of the EM structures the generalized eigenvalue problem of (2.7) has to be solved. Such calculations are very time consuming, since the FEM formulation of (2.7) often leads to a very large system of equations which needs to be solved over a broad frequency spectrum.

For the case of scattering problems, the functional for boundary value problem defined in (2.1) in accordance with the general variational principle can also be represented in the presence of excitation $\boldsymbol{E}^{inc}$ as [27]

$$\begin{aligned} F(\boldsymbol{E}) = \frac{1}{2}\iiint_V \left[[\mu]^{-1}(\nabla \times \boldsymbol{E}) \cdot (\nabla \times \boldsymbol{E}) - k^2 [\tilde{\varepsilon}_r] \boldsymbol{E} \cdot \boldsymbol{E}^* \right] dV \\ + \sum_{i=1}^{p} \left\{ \left[\iint_{\Gamma_i} \frac{j\beta}{2} (\hat{n} \times \boldsymbol{E}) \cdot (\hat{n} \times \boldsymbol{E}) - 2j\beta \boldsymbol{E} \cdot \boldsymbol{E}^{inc} \right] dS \right\} \end{aligned} \tag{2.9}$$

where $\gamma = \alpha + j\beta$ is the complex propagation constant; V denotes the volume of the structure; S denotes the surface enclosing V and $\hat{n}$ is outward normal to S and p is the total number of ports. The FEM discretization of (2.9) when there is finite conductivity using vector basis functions results a matrix equation as

$$(\boldsymbol{A}_0 + \boldsymbol{A}_1 s + \boldsymbol{A}_2 s^2 + \boldsymbol{A}_3 j\beta)\boldsymbol{e}_s = j\beta \boldsymbol{b} \tag{2.10}$$

where $s = j\omega$ is the angular frequency, β is the propagation constant and is a function of frequency, the matrices $\boldsymbol{A}_0, \boldsymbol{A}_1, \boldsymbol{A}_2, \boldsymbol{A}_3$ and $\boldsymbol{b}$ are given by

$$\boldsymbol{A}_{0,ij} = \iiint_V \frac{1}{\mu} \nabla \times \boldsymbol{N}_i \cdot \nabla \times \boldsymbol{N}_j dV \tag{2.11}$$

$$\boldsymbol{A}_{1,ij} = \iiint_V \sigma \boldsymbol{N}_i \cdot \boldsymbol{N}_j dV \tag{2.12}$$

$$\boldsymbol{A}_{2,ij} = \iiint_V \varepsilon \boldsymbol{N}_i \cdot \boldsymbol{N}_j dV \tag{2.13}$$

$$\boldsymbol{A}_{3,ij} = \iiint_V \boldsymbol{S}_i \cdot \boldsymbol{S}_j dV \tag{2.14}$$

$$\boldsymbol{b}_i = -2\iint_S \boldsymbol{S}_i \cdot (\boldsymbol{E}^{inc} \times \hat{n}) dS \tag{2.15}$$

where $\boldsymbol{S}_i$ is the vector basis functions and $\boldsymbol{S}_i = \hat{n} \times \boldsymbol{N}_i$ where $\boldsymbol{N}_i$ are the vector basis functions that have unit tangential component at edge *i*, $\boldsymbol{A}_0 \in \Re^{N \times N}$, $\boldsymbol{A}_1 \in \Re^{N \times N}$, $\boldsymbol{A}_2 \in \Re^{N \times N}$ and $\boldsymbol{A}_3 \in \Re^{N \times N}$ are the sparse matrices obtained through the FEM formulation. $\boldsymbol{e}_s \in C^N$ is the vector of unknown variables in the approximation of $\boldsymbol{E}$, $\boldsymbol{b} \in \Re^N$ in the vector of the incident field and N is the total number of variables in the FEM formulation. In case of no finite conductivity (2.10) can be simplified as

$$(\overline{\boldsymbol{A}}_0 + \overline{\boldsymbol{A}}_1 k + \overline{\boldsymbol{A}}_2 k^2)\boldsymbol{e}_k = k\boldsymbol{b} \tag{2.16}$$

where $\boldsymbol{e}_k \in C^N$ in the vector of unknowns and $k = j\beta$. The matrices $\overline{\boldsymbol{A}}_0, \overline{\boldsymbol{A}}_1$ and $\overline{\boldsymbol{A}}_2$ are as follows

$$\overline{\boldsymbol{A}}_0 = \boldsymbol{A}_0 - (\frac{k_t^2}{\varepsilon_0 \mu_0})\boldsymbol{A}_2 \tag{2.17}$$

$$\overline{\boldsymbol{A}}_1 = \boldsymbol{A}_3 \tag{2.18}$$

$$\overline{\boldsymbol{A}}_0 = (\frac{1}{\varepsilon_0 \mu_0})\boldsymbol{A}_2 \tag{2.19}$$

Equations (2.10) and (2.14) can be rewritten in a general linear network form as

$$\boldsymbol{Y}(s) \cdot \boldsymbol{X}(s) = \boldsymbol{b}(s) \tag{2.20}$$

where $\boldsymbol{Y}(s) \in C^{N \times N}$ is the transfer function of the system; $\boldsymbol{X}(s) \in C^{N}$ is the vector of unknown variables; $\boldsymbol{b}(s) \in C^{N}$ represents the excitation of the network; N is the number of unknown variables in $\boldsymbol{X}(s)$ and s is the angular frequency. Complexity of such system of equations often leads to large system matrices in (2.20) and as a result simulation of which is computationally expensive.

One way to combat such computational complexity of FEM solutions is to use MOR techniques. In the following sections, the MOR algorithms used to perform eigen-analysis and calculate the scattering parameters of microwave systems are briefly reviewed. In addition, MOR techniques to calculate sensitivities are also described.

2.3. Simulation Techniques based on MOR

To efficiently solve the eigenvalue problem of (2.7), MOR techniques based on hyper-perturbation Taylor series expansion [28]-[30], asymptotic waveform evaluation [8]-[9] and singular value decomposition [29]-[30] have been proposed. To obtain reduced order models for (2.20), MOR techniques are either based on explicit moment matching based on direct Padé approximants [32]-[34] or implicit moment matching based on projecting large matrices on its dominant eigenspace [30], [36]-[39], [42]. The following sections briefly reviews MOR techniques to efficiently solve the system equations in (2.7) and (2.20).

2.3.1. SVD Based MOR for Eigenvalue Problems

Modal analysis of the EM structures corresponds to solving a generalized eigenvalue problem of (2.7). One approach to derive a reduced order model for (2.7) is based on using modified perturbation theory and singular value decomposition [28]-[30]. This approach expands the eigenvectors $\boldsymbol{E}(k)$ and eigenvalues $\lambda(k)$ of (2.7) into a Taylor series at $k = k_0$ as

$$\boldsymbol{E}(k) = \sum_{i=0}^{M} \boldsymbol{E}_i (k - k_0)^i \tag{2.21}$$

$$\lambda(k,h) = \sum_{i=0}^{M} \lambda_i (k - k_0)^i \tag{2.22}$$

Substituting (2.8), (2.21)-(2.22) into (2.7) and matching coefficients of corresponding powers of $(k - k_0)$ yields the following recursive relationship

$$(\boldsymbol{A}_0 - \lambda_0 \boldsymbol{B}_0)\boldsymbol{E}_1 = \lambda_1 \boldsymbol{B}_0 \boldsymbol{E}_0 - (\boldsymbol{A}_1 - \lambda_0 \boldsymbol{B}_1)\boldsymbol{E}_0$$

$$\begin{aligned}(\boldsymbol{A}_0 - \lambda_0 \boldsymbol{B}_0)\boldsymbol{E}_2 = {} & \lambda_2 \boldsymbol{B}_0 \boldsymbol{E}_0 - (\boldsymbol{A}_1 - \lambda_0 \boldsymbol{B}_1)\boldsymbol{E}_1 \\ & - (\boldsymbol{A}_2 - \lambda_0 B_2)\boldsymbol{E}_0 + \lambda_1 (\boldsymbol{B}_0 \boldsymbol{E}_1 + \boldsymbol{B}_1 \boldsymbol{E}_0)\end{aligned}$$

$$\vdots$$

$$\begin{aligned}(\boldsymbol{A}_0 - \lambda_0 \boldsymbol{B}_0)\boldsymbol{E}_M = {} & \lambda_M \boldsymbol{B}_0 \boldsymbol{E}_0 - \\ & \sum_{i=1}^{\min(2,M)} (\boldsymbol{A}_i - \lambda_0 \boldsymbol{B}_i)\boldsymbol{E}_{M-i} + \sum_{i=1}^{M-1} \lambda_i \cdot \sum_{j=0}^{\min(2,M-i)} \boldsymbol{B}_j \boldsymbol{E}_{M-i-j}\end{aligned} \tag{2.23}$$

To obtain the Taylor series coefficients of (2.21)-(2.22) from (2.23), equation (2.7) must first be solved at k_0 to obtain the eigenvalue λ_0 and corresponding eigenvector $\boldsymbol{E}_0$. This

can be done by using the Lanczos algorithm as reported in [28], [30]. Since $\boldsymbol{E}_0$ is an eigenvector of (2.7), then the following relationship holds true $\boldsymbol{E}_0^{\mathrm{H}}(\boldsymbol{A}_0 - \lambda_0 \boldsymbol{B}_0) = 0$ [28]-[30], where the superscript H denotes the Hermitian of the matrix. Therefore, by multiplying the first equation of (2.23) by $\boldsymbol{E}_0^{\mathrm{H}}$ will make the left-hand side disappear and λ_1 can be found. With the knowledge of λ_1 the first equation of (2.23) can be used to find $\boldsymbol{E}_1$. This process is repeated recursively to find the higher order polynomial coefficients λ_i and $\boldsymbol{E}_i$, where $i = [0,1,...,M]$. Once all the required Taylor series coefficients with respect to k are evaluated, the subspace $\boldsymbol{K}$ is constructed as $\boldsymbol{K} = [\boldsymbol{E}_0, \boldsymbol{E}_1,..., \boldsymbol{E}_M]$. As the number of Taylor coefficients increase, the matrix $\boldsymbol{K}$ becomes ill-conditioned. As a result, to obtain a more accurate reduced order system, the matrix $\boldsymbol{K}$ is converted into orthonormal matrix $\boldsymbol{Q}$ using singular value decomposition [28]-[30]. The reduced order model is obtained by a change of variables as

$$\boldsymbol{E}(k) = \boldsymbol{Q}\hat{\boldsymbol{E}}(k) \tag{2.24}$$

Substituting (2.24) into (2.7) and pre-multiplying by $\boldsymbol{Q}^H$ yields

$$(\hat{\boldsymbol{A}}(k) - \lambda(k)\hat{\boldsymbol{B}}(k)) \cdot \hat{\boldsymbol{E}}(k) = 0 \tag{2.25}$$

where

$$\hat{\boldsymbol{A}}(k) = \boldsymbol{Q}^H \boldsymbol{A}(k)\, \boldsymbol{Q}$$

$$\hat{\boldsymbol{B}}(k) \cdot = \boldsymbol{Q}^H \boldsymbol{B}(k)\, \boldsymbol{Q} \tag{2.26}$$

The size of the reduced order model depends on the order *M*, which is very small compared to the size of the original system. Once the reduced system of (2.25) is obtained, it can be applied to perform fast frequency sweeps of electromagnetic eigenvalue problems. However if one decides to change a parameter in the system, the reduced order model of (2.25) is no longer valid and a new reduced order model needs to be calculated. This is due to the fact that the moments are captured only with respect to frequency.

2.3.2. Moment Matching Based MOR

For the solution of (2.20), MOR techniques can be broadly classified into two main categories: approaches based on explicit moment matching based on direct Padé approximants and implicit moment matching based on projecting large matrices on its dominant eigenspace.

Explicit moment matching techniques calculate the actual moments of (2.10) and (2.16) to obtain a reduced order system. However, these methods are limited to low order approximations, due to the fact that the higher order moments converge to the largest eigenvalue of the system and are almost identical or parallel to each other [15]-[16], [43]. As a result, the additional higher order moments add no new information to the reduced order model. On the other hand, Krylov subspace methods based on congruent transformations capture the system moments implicitly by using Arnoldi process [44] to provide high order approximations. A general approach used to apply the Arnoldi process for polynomial matrix equations in (2.16) is to convert it to a linear system by using extra state variables as [12], [14]-[19], [46] as

$$(s\boldsymbol{C}+\boldsymbol{G})\boldsymbol{X}=\boldsymbol{B} \tag{2.27}$$

where

$$\boldsymbol{G}=\begin{bmatrix}\overline{\boldsymbol{A}}_1 & \boldsymbol{I}_N\\ -\overline{\boldsymbol{A}}_0 & \boldsymbol{0}\end{bmatrix};\quad \boldsymbol{C}=\begin{bmatrix}\overline{\boldsymbol{A}}_1 & \boldsymbol{I}_N\\ -\overline{\boldsymbol{A}}_0 & \boldsymbol{0}\end{bmatrix};$$

$$\boldsymbol{X}=\begin{bmatrix}\boldsymbol{e}_k\\ \boldsymbol{e}'_k\end{bmatrix};\quad \boldsymbol{B}=\begin{bmatrix}\boldsymbol{b}\\ \boldsymbol{0}\end{bmatrix} \tag{2.28}$$

where $\boldsymbol{I}_N \in \Re^{N\times N}$ is the identity matrix and $\boldsymbol{e}'_x \in C^N$ is the vector of extra unknown variables. The system of equations (2.27) has linear dependency with respect to *s*, so that the Arnoldi algorithm is directly applicable.

To obtain a reduced order model the moments of the network need to be evaluated. To illustrate this concept, for both explicit and implicit moment matching techniques, consider a single-input single-output linear system and let *H(s)* be the transfer function. Using a Maclaurin series expansion, *H(s)* can be expressed as

$$H(s) \approx m_o + m_1 s + m_2 s^2 + ... \tag{2.29}$$

where m_i is referred to as the i^{th} moment of *H(s)*. To construct a reduced-order model using explicit moment matching techniques such as Asymptotic Waveform Evaluation (AWE), the series expansion of (2.29) is converted to a rational function using Padé approximation as

$$H(s) \approx m_o + m_1 s + m_2 s^2 + ... m_{N+L-1} s^{N+L-1} \approx \frac{a_0 + a_1 s + ... + a_L s^L}{1 + b_1 s + ... + b_N s^N} \tag{2.30}$$

The coefficients a_i and b_i are obtained by cross multiplying the denominator of (2.28) and equating similar powers of s. In general the system of equations can be represented as

$$\begin{bmatrix} m_{L-N+1} & m_{L-N+2} & \cdots & m_L \\ m_{L-N+2} & m_{L-N+3} & \cdots & m_{L+1} \\ \vdots & \vdots & & \vdots \\ m_L & m_{L+2} & \cdots & m_{N+L-1} \end{bmatrix} \begin{bmatrix} b_N \\ b_{N-1} \\ \vdots \\ b_1 \end{bmatrix} = - \begin{bmatrix} m_{L+1} \\ m_{L+2} \\ \vdots \\ m_{L+N} \end{bmatrix}$$

$$\begin{aligned} a_0 &= m_0 \\ a_1 &= m_1 + b_1 m_0 \\ &\cdots \\ a_L &= m_L + \sum_{i=1}^{min(L,N)} b_i m_{L-i} \end{aligned} \tag{2.31}$$

The moments of (2.27) can be calculate by replacing $\boldsymbol{X}$ with a Maclaurin series expansion, gives

$$(s\boldsymbol{C} + \boldsymbol{G})(\boldsymbol{M}_0 + \boldsymbol{M}_1 s + \boldsymbol{M}_2 s^2 + ...) = \boldsymbol{B} \tag{2.32}$$

Equating the coefficients of similar powers of s on both sides yields

$$\begin{aligned} \boldsymbol{G}\boldsymbol{M}_0 &= \boldsymbol{B} & \boldsymbol{M}_0 &= \boldsymbol{G}^{-1}\boldsymbol{B} \\ \boldsymbol{C}\boldsymbol{M}_0 + \boldsymbol{G}\boldsymbol{M}_1 &= \boldsymbol{0} & \boldsymbol{M}_1 &= -\boldsymbol{G}^{-1}\boldsymbol{C}\boldsymbol{M}_0 \\ \boldsymbol{C}\boldsymbol{M}_1 + \boldsymbol{G}\boldsymbol{M}_2 &= \boldsymbol{0} & \boldsymbol{M}_2 &= -\boldsymbol{G}^{-1}\boldsymbol{C}\boldsymbol{M}_1 \\ &\cdots & &\cdots \\ \boldsymbol{C}\boldsymbol{M}_{k-1} + \boldsymbol{G}\boldsymbol{M}_k &= \boldsymbol{0} & \boldsymbol{M}_k &= -\boldsymbol{G}^{-1}\boldsymbol{C}\boldsymbol{M}_{k-1} \end{aligned} \tag{2.33}$$

Substituting $\boldsymbol{A} = -\boldsymbol{G}^{-1}\boldsymbol{C}$ and $\boldsymbol{R} = \boldsymbol{G}^{-1}\boldsymbol{B}$ into (2.33) yields

$$\begin{aligned} \boldsymbol{M}_0 &= \boldsymbol{R} \\ \boldsymbol{M}_k &= \boldsymbol{A}\boldsymbol{M}_{k-1} \end{aligned} \tag{2.34}$$

Equation (2.34) yields a closed form relationship for the computation of the moments $\boldsymbol{M}_k$. As shown in (2.33), only one matrix inversion is required to calculate the moments. As a result the main computational cost to calculate the moments is one lower-upper decomposition for each expansion point and one forward-backward substitution for each moment. This significantly reduces the simulation time of linear circuits since the original system requires many matrix inversions to solve the system at different frequency points.

Explicit moment matching techniques based on AWE is limited to a low order rational approximation, since (2.31) becomes an ill-conditioned matrix as the number of moments increases. In addition, Padé approximants may produce unstable poles and provide no estimates for error bounds. To address some of the difficulties with single Padé expansition complex frequency hopping (CFH) has been developed which relies on multiple expansion points to construct a unified rational function. However in both AWE and CFH there is no guarantee that the reduced order model is passive [43].

Implicit moment matching techniques use Krylov subspace approaches to project large matrices on its dominant eigenspace. The moments calculated using (2.33) are used to form the moment matrix $\boldsymbol{K}$ as

$$\boldsymbol{K} = \left\lfloor \boldsymbol{M}_0 \;\; \boldsymbol{M}_1 \;\; \boldsymbol{M}_2 .... \boldsymbol{M} \right\rfloor = \left[\boldsymbol{R} \;\; \boldsymbol{RA} \;\; \boldsymbol{RA}^2 .... \boldsymbol{RA}^q \right] \tag{2.35}$$

The matrix $\boldsymbol{K}$ becomes an ill-conditioned matrix as the number of moments increase [43]. To obtain more accurate reduced order models, implicit moment matching techniques such as the Arnoldi algorithm are used to convert the matrix $\boldsymbol{K}$ into an orthonormal matrix $\boldsymbol{Q}$ as

$$colsp(\boldsymbol{Q}) = colsp(\boldsymbol{K}) \qquad \boldsymbol{Q}^T\boldsymbol{Q} = \boldsymbol{I} \tag{2.36}$$

where both matrices $\boldsymbol{K}$ and $\boldsymbol{Q}$ span the same column space and $\boldsymbol{I}$ is the identity matrix. An orthonormal matrix satisfies the following conditions:

$$\boldsymbol{Q} = \lfloor \boldsymbol{q}_0 \ \boldsymbol{q}_1 \ \boldsymbol{q}_2 \cdots \boldsymbol{q}_q \rfloor$$

$$\begin{aligned} &\|\boldsymbol{q}_i\| = 1 \\ &\boldsymbol{q}_m\boldsymbol{q}_n = 0; \qquad \forall m \neq n \end{aligned} \tag{2.37}$$

The reduced-order system is obtained by a change of variables in (2.27),

$$\boldsymbol{X} = \boldsymbol{Q}\hat{\boldsymbol{X}} \tag{2.38}$$

where $\hat{\boldsymbol{X}}$ contains the variables of the reduced order system. The reduced order system is obtained by congruent transformation by substituting (2.38) into (2.27) and pre-multiplying by $\boldsymbol{Q}^{\mathrm{T}}$ yields

$$(s\hat{\boldsymbol{C}} + \hat{\boldsymbol{G}})\hat{\boldsymbol{X}} = \hat{\boldsymbol{B}} \tag{2.39}$$

where

$$\hat{\boldsymbol{G}} = \boldsymbol{Q}^T\boldsymbol{G}\boldsymbol{Q} \qquad \hat{\boldsymbol{C}} = \boldsymbol{Q}^T\boldsymbol{C}\boldsymbol{Q} \qquad \hat{\boldsymbol{B}} = \boldsymbol{Q}^T\boldsymbol{B} \tag{2.40}$$

The orthonormal matrix $\boldsymbol{Q}$ is generated using the Arnoldi algorithm as described in Fig. 2.1, where “orthonormalize” refers to the Modified Gram-Schmidt (MGS) orthonormalization procedure. The basic idea of the Arnoldi algorithm is to exploit the relationship between successive moments of (2.35) which forms a Krylov subspace.

While the Arnoldi algorithm yields numerically more accurate results when compare to explicitly calculating the moments, the Arnoldi algorithm is not directly applicable for microwave systems that have arbitrary functions of frequency due to material properties and boundary conditions. This is due to the fact the relationship between successive moments does not satisfy the pattern of (2.35). Arnoldi algorithms have been extended to second order polynomial systems as well as multi-order polynomial systems [56]-[57], [60]-[61]. Approaches to model distributed systems with arbitrary functions of frequency are either based on rational curve fitting and applying multiorder Arnoldi [57] or to treat the arbitrary frequency functions as separate variables and apply multidimensional subspace methods [24]-[25], [47].

Block Arnoldi (inputs : $\boldsymbol{G}, \boldsymbol{C}, \boldsymbol{B}, s_0 \rightarrow$ output : $\boldsymbol{Q}$)
$\boldsymbol{M} = (\boldsymbol{G} + s_0 \boldsymbol{C})^{-1}$
$\boldsymbol{R} = \boldsymbol{M}\boldsymbol{B}$
$\boldsymbol{z}_0 = \boldsymbol{R}$
$[\boldsymbol{Q}_0] = orthonorma\ lize\ (\mathrm{Re}[\boldsymbol{z}_0] \quad \mathrm{Im}[\boldsymbol{z}_0])$
for j $\leftarrow 1$ to k
  $\boldsymbol{z}_j = -\boldsymbol{M}\boldsymbol{C}\boldsymbol{q}_{j-1}$
  for i $\leftarrow 0$ to j -1
    $\boldsymbol{h} = \boldsymbol{q}_i^T \boldsymbol{z}_j$
    $\boldsymbol{z}_j = \boldsymbol{z}_j - \boldsymbol{q}_i \boldsymbol{h}$
  end
$[\boldsymbol{Q}_j] = orthonorma\ lize\ (Re[\boldsymbol{z}_j] \quad Im[\boldsymbol{z}_j])$
end
$\boldsymbol{Q} = [\boldsymbol{Q}_0 \quad \boldsymbol{Q}_1 \quad \boldsymbol{Q}_2 \quad \cdots \quad \boldsymbol{Q}_k]$
Return($\boldsymbol{Q}$)

Fig.2.1. Block Arnoldi Algorithm for expansion about a complex frequency point $s = s_0$.

2.3.3. Sensitivity Analysis Using MOR Techniques

Sensitivity analysis is important to determine which circuit parameters significantly influence the response of the system. In addition, sensitivity analysis provides gradient information needed for optimization. Among the techniques used to calculate sensitivities, the adjoint method has been found to be the most efficient [86], [92]. The following section briefly reviews the adjoint method using model order reduction techniques.

Consider the linear network described by (2.20) in the frequency domain. Let λ be a design parameter of the network. The adjoint or transpose method calculates sensitivity of a specific output with respect to the circuit parameters. Let the output variable be as following

$$\Phi = \boldsymbol{d}^T \boldsymbol{X} \tag{2.41}$$

where Φ is the scaler variable of interest, $\boldsymbol{d}$ is a constant vector that selects the output of interest and the superscript T denotes the transpose of matrix. Differentiating (2.20) and (2.41) with respect to parameter λ yields

$$\frac{d\Phi}{d\lambda} = \boldsymbol{d}^T \frac{d\boldsymbol{X}}{d\lambda} \tag{2.42}$$

$$\frac{d\boldsymbol{X}}{d\lambda} = -\boldsymbol{Y}^{-1}\left(\frac{d\boldsymbol{A}}{d\lambda}\boldsymbol{X} - \frac{d\boldsymbol{b}}{d\lambda}\right) \tag{2.43}$$

Substituting (2.43) into (2.42) yields

$$\frac{d\Phi}{d\lambda} = \left(\boldsymbol{X}^{a}\right)^{T}\left(\frac{d\boldsymbol{A}}{d\lambda}\boldsymbol{X} - \frac{d\boldsymbol{b}}{d\lambda}\right) \tag{2.44}$$

where $\boldsymbol{X}^{a}$ is the solution of the adjoint network defined as

$$\boldsymbol{A}^{\boldsymbol{T}}\boldsymbol{X}^{a} = -\boldsymbol{d} \tag{2.45}$$

Note, that the solution of the adjoint variable network does not require additional lower-upper decompositions to invert $\boldsymbol{A}^{\boldsymbol{T}}$ since the lower-upper matrices are known from the solution of (2.20). This leads to significant computational savings, since the sensitivities with respect to all design parameters can be obtained with only one forward-backward substitution to solve (2.44).

The find magnitude and phase values of the sensitivities Let the response of the system be expressed in terms of the phase θ and magnitude $|\Phi|$ as

$$\Phi = |\Phi| e^{j\theta} \tag{2.46}$$

The sensitivity of the magnitude or absolute value of the function is defined as $d|\Phi|/d\lambda$. The value of $d|\Phi|/d\lambda$ is referred to the absolute sensitivity. To calculate $d|\Phi|/d\lambda$ and $d\theta/d\lambda$, (2.46) is expressed as

$$ln\Phi = ln|\Phi| + j\theta \tag{2.47}$$

Differentiating (2.47)**Error! Reference source not found.** with respect to a circuit parameter λ,

$$\frac{1}{\Phi}\frac{d\Phi}{d\lambda} = \frac{1}{|\Phi|}\frac{d|\Phi|}{d\lambda} + j\frac{d\theta}{d\lambda} \tag{2.48}$$

The real and imaginary part of (2.48) can be split into two equations as

$$\frac{d|\Phi|}{d\lambda} = |\Phi| \operatorname{Re}\left(\frac{1}{\Phi}\frac{d\Phi}{d\lambda}\right) \tag{2.49}$$

$$\frac{d\theta}{d\lambda} = \operatorname{Im}\left(\frac{1}{\Phi}\frac{d\Phi}{d\lambda}\right) \tag{2.50}$$

where “Re” and “Im” denote the real and imaginary parts. Equations (2.49) and (2.50) calculate the absolute and phase sensitivities, respectively.

Recently MOR techniques have been used to perform sensitivity analysis of distributed interconnects and microwave circuits [80], [89]-[90]. The methodologies of [80] and [89] calculate moments for (2.20) and (2.45), to obtain reduced order models for both the original and adjoint networks. In [90], the sensitivities are derived from the reduced order model of the original network by finding the derivative of the orthogonal basis. However, all these MOR-sensitivity algorithms conserve the original system moments only with respect to frequency. As a result, a new reduced order system is required each time a design parameter is changed.

Chapter 3

3. Parameterized Model Order Reduction on Eigenvalue Equations

3.1. Introduction

In this work, a parameterized model reduction technique is developed to perform eigenanalysis of waveguiding structures. The proposed methodology uses modified perturbation theory to calculate a multidimensional Taylor series and singular value decomposition to perform reduction directly on the FEM eigenvalue equations. This procedure results in a parameterized reduced order model that is valid over a user defined range of design parameter values (such as material properties, geometrical parameters). Such an approach is significantly more CPU efficient in optimization and design space exploration problems since a new reduced model is not required when a design parameter is modified. Numerical examples are presented to illustrate the validity of the proposed technique.

This chapter is organized as follows. Section 3.2 describes the eigenvalue problem derived from the FEM formulation of the vector wave equations. The proposed parameterized model reduction technique is described in section 3.3. Numerical examples are provided is section 3.4.

3.2. Formulation of microwave system

Applying Galerkin's procedure to the vector wave equation of (2.1) yields a linear sparse

eigenvalue problem of (2.7). To derive a parametric reduced order model for (2.7), the system is expressed as a function of the frequency variable *k* and other design parameters as

$$(\boldsymbol{A}(k,\bar{h}) - \lambda(k,\bar{h})\boldsymbol{B}(k,\bar{h})) \cdot \boldsymbol{E}(k,\bar{h}) = 0 \tag{3.1}$$

where

$$\begin{aligned} \boldsymbol{A}(k,\bar{h}) &= \boldsymbol{A}_0(\bar{h}) + k\boldsymbol{A}_1(\bar{h}) + k^2\boldsymbol{A}_2(\bar{h}) \\ \boldsymbol{B}(k,\bar{\lambda}) &= \boldsymbol{B}_0(\bar{h}) + k\boldsymbol{B}_1(\bar{h}) + k^2\boldsymbol{B}_2(\bar{h}) \end{aligned} \tag{3.2}$$

and $\bar{h} = [h_1, h_2 .....h_n]$ are the design parameters of interest in the system.

3.3. Parameterized Reduced Order Model

3.3.1. Parametric System Formulation

The design parameters of (3.1) can be material properties such as the permittivity, permeability, and conductivity whose dependencies in the system are known directly. However, in certain cases, the dependence on parameters (such as geometrical variations) in the electromagnetic model is not known explicitly. In order to include geometrical design parameters in the reduced order model, a polynomial fitting algorithm for parametric model reduction is used [24], [46]-[47].

The polynomial fitting based approach samples the matrices at different points in the parameter space, and fits the entries with polynomials. This technique requires that the discretized mesh for all sample points in the parameter space is identical (i.e., they have

the same number of degrees of freedom and their corresponding locations in the system matrices are same). For a given matrix $\boldsymbol{A}_0(h_1.....h_n)$, the polynomial fit $\boldsymbol{A}'_0(h_1.....h_n)$ is

$$\boldsymbol{A}'_0(h_1.....h_n) = \boldsymbol{A}'_{00} + \sum_i h_i \boldsymbol{A}'_{0i} + \sum_{i,j} h_i h_j \boldsymbol{A}'_{0i,j}$$

$$+ \sum_{i,j,k} h_i h_j h_k \boldsymbol{A}'_{0i,j,k} + \cdots \quad i, j, k = 1, \ldots, n \tag{3.3}$$

Once the system matrices are calculated as a function of design parameters using a polynomial fit, they are substituted in (3.1) to derive a parameterized reduced order model. In Section 3.4, a step by step approach of generating the reduced order model using the polynomial fitting technique is illustrated.

3.3.2. Computation of Parameterized Reduced Order Model

The computation of the parameterized reduced order model expands the quantities of (3.1) into a multidimensional Taylor series expansion with respect to the wave number *k* and the design parameters $\bar{h}$. For ease of presentation and without the loss of generality, the method is described for the case when there is only one design parameter $\bar{h} = [h]$. The eigenvectors $\boldsymbol{E}(k,h)$ and eigenvalues $\lambda(k,h)$ of (3.1) are expanded into a multidimensional Taylor series at $k = k_0$ and $h = h_0$, expressed as

$$\boldsymbol{E}(k,h) = \sum_{i=0}^{M} \boldsymbol{E}_{i0} (k - k_0)^i + \sum_{j=1}^{N} \boldsymbol{E}_{0j} (h - h_0)^j +$$

$$\sum_{i=1} \sum_{j=1} \boldsymbol{E}_{ij} (k - k_0)^i (h - h_0)^j \tag{3.4}$$

$$\lambda(k,h) = \sum_{i=0}^{M} \lambda_{i0} (k - k_0)^i + \sum_{j=1}^{N} \lambda_{0j} (h - h_0)^j + \sum_{i=1} \sum_{j=1} \lambda_{ij} (k - k_0)^i (h - h_0)^j \tag{3.5}$$

where the first and second summation terms of (3.4) and (3.5) correspond to the self-terms with respect to *k* and *h*, respectively, and the double summation terms of (3.4) and (3.5) correspond to the cross terms. The matrices $\boldsymbol{A}(k,h)$ and $\boldsymbol{B}(k,h)$ of (3.1) are also written as multidimensional series as

$$\boldsymbol{A}(k,h) = \sum_{i=0} \boldsymbol{A}_{i0} (k - k_0)^i + \sum_{j=1} \boldsymbol{A}_{0j} (h - h_0)^j + \sum_{i=1} \sum_{j=1} \boldsymbol{A}_{ij} (k - k_0)^i (h - h_0)^j \tag{3.6}$$

$$\boldsymbol{B}(k,h) = \sum_{i=0} \boldsymbol{B}_{i0} (k - k_0)^i + \sum_{j=1} \boldsymbol{B}_{0j} (h - h_0)^j + \sum_{i=1} \sum_{j=1} \boldsymbol{B}_{ij} (k - k_0)^i (h - h_0)^j \tag{3.7}$$

When the design parameter *h* represents a material property such as the permittivity, permeability, or conductivity, the dependence on the design parameter in the system is known and the matrices $\boldsymbol{A}_{ij}$ and $\boldsymbol{B}_{ij}$ are determined directly form the FEM formulation. For the case when the dependency of the design parameter *h* is not known explicitly (i.e. such as geometrical variations), the matrices of (3.6) and (3.7) are obtained using a polynomial fitting algorithm for parametric model reduction as described in section 3.4.1.

The Taylor series coefficients of (3.4) and (3.5) are obtained following a procedure

similar to [28] and [30], except in the proposed work it is extended to include design parameter variations. Substituting (3.4)-(3.7) into (3.1) and matching coefficients of corresponding powers of $(k-k_0)$ yields the following recursive relationship

$$(\boldsymbol{A}_{00}-\lambda_{00}\boldsymbol{B}_{00})\boldsymbol{E}_{10}=\lambda_{10}\boldsymbol{B}_{00}\boldsymbol{E}_{00}-(\boldsymbol{A}_{10}-\lambda_{00}\boldsymbol{B}_{10})\boldsymbol{E}_{00}$$

$$\begin{aligned}(\boldsymbol{A}_{00}-\lambda_{00}\boldsymbol{B}_{00})\boldsymbol{E}_{20}=\lambda_{20}\boldsymbol{B}_{00}\boldsymbol{E}_{00}-(\boldsymbol{A}_{10}-\lambda_{00}\boldsymbol{B}_{10})\boldsymbol{E}_{10}-\\(\boldsymbol{A}_{20}-\lambda_{00}B_{20})\boldsymbol{E}_{00}+\lambda_{10}(\boldsymbol{B}_{00}\boldsymbol{E}_{10}+\boldsymbol{B}_{10}\boldsymbol{E}_{00})\end{aligned}$$

$$\vdots$$

$$\begin{aligned}(\boldsymbol{A}_{00}-\lambda_{00}\boldsymbol{B}_{00})\boldsymbol{E}_{M0}=\lambda_{M0}\boldsymbol{B}_{00}\boldsymbol{E}_{00}-\sum_{i=1}^{\min(2,M)}(\boldsymbol{A}_{i0}-\lambda_{00}\boldsymbol{B}_{i0})\boldsymbol{E}_{(M-i)0}+\\\sum_{i=1}^{M-1}\lambda_{i0}\cdot\sum_{j=0}^{\min(2,M-i)}\boldsymbol{B}_{j0}\boldsymbol{E}_{(M-i-j)0}\end{aligned}\tag{3.8}$$

Similarly, matching coefficients of corresponding powers of $(h-h_0)$ yields

$$(\boldsymbol{A}_{00}-\lambda_{00}\boldsymbol{B}_{00})\boldsymbol{E}_{01}=\lambda_{01}\boldsymbol{B}_{00}\boldsymbol{E}_{00}-(\boldsymbol{A}_{01}-\lambda_{00}\boldsymbol{B}_{01})\boldsymbol{E}_{00}$$

$$\begin{aligned}(\boldsymbol{A}_{00}-\lambda_{00}\boldsymbol{B}_{00})\boldsymbol{E}_{02}=\lambda_{02}\boldsymbol{B}_{00}\boldsymbol{E}_{00}-(\boldsymbol{A}_{01}-\lambda_{00}\boldsymbol{B}_{01})\boldsymbol{E}_{01}-\\(\boldsymbol{A}_{02}-\lambda_{00}B_{02})\boldsymbol{E}_{00}+\lambda_{01}(\boldsymbol{B}_{00}\boldsymbol{E}_{01}+\boldsymbol{B}_{01}\boldsymbol{E}_{00})\end{aligned}$$

$$\vdots$$

$$\begin{aligned}(\boldsymbol{A}_{00}-\lambda_{00}\boldsymbol{B}_{00})\boldsymbol{E}_{0N}=\lambda_{0N}\boldsymbol{B}_{00}\boldsymbol{E}_{00}-\sum_{i=1}^{\min(2,N)}(\boldsymbol{A}_{0i}-\lambda_{00}\boldsymbol{B}_{0i})\boldsymbol{E}_{0(N-i)}+\\\sum_{i=1}^{N-1}\lambda_{0i}\cdot\sum_{j=0}^{\min(2,N-i)}\boldsymbol{B}_{0j}\boldsymbol{E}_{0(N-i-j)}\end{aligned}\tag{3.9}$$

The cross-terms $(k-k_0)^M(h-h_0)^N$, are also computed by matching coefficients of

similar powers as

$$\sum_{i=0}^{M}\sum_{j=0}^{N}\boldsymbol{A}_{ij}\boldsymbol{E}_{M-i,N-j}=\sum_{i=0}^{M}\sum_{j=0}^{N}\lambda_{ij}\cdot\sum_{p=0}^{M-i}\sum_{q=0}^{N-j}\boldsymbol{B}_{pq}\boldsymbol{E}_{M-i-p,N-j-q}\qquad \text{for}\begin{cases}M\geq 1\\N\geq 1\end{cases}\qquad(3.10)$$

To obtain the Taylor series coefficients of (3.4)-(3.5) from (3.8)-(3.10), equation (3.1) must first be solved at k_0 and h_0 to obtain the eigenvalue λ_{00} and corresponding eigenvector $\boldsymbol{E}_{00}$. This can be done by using the Lanczos algorithm as reported in [28]-[30]. Since $\boldsymbol{E}_{00}$ is an eigenvector of (3.1), then the following relationship holds true $\boldsymbol{E}_{00}^{\mathrm{H}}(\boldsymbol{A}_{00}-\lambda_{00}\boldsymbol{B}_{00})=0$ [28]- [30], where the superscript *H* denotes the Hermitian of the matrix. Therefore, by multiplying the first equation of (3.8) and (3.9) by $\boldsymbol{E}_{00}^{\mathrm{H}}$ will make the left-hand side disappear and λ_{10} and λ_{01} can be found. With the knowledge of λ_{10} and λ_{01} the first equation of (3.8) and (3.9) can be used to find $\boldsymbol{E}_{10}$ and $\boldsymbol{E}_{01}$, respectively. This process is repeated recursively to find the higher order polynomial coefficients $\lambda_{i0}, \boldsymbol{E}_{i0}, \lambda_{0j}$ and $\boldsymbol{E}_{0j}$, where $i=[0,1,...,M]$ and $j=[0,1,...,N]$. To find the cross-terms λ_{ij} and $\boldsymbol{E}_{ij}$ using (3.10) a similar procedure is followed. The equations of (3.10) are arranged in a form similar to (3.8) and (3.9) where the left hand side is expressed as $(\boldsymbol{A}_{00}-\lambda_{00}\boldsymbol{B}_{00})\boldsymbol{E}_{ij}$ and the right hand side contains remaining terms. By multiplying (3.10) by $\boldsymbol{E}_{00}^{\mathrm{H}}$ will make the $\boldsymbol{E}_{ij}$ term disappear and the corresponding λ_{ij} can be determined. With the knowledge of λ_{ij}, equation (3.10) can be used to determine the corresponding eigenvector $\boldsymbol{E}_{ij}$. This process is repeated to find the higher order cross-terms.

Once all the required Taylor series coefficients with respect to *k* and *h* are evaluated,

the multidimensional subspace $\boldsymbol{K}$ is constructed as

$$\boldsymbol{K} = \left[\boldsymbol{M}^{k} \quad \boldsymbol{M}^{h} \quad \boldsymbol{M}^{X}\right] \tag{3.11}$$

where $\boldsymbol{M}^{k} = [\boldsymbol{E}_{00}, \boldsymbol{E}_{10}, ..., \boldsymbol{E}_{M0}]$ contains the series coefficients corresponding to powers of $(k - k_0)$, $\boldsymbol{M}^{h} = [\boldsymbol{E}_{01}, ..., \boldsymbol{E}_{0N}]$ contains the series coefficients corresponding to powers of $(h - h_0)$ and $\boldsymbol{M}^{X} = [\boldsymbol{E}_{11}, ..., \boldsymbol{E}_{ij}, ...]$ contains the cross-term coefficients. For the case when a reduced order model with multiple parameters is required, the multidimensional subspace $\boldsymbol{K}$ becomes

$$\boldsymbol{K} = \left[\boldsymbol{M}^{k} \quad \boldsymbol{M}^{h_1} ... \quad \boldsymbol{M}^{h_n} \quad \boldsymbol{M}^{X}\right] \tag{3.12}$$

where $\boldsymbol{M}^{h_i}$ contains the series coefficients corresponding to the self-terms of parameter h_i. Since the matrix $\boldsymbol{K}$ is generally ill-conditioned, it is converted into an orthonormal matrix $\boldsymbol{Q}$ using singular value decomposition as in [29]-[30]. The parametric reduced order model is obtained by a change of variables as

$$\boldsymbol{E}(k,\bar{h}) = \boldsymbol{Q}\hat{\boldsymbol{E}}(k,\bar{h}) \tag{3.13}$$

where $\hat{\boldsymbol{E}}(k,\bar{h}) \in \Re^{q}$; $q = q_k + \sum_{i=1}^{n} q_{h_i} + q_x$; q_k, q_{h_i} and q_x are the number of columns in $\boldsymbol{M}^{k}$, $\boldsymbol{M}^{h_i}$ and $\boldsymbol{M}^{X}$, respectively. Substituting (3.13) into (3.1) and pre-multiplying by $\boldsymbol{Q}^{H}$ yields

$$(\hat{\boldsymbol{A}}(k,\bar{h}) - \lambda(k,\bar{h})\hat{\boldsymbol{B}}(k,\bar{h})) \cdot \hat{\boldsymbol{E}}(k,\bar{h}) = 0 \tag{3.14}$$

where

$$\hat{\boldsymbol{A}}(k,\bar{h}) = \boldsymbol{Q}^H \boldsymbol{A}(k,\bar{h})\,\boldsymbol{Q}$$

$$\hat{\boldsymbol{B}}(k,\bar{h})\cdot = \boldsymbol{Q}^H \boldsymbol{B}(k,\bar{h})\,\boldsymbol{Q} \tag{3.15}$$

The size of the parameterized reduced order model depends on the order q which is very small compared to the size of the original system. Once the reduced system of (3.14) is obtained, it can be used to perform fast frequency sweeps of electromagnetic eigenvalue problems that are valid within a user defined range of design parameters and frequency.

3.3.3. Selecting the Order of the Reduced Order Model

The accuracy of the parameterized reduced order model can be verified by examining the residual error which is defined as [28]-[30],

$$\varepsilon = \frac{\left\|(\boldsymbol{A}(k,\bar{h}) - \lambda(k,\bar{h})\boldsymbol{B}(k,\bar{h}))\cdot \boldsymbol{E}(k,\bar{h})\right\|}{\left\|\boldsymbol{E}(k,\bar{h})\right\|} \tag{3.16}$$

where $\lambda(k,\bar{h})$ and $\boldsymbol{E}(k,\bar{h})$ are the approximate solutions given by (3.13). If the residual error ε is below a given tolerance for the specified ranges of design parameters and frequency, then the reduced order model is assumed to be accurate and the reduction process is terminated. Otherwise additional Taylor series coefficients or multiple expansion points can be used in (3.13) to improve the accuracy of the reduced order system.

3.4. Numerical Examples

In this section, numerical examples of a dielectric loaded rectangular waveguide and a microstrip line are presented. All computations are performed on a Pentium 4 (2.8GHz) PC with 2048 MB memory. The developed algorithm was programmed in MATLAB using *sptarn* function to solve the generalized eigenvalue problem [49].

3.4.1. Example I: Partially-Filled Rectangular Waveguide

A partially dielectric filled rectangular waveguide proposed in [29], is shown in Fig. 3.1a. The waveguide structure is discretized using Lagrange-quadratic elements [27] and the total number of degrees of freedom in the original system of (3.1) is equal to 1978. The bandwidth of interest for this problem ranges from normalized frequency $k_0 b$ =1.5 to 6. Two parameterized reduced order models are generated to study the dispersion curves of the waveguide. The first reduced system models the variation with respect to frequency *k* and the relative dielectric permittivity which ranges from ε_r =1.5 to 5. The second reduced system includes an additional design parameter which represents the boundary position of the dielectric medium and ranges from d=b to 1.3b (labeled in Fig. 3.1a).

To obtain the first parameterized reduced order model, the matrices $\boldsymbol{A}_i$ and $\boldsymbol{B}_i$ of

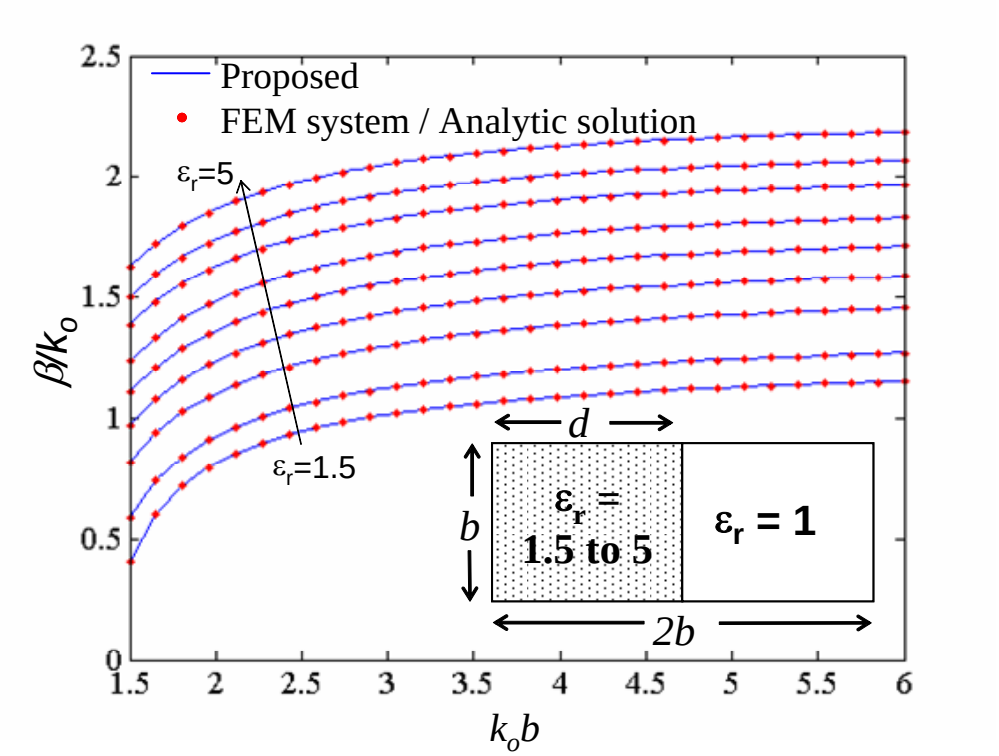

(a)

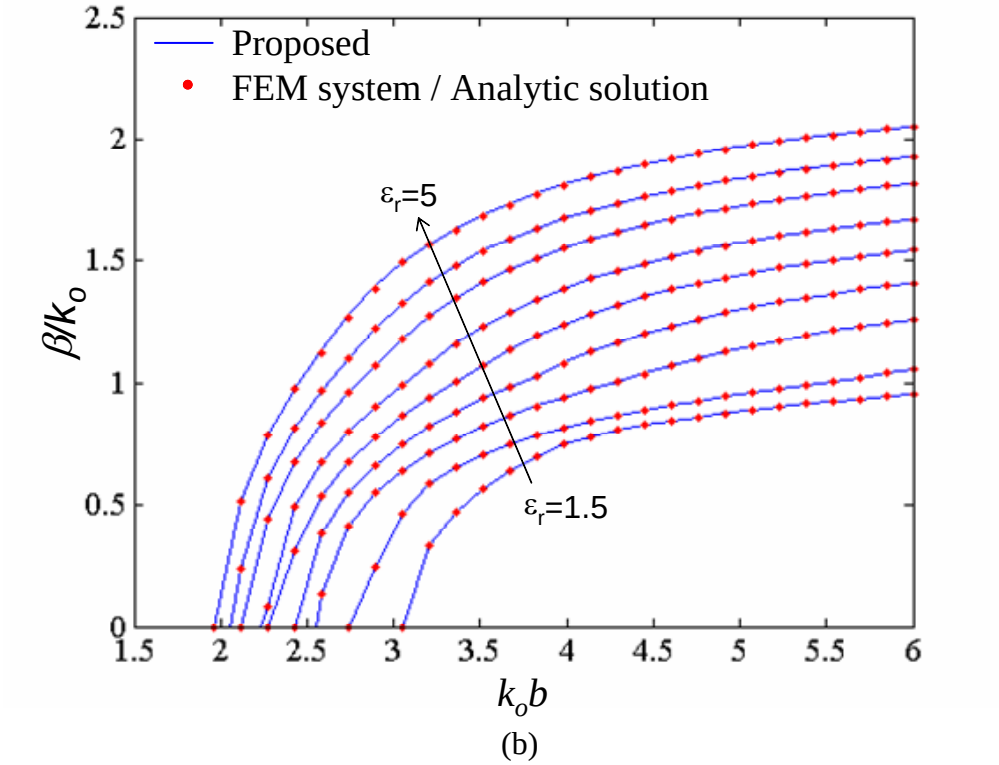

(b)

Fig. 3.1. Dielectric-loaded rectangular waveguide and the dispersion curves of the lowest four modes as ε_r ranges from 1.5 to 5 (a) mode 1 and physical geometry of waveguide (b) mode 4.

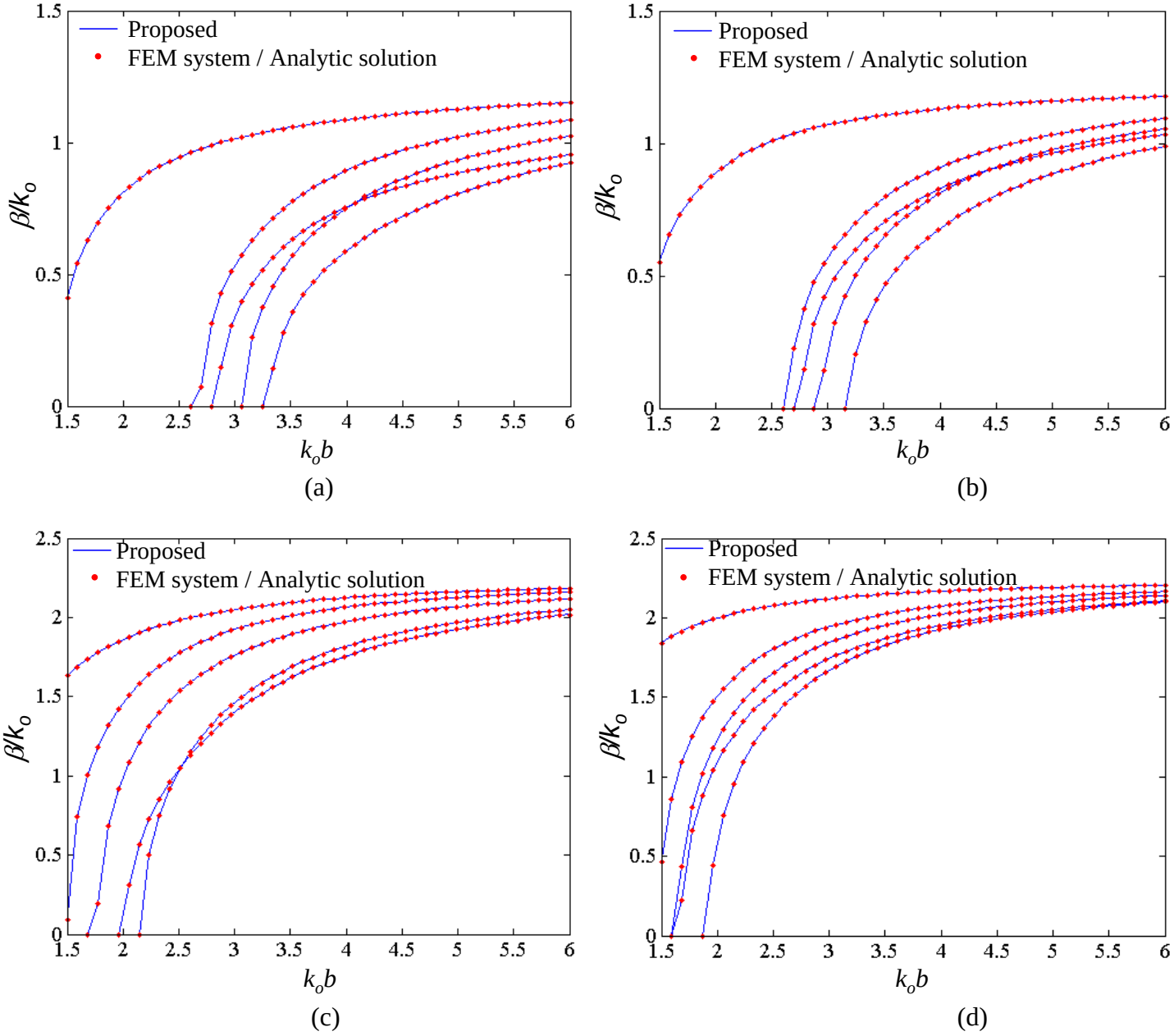

Fig. 3.2. Dispersion curves of the lowest five modes at the four extreme corners of parameter ranges for ε_r and d (a) At ε_r =1.5 and d=b (b) At ε_r =1.5 and d=1.3b (c) At ε_r =5 and d=b (d) At ε_r =5 and d=1.3b.

(3.6) where $i=[0,1,2]$ have a linear dependency with respect to ε_r and are expressed as

$$\boldsymbol{A}_i(\varepsilon_r,d)=\boldsymbol{A}_{i0}(d)+\varepsilon_r\boldsymbol{A}_{i1}(d)$$
$$\boldsymbol{B}_i(\varepsilon_r,d)=\boldsymbol{B}_{i0}(d)+\varepsilon_r\boldsymbol{B}_{i1}(d) \quad (3.17)$$

TABLE 3.1
COMPUTATIONAL INFORMATION – EXAMPLE I

Solution Method	Size	CPU Time to generate reduced system	Simulation Time	Savings in Size	Speed Up Factor
Original System*	1978	-	5 hrs and 46 min	-	-
Proposed*	32	108 sec	4 min and 2 sec	98%	86
Original System**	1978	-	57 hrs and 2 min		-
Proposed**	40	135 sec	50 min and 20 sec	97%	68

* 2500 simulations corresponding to 50 different frequency points and 50 different values of ε_r.
** 25000 simulations corresponding to 50 different frequency points, 50 different values of ε_r and 10 different values of *d*.

and the boundary position of the dielectric medium is set to *d*=*b*. To derive compact parametric reduced order models with residual error of less than $\varepsilon < 10^{-5}$ for the first four modes, two expansion points were selected at normalized frequency $k_0 b$=2 and ε_r =3.25 and at $k_0 b$=4.5 and ε_r =3.25. Each expansion point used 7 Taylor coefficients for *k*, 5 Taylor coefficients for ε_r and 4 cross-terms resulting in a reduced order system of size 32x32. Fig. 3.1 shows the dispersion curves for the first and forth modes as a function of normalized frequency and ε_r. Both the reduced order model and the analytical solution for this structure are in agreement. The accuracy of two different reduced order systems of size 32x32 and 8x8 is verified by checking the residual error of the dominant mode using (3.19). The simulations were performed at 50 different frequency points and 50 different ε_r values as described in Table I. The 32x32 model corresponds to the plots of Fig. 3.1 and has a maximum residual error of $4.5 \cdot 10^{-6}$, while the 8x8 model uses 2 Taylor coefficients for *k* and 1 Taylor coefficient for ε_r and 1 cross-term at the same expansion points and has a maximum residual error of 0.89.

To obtain a parameterized reduced order model that includes the boundary position variable *d*, the following procedure is followed based on a polynomial fitting approach.

1. At first, a number of evaluation points of the design parameter *d* were chosen. Here 10 test points (d_i , i = 1,….10) between $d=b$ and $1.3b$ are considered.
2. The matrices $\boldsymbol{A}_{i0}, \boldsymbol{A}_{i1}, \boldsymbol{B}_{i0}$, and $\boldsymbol{B}_{i1}$ of (3.20) depends on '*d*'. At each test point d_i, the matrices $\boldsymbol{A}_{i0}, \boldsymbol{A}_{i1}, \boldsymbol{B}_{i0}$, and $\boldsymbol{B}_{i1}$ are calculated. The crucial point in this technique is that the finite element mesh for all the test points is identical (i.e., they have the same number of degrees of freedom and their corresponding locations in the system matrices are same). For each of the test points, the mesh was adjusted in the areas close to where the geometry has been perturbed.
3. The elements of the matrices $\boldsymbol{A}_{i0}, \boldsymbol{A}_{i1}, \boldsymbol{B}_{i0}$, and $\boldsymbol{B}_{i1}$ which are affected by the mesh adjustments at each test point d_i, are then fitted to a low order polynomial. This example required a quadratic fit for the matrices since Lagrange-quadratic elements were used and are expressed as

$$\boldsymbol{A}_{i0}(d) = \boldsymbol{A}_{i00} + d\boldsymbol{A}_{i01} + d^2\boldsymbol{A}_{i02};$$

$$\boldsymbol{A}_{i1}(d) = \boldsymbol{A}_{i10} + d\boldsymbol{A}_{i11} + d^2\boldsymbol{A}_{i12};$$

$$\boldsymbol{B}_{i0}(d) = \boldsymbol{B}_{i00} + d\boldsymbol{B}_{i01} + d^2\boldsymbol{B}_{i02};$$

$$\boldsymbol{B}_{i1}(d) = \boldsymbol{B}_{i10} + d\boldsymbol{B}_{i11} + d^2\boldsymbol{B}_{i12}$$

4. In order to find an accurate fit for $\boldsymbol{A}_{i0}$, the least squares method is used to calculate the three coefficients $\boldsymbol{A}_{i00}, \boldsymbol{A}_{i01}$ and $\boldsymbol{A}_{i02}$ of the second order polynomial matching the 10 test points as

$$\begin{bmatrix} 1 & d_1 & d_1^2 \\ 1 & d_2 & d_2^2 \\ \vdots & \vdots & \vdots \\ 1 & d_{10} & d_{10}^2 \end{bmatrix} \begin{bmatrix} A_{i00}^{j,k} \\ A_{i01}^{j,k} \\ A_{i02}^{j,k} \end{bmatrix} = \begin{bmatrix} A_{i0}^{j,k} \big| d = d_1 \\ A_{i0}^{j,k} \big| d = d_2 \\ \vdots \\ A_{i0}^{j,k} \big| d = d_{10} \end{bmatrix}$$

where *j*, *k* denotes the element indices of the matrix. A similar procedure was used to fit the elements of matrices $\boldsymbol{A}_{i1}$, $\boldsymbol{B}_{i0}$, and $\boldsymbol{B}_{i1}$.

5. The parametric system is then expressed as in (3.9) and (3.10) and the technique proposed in section III is used to generate a parameterized reduced order system as a function of *k*, ε_r and *d*.

For this example, two expansion points were selected at normalized frequency $k_0 b$=2, ε_r=3.25 and d=1.15b and at $k_0 b$=4.5, ε_r=3.25 and d=1.15b to derive parametric reduced order models with residual error of less than $\varepsilon < 10^{-5}$. Each expansion point used 7 Taylor coefficients for *k*, 5 Taylor coefficients for ε_r, 3 Taylor coefficients for *d* and 5 cross-terms resulting in a reduced order system of size 40x40. Fig. 3.2 shows the dispersion curves of the first five modes as a function of normalized frequency at the four extreme corners of parameter ranges for ε_r and *d*. Table 3.1 compares the total size, CPU times to generate the parametric reduced order models and simulation times. A speed up of 68 to 86 was achieved using the proposed approach when compared to the original simulation time.

3.4.2. Example II: Microstrip Line

A shielded microstrip transmission line with perfect conductors on an isotropic lossless substrate proposed in [30] is shown in Fig. 3.3a. The structure is discretized

using Lagrange-quadratic elements [27] and the total number of degrees of freedom in the original system of (3.2) is equal to 10359. The proposed parameterized model order reduction technique is used to model variations with respect to frequency, relative permittivity ε_r, and the conductor width *w*. The bandwidth of interest is from 1GHz to 15GHz, the relative permittivity ranges from ε_r =5 to 10 and the conductor width ranges from *w* =1.27 mm to 1.65 mm. To include the parameter variation of the conductor width *w*, the polynomial fitting approach is used following the procedure similar to Example I. The expansion point for frequency and the design parameters is chosen to be in the middle of the range of interest. Applying the proposed algorithm with 10 Taylor coefficients for *k*, 7 Taylor coefficients for ε_r, 4 Taylor coefficients for *w*, and 4 cross-terms, the dispersion curves for the first two modes can be obtained. Fig. 3.3 shows the dispersion curves as a function of frequency at the four extreme corners of parameter ranges for ε_r and *w*. The reduced order model obtained using the proposed approach shows good agreement with the results of the original FEM model.

To study the dispersion curves of higher order modes, the same structure is also analyzed from 15 GHz to 20GHz, while the parameter range for ε_r and *w* are kept the same. Once again, the expansion point for frequency and the design parameters are chosen to be in the middle of the range of interest. For this example, the reduced order model used 10 Taylor coefficients for *k*, 7 Taylor coefficients for ε_r, 4 Taylor coefficients for *w*, and 4 cross-terms. Fig. 3.4 shows the dispersion curves as a function of frequency at the four extreme corners of parameter ranges for ε_r and *w*. In Fig. 3.4c the dispersion curves of modes eight and nine degenerate and merge into complex conjugate modes.

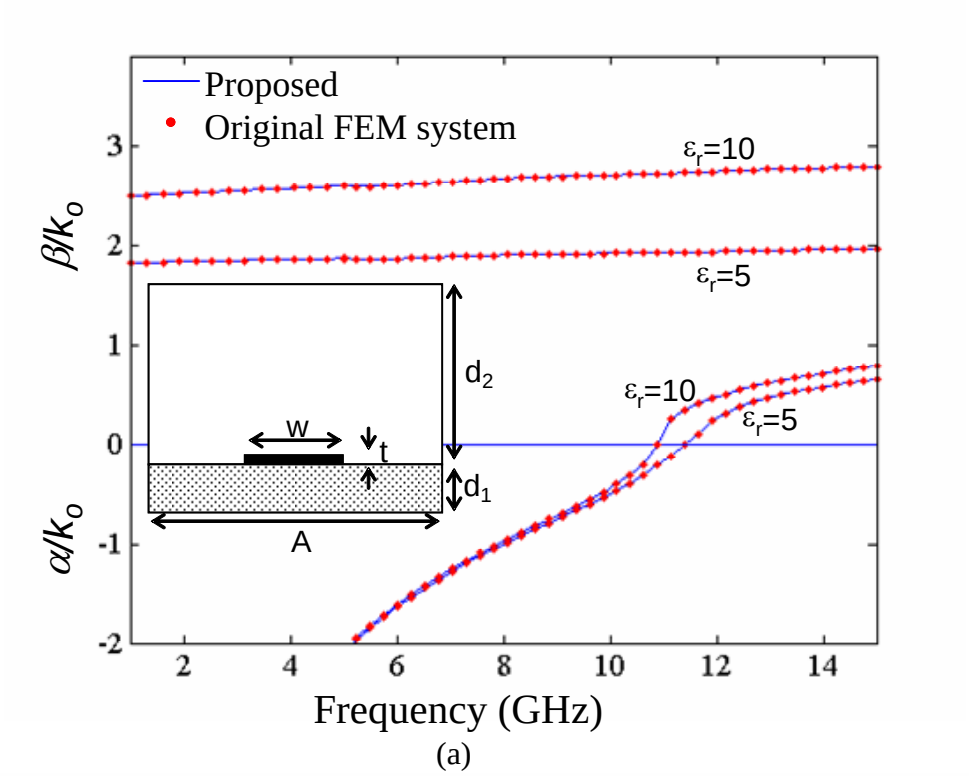

(a)

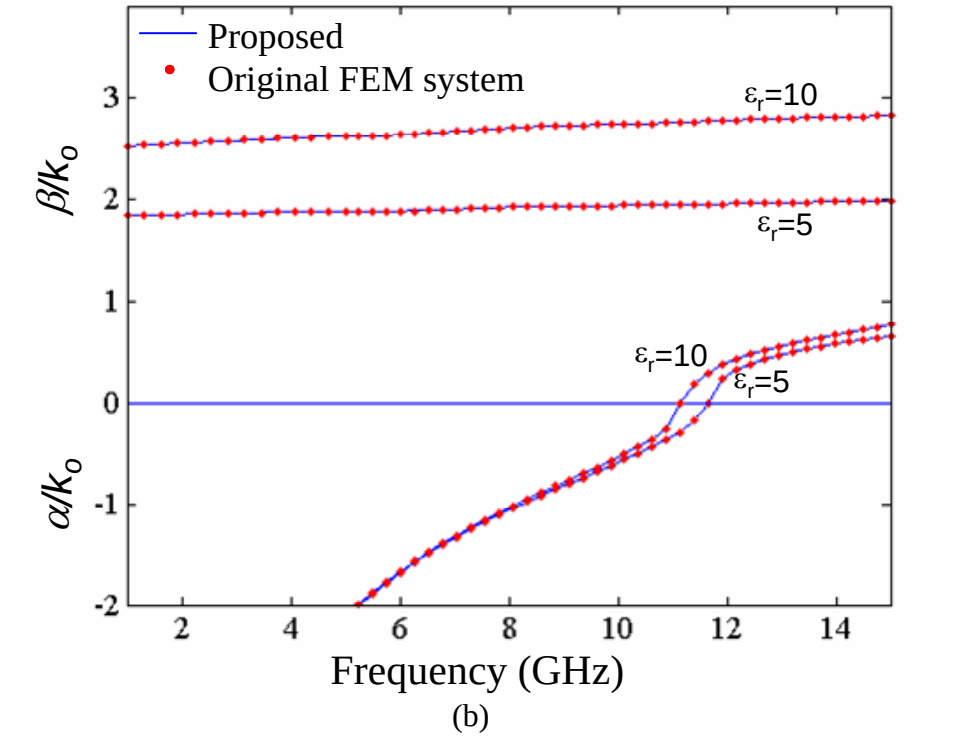

(b)

Fig. 3.3. Lossless microstrip line and the dispersion curves of the first two modes at the four extreme corners of parameter ranges for ε_r and w (a) At w=1.27 mm for ε_r =5 and ε_r =10, (b) At w=1.65 mm for ε_r =5 and ε_r =10. In all cases A=12.7 mm, d_1=1.27 mm, d_2=11.43 mm and t=0.127 mm.

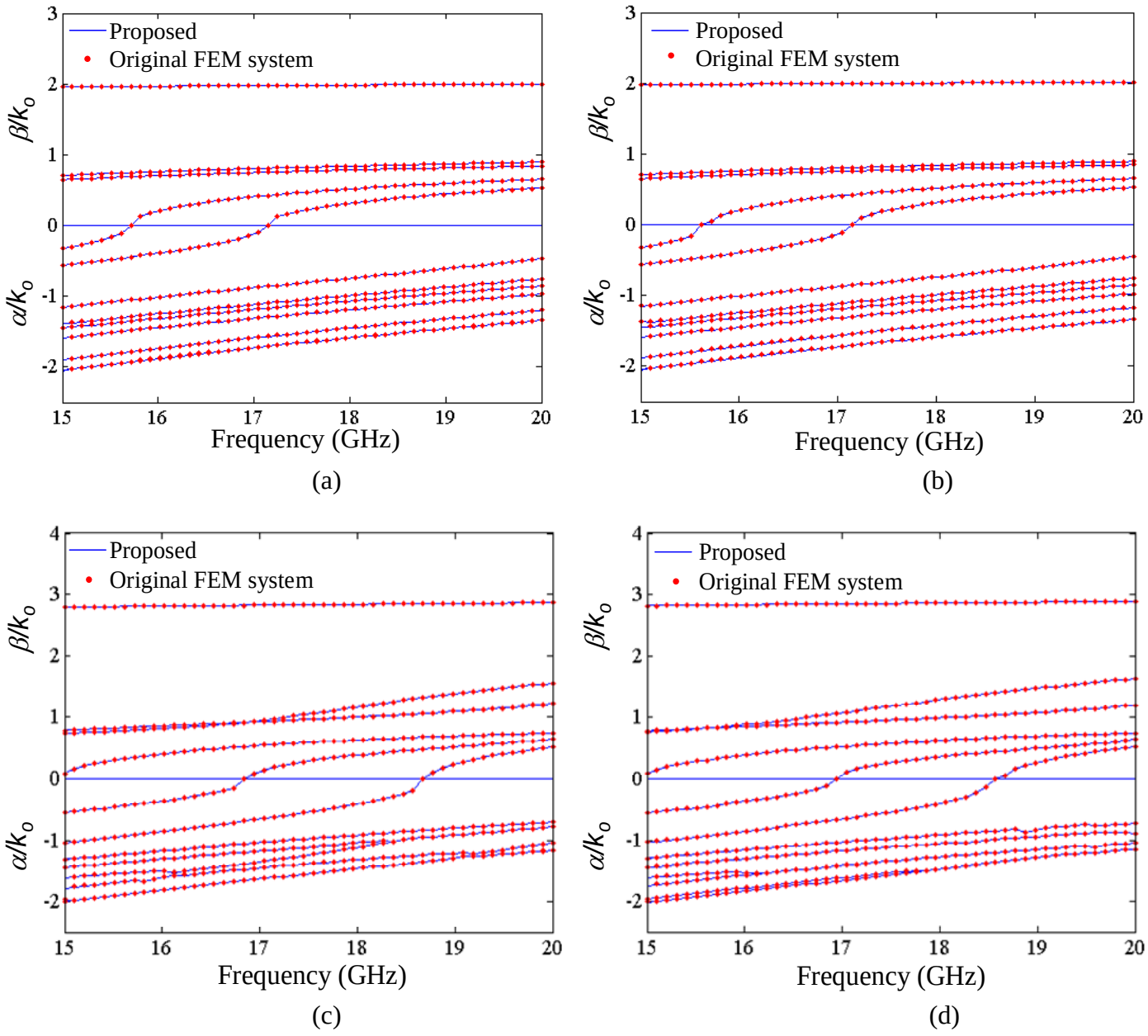

Fig. 3.4. Dispersion curves of the lowest twelve modes at the four extreme corners of parameter ranges for ε_r and w (a) At ε_r =5 and w=1.27 mm (b) At ε_r =5 and w=1.65 mm (c) At ε_r =10 and w=1.27 mm (d) At ε_r =10 and w=1.65 mm.

Similarly, in Fig. 3.4d the dispersion curve of modes nine and ten as well as eleven and twelve also degenerate and merge into complex conjugate modes. This phenomenon is accurately described by the reduced order model, illustrating the accuracy of the proposed

method over broad ranges of frequency and design parameter variations. Table 3.2 compares the total size, CPU times to generate the parametric reduced order models and simulation times. For this example a speed up of 95 to 137 was achieved.

TABLE 3.2
COMPUTATIONAL INFORMATION – EXAMPLE II

Solution Method	Size	CPU Time to generate reduced system	Simulation Time	Savings in Size	Speed Up Factor
Original System (1-15GHz)	10359	-	22 hrs and 51 min.	-	-
Proposed (1-15GHz)	25	308 sec	10 min and 2 sec	99.75%	137
Original System (15-20GHz)	10359	-	27 hrs and 23 min.	-	-
Proposed (15-20GHz)	25	317 sec	17 min and 23 sec	99.75%	95

375 simulations corresponding to 15 different frequency points, 5 different values of ε_r and 5 different values of *w*.

Chapter 4

4. Parameterized Model Order Reduction of Electromagnetic Systems using Multi-Order Arnoldi

4.1. Introduction

In this chapter, a parameterized MOR technique is developed for distributed electromagnetic systems that have arbitrary functions of frequency due to material properties, boundary conditions and delay elements. The proposed algorithm directly differentiates the network equations and uses multi-order Arnoldi method to calculate the moments, without having to perform rational curve fitting or introduce separate variables to approximate the arbitrary functions of frequency. The developed algorithm is also extended to implicitly calculate the moments with respect to arbitrary function design parameters as well as the cross-moments. This procedure results in a parameterized reduced order model that is valid over a user defined range of design parameters while preserving the form of the original system. Numerical examples are provided to illustrate the validity of the proposed technique.

This chapter is organized as follows. Section 4.2 describes the proposed parameterized multi-order Arnoldi model reduction technique. Numerical examples are provided in section 4.3.

4.2. Parameterized Multi-Order Arnoldi for Systems with Arbitrary Functions

4.2.1. Computation of Reduced Order Model

For the case of scattering problems, applying Galerkin's procedure to the vector wave equation of (2.1) yields a linear sparse algebraic system of (2.20). To derive a parametric reduced order model for (2.20), the system is expressed as a function of the frequency and other design parameters as

$$\boldsymbol{Y}(s,\bar{h})\cdot\boldsymbol{X}(s,\bar{h})=\boldsymbol{b}(s,\bar{h}) \tag{4.1}$$

where $\boldsymbol{Y}(s,\bar{h})\in C^{\varphi\times\varphi}$ is the transfer function of the system; $\boldsymbol{X}(s,\bar{h})\in C^{\varphi}$ is the vector of unknown variables; $\boldsymbol{b}(s,\bar{h})\in C^{\varphi}$ represents the excitation of the network; $\bar{h}=[h_1,h_2,\ldots,h_n]$ are the design parameters of interest; and φ is the number of unknown variables in $\boldsymbol{X}(s,\bar{h})$. It is assumed that the system of (4.1) has arbitrary functions of frequency due to material properties, boundary conditions and delay elements, as well as arbitrary functions of design parameters, which makes the calculation of the moments using traditional Arnoldi methods a challenging task. In this section, a multi-order Arnoldi method is described to accurately calculate the moments of reduced order models for arbitrary functions of frequency and design parameters.

The computation of the parameterized reduced order model expands (4.1) into a multidimensional Taylor series with respect to frequency and design parameters $\bar{h}$. For ease of presentation and without loss of generality, the method is described for the case when there is only one design parameter of interest $\bar{h}=[h]$. The computation of the

parameterized reduced order model begins with the evaluation of the multidimensional subspace. This is accomplished by calculating the moments of $\boldsymbol{X}(s,h)$ with respect to frequency s and design parameter h as well as the cross moments. The moments of $\boldsymbol{X}(s,h)$ are computed by expanding $\boldsymbol{Y}(s,h)$ and $\boldsymbol{b}(s,h)$ into a multi-dimensional Taylor series as

$$\begin{aligned}\boldsymbol{Y}(s,h)\big|_{s_0,h_0} = &\sum_{i=0}^{n}\frac{1}{i!}\frac{\partial^i}{\partial s^i}\boldsymbol{Y}(s,h)\bigg|_{s_0,h_0}(s-s_0)^i + \\ &\sum_{i=1}^{m}\frac{1}{i!}\frac{\partial^i}{\partial h^i}\boldsymbol{Y}(s,h)\bigg|_{s_0,\lambda_0}(h-h_0)^i + \\ &\sum_{i=1}\sum_{j=1}\frac{1}{i!\,j!}\frac{\partial^i\partial^j}{\partial s^i\partial h^j}\boldsymbol{Y}(s,h)\bigg|_{s_0,\lambda_0}(s-s_0)^i(h-h_0)^j\end{aligned} \tag{4.2}$$

$$\begin{aligned}\boldsymbol{b}(s,h)\big|_{s_0,h_0} = &\sum_{i=0}^{n}\frac{1}{i!}\frac{\partial^i}{\partial s^i}\boldsymbol{b}(s,h)\bigg|_{s_0,\lambda_0}(s-s_0)^i + \\ &\sum_{i=1}^{m}\frac{1}{i!}\frac{\partial^i}{\partial h^i}\boldsymbol{b}(s,h)\bigg|_{s_0,\lambda_0}(h-h_0)^i + \\ &\sum_{i=1}\sum_{j=1}\frac{1}{i!\,j!}\frac{\partial^i\partial^j}{\partial s^i\partial h^j}\boldsymbol{b}(s,h)\bigg|_{s_0,\lambda_0}(s-s_0)^i(h-h_0)^j\end{aligned} \tag{4.3}$$

where s_o and h_o are the expansion points of the Taylor series. The first and second summation terms of (4.2) correspond to the self-terms with respect to s and h respectively, and the double summation term of (4.2) corresponds to the cross terms. Assuming that the transfer function $\boldsymbol{Y}(s,h)$ and forcing function $\boldsymbol{b}(\mathrm{s},h)$ are known and differentiable, the Taylor series coefficients of (4.2) and (4.3) can be determined by differentiating $\boldsymbol{Y}(s,h)$ and $\boldsymbol{b}(\mathrm{s},h)$ with respect to s and h. Similarly, $\boldsymbol{X}(s,h)$ is also expanded into a multidimensional power series as

$$\boldsymbol{X}(s,h) = \sum_{i=0}^{n} \boldsymbol{M}_{i0}^{s} (s - s_0)^i + \sum_{i=1}^{m} \boldsymbol{M}_{0i}^{h} (h - h_0)^i + \sum_{i=1}\sum_{j=1} \boldsymbol{M}_{ij}^{sh} (s - s_0)^i (h - h_0)^j \tag{4.4}$$

Substituting (4.2)-(4.4) into (4.1) and matching coefficients of corresponding powers of s yields the following recursive relationship:

$$\boldsymbol{Y}(s_0, h_0) \cdot \boldsymbol{M}_{00}^{s} = \boldsymbol{b}(s_0, h_0)$$

$$\vdots$$

$$\boldsymbol{Y}(s_0, h_0) \cdot \boldsymbol{M}_{i0}^{s} = -\left(\sum_{j=1}^{i} \frac{1}{j!} \frac{\partial^j}{\partial s^j} \boldsymbol{Y}(s,h)\Big|_{s_0,h_0} \cdot \boldsymbol{M}_{i-j,0}^{s} \right) + \frac{\partial^i}{\partial s^i} \boldsymbol{b}(s,h)\Big|_{s_0,h_0} \tag{4.5}$$

Similarly, matching coefficients of corresponding powers of h, yields

$$\boldsymbol{Y}(s_0, h_0) \cdot \boldsymbol{M}_{0i}^{h} = -\left(\sum_{j=1}^{i} \frac{1}{j!} \frac{\partial^j}{\partial h^j} \boldsymbol{Y}(s,h)\Big|_{s_0,h_0} \cdot \boldsymbol{M}_{i-j,0}^{h} \right) + \frac{\partial^i}{\partial h^i} \boldsymbol{b}(s,h)\Big|_{s_0,h_0} \tag{4.6}$$

The cross-moments of $(s - s_0)^i (h - h_0)^j$ are also computed by matching coefficients of similar powers as

$$\boldsymbol{Y}(s_0, h_0) \boldsymbol{M}_{ij}^{sh} = -\left(\sum_{p=0}^{i}\sum_{q=0}^{j} \frac{1}{p!q!} \frac{\partial^p}{\partial s^p} \frac{\partial^q}{\partial h^q} \boldsymbol{Y}(s,h)\Big|_{s_0,h_0} \cdot \boldsymbol{M}_{i-p,j-q}^{sh} \right) + \frac{\partial^i}{\partial s^i} \frac{\partial^j}{\partial h^j} \boldsymbol{b}(s,h)\Big|_{s_0,h_0} \tag{4.7}$$

Once all the required moments with respect to s and h are evaluated, the multidimensional subspace $\boldsymbol{K}$ is constructed as

$$\boldsymbol{K} = colsp\left(\begin{bmatrix} \boldsymbol{M}^{s} & \boldsymbol{M}^{h} & \boldsymbol{M}^{X} \end{bmatrix} \right) \tag{4.8}$$

where $\boldsymbol{M}^{s} = [\boldsymbol{M}_{00}^{s}, \boldsymbol{M}_{10}^{s}, \ldots, \boldsymbol{M}_{n0}^{s}]$ contains the series coefficients corresponding to powers of $(s - s_0)^i$, $\boldsymbol{M}^{h} = [\boldsymbol{M}_{01}^{h}, \boldsymbol{M}_{02}^{h}, \ldots, \boldsymbol{M}_{0m}^{h}]$ contains the series coefficients corresponding to powers of $(h - h_0)^i$ and $\boldsymbol{M}^{X} = [\boldsymbol{M}_{11}^{sh}, \ldots, \boldsymbol{M}_{ij}^{sh}, \ldots]$ contains the cross-term coefficients. The main computational complexity to calculate the moments of the reduced order system using (4.5)-(4.7), requires solving the original network at s_o and h_o (i.e. inverting $\boldsymbol{Y}(s_0, h_0)$). Hence the calculation of the first moment requires one lower-upper decomposition and one forward-backward substitution, while each additional moment requires only one forward-backward substitution [43]-[44]. Since the major cost of solving the original network is the lower-upper decompositions at different frequencies and design parameters, moment matching techniques yield very high speed advantage due to the fact that only one lower-upper decomposition is required for each expansion point to create the model. Furthermore, the size of the reduced order system is usually significantly smaller and hence less computationally expensive than the original system.

For the case when a reduced order model with multiple parameters is required, the multidimensional subspace $\boldsymbol{K}$ becomes

$$\boldsymbol{K} = colsp\left(\begin{bmatrix} \boldsymbol{M}^{h_0} & \boldsymbol{M}^{h_1} & \cdots & \boldsymbol{M}^{h_N} & \boldsymbol{M}^{X} \end{bmatrix}\right) \tag{4.9}$$

where $\boldsymbol{M}^{h_0}$ may correspond to the Laplace frequency moments similar to (4.8) and $\boldsymbol{M}^{h_i}$ are the self-term moment matrices corresponding to parameter h_i. Since the matrix $\boldsymbol{K}$ is generally ill-conditioned, Arnoldi methods are usually used to convert (4.8) and (4.9) into an orthonormal matrix $\boldsymbol{Q}$ [43]. However, the original Arnoldi algorithm is only applicable for systems that have linear dependency with respect to frequency (i.e. $\boldsymbol{Y} = \boldsymbol{G} + s\boldsymbol{C}$) [44].

Since the network of (4.1) is assumed to exhibit arbitrary functions of frequency and design parameters, the traditional Arnoldi algorithm is not directly applicable. To address this issue, a multi-order Arnoldi algorithm is described to create parameterized reduced order models for arbitrary functions of frequency and design parameters by implicitly calculating the orthonormal subspace derived from the self-moments and cross-moments.

The description of the proposed multi-order Arnoldi algorithm for the two parameter case is provided in Fig. 4.1, where

$$\boldsymbol{A}_{i0}^{s} = -\left(\boldsymbol{Y}(s_0, h_0)\right)^{-1} \frac{1}{i!} \frac{\partial^i}{\partial s^i} \boldsymbol{Y}(s,h)\Big|_{s_0,h_0} \tag{4.10}$$

$$\boldsymbol{A}_{0i}^{h} = -\left(\boldsymbol{Y}(s_0, h_0)\right)^{-1} \frac{1}{i!} \frac{\partial^i}{\partial h^i} \boldsymbol{Y}(s,h)\Big|_{s_0,h_0} \tag{4.11}$$

$$\boldsymbol{A}_{ij}^{sh} = -\left(\boldsymbol{Y}(s_0, h_0)\right)^{-1} \frac{1}{i!\,j!} \frac{\partial^i \partial^j}{\partial s^i \partial h^j} \boldsymbol{Y}(s,h)\Big|_{s_0,h_0} \tag{4.12}$$

$$\boldsymbol{B}_{i}^{s} = \left(\boldsymbol{Y}(s_0, h_0)\right)^{-1} \frac{\partial^i}{\partial s^i} \boldsymbol{b}(s,h)\Big|_{s_0,h_0} \tag{4.13}$$

$$\boldsymbol{B}_{i}^{h} = \left(\boldsymbol{Y}(s_0, h_0)\right)^{-1} \frac{\partial^i}{\partial h^i} \boldsymbol{b}(s,h)\Big|_{s_0,h_0} \tag{4.14}$$

$$\boldsymbol{B}_{ij}^{sh} = \left(\boldsymbol{Y}(s_0, h_0)\right)^{-1} \frac{\partial^i \partial^j}{\partial s^i \partial h^j} \boldsymbol{b}(s,h)\Big|_{s_0,h_0} \tag{4.15}$$

and n_s^c and n_h^c determine the number of cross-moments with respect to s and h respectively, for the reduced order system. The multi-order Arnoldi algorithm described

MULTI-ORDER ARNOLDI $\left(\boldsymbol{Y}(s,\lambda), n_s, n_\lambda, n_s^c, n_\lambda^c\right)$

$\boldsymbol{Q}^{Total} \leftarrow \phi$ *// Initialize* $\boldsymbol{Q}^{Total}$ *to an empty set*

$\boldsymbol{q}_{00} = \boldsymbol{M}_{00} / \|\boldsymbol{M}_{00}\|$

for $i_s^c \leftarrow 0$ to n_s^c

  for $i_\lambda^c \leftarrow 0$ to n_λ^c

    if ($i_s^c \neq 0$ or $i_\lambda^c \neq 0$)

$$\boldsymbol{z} = \sum_{i_1}^{i_s^c} \sum_{i_0}^{i_\lambda^c} \boldsymbol{A}_{i_1,i_0} \boldsymbol{q}_{i_s^c - i_1, i_\lambda^c - i_0} + \boldsymbol{B}_{ij}$$

      for $i_1 \leftarrow 0$ to i_s^c

        for $i_0 \leftarrow 0$ to i_λ^c

          if $(i_1 < i_s^c)\,\&\,(i_0 < i_\lambda^c)$

$\boldsymbol{h} = (\boldsymbol{q}_{i_1,i_0})^T \boldsymbol{z}$

$\boldsymbol{z} = \boldsymbol{z} - \boldsymbol{h}\boldsymbol{q}_{i_1,i_0}$

          end if

        end for

      end for

$\boldsymbol{q}_{i_1,i_0} \leftarrow orthogonalize(\boldsymbol{z})$ //Orthogonalization Process//

    end if

  end for

end for

$\boldsymbol{Q}^{Total} = [\boldsymbol{Q}^{Total}\ \boldsymbol{q}_{i_1,i_0}]$

for $i \leftarrow n_s^c + 1$ to n_s

⋮

⋮

$$\boldsymbol{z} = \sum_{j=1}^{j=i} \boldsymbol{A}_{j0} \boldsymbol{q}_{(i-j)0} + \boldsymbol{B}_i$$

  for $j \leftarrow 0$ to $i-1$

$\boldsymbol{h} = (\boldsymbol{q}_{j0})^T \boldsymbol{z}$

$\boldsymbol{z} = \boldsymbol{z} - \boldsymbol{h}\boldsymbol{q}_{j0}$

  end for

$\boldsymbol{q}_{i0} \leftarrow orthonormalize(\boldsymbol{z})$

end for

$\boldsymbol{Q}^s = [\boldsymbol{q}_{00}, \boldsymbol{q}_{10}, \ldots, \boldsymbol{q}_{n_s 0}]$

$\boldsymbol{Q}^{Total} = [\boldsymbol{Q}^{Total}\ \boldsymbol{Q}^s]$

for $i \leftarrow n_\lambda^c + 1$ to n_λ

$$\boldsymbol{z} = \sum_{j=1}^{j=i} \boldsymbol{A}_{0j} \boldsymbol{q}_{0(i-j)} + \boldsymbol{B}_i$$

  for $j \leftarrow 0$ to $i-1$

$\boldsymbol{h} = (\boldsymbol{q}_{0j})^T \boldsymbol{z}$

$\boldsymbol{z} = \boldsymbol{z} - \boldsymbol{h}\boldsymbol{q}_{0j}$

  end for

$\boldsymbol{q}_{0i} \leftarrow orthonormalize(\boldsymbol{z})$

end for

$\boldsymbol{Q}^\lambda = [\boldsymbol{q}_{00}, \boldsymbol{q}_{01}, \ldots, \boldsymbol{q}_{0 n_\lambda}]$

$\boldsymbol{Q}^{Total} = [\boldsymbol{Q}^{Total}\ \boldsymbol{Q}^\lambda]$

return($\boldsymbol{Q}^{Total}$)

Fig.4.1. Multi-Order Block Arnoldi Procedure including self-terms; with respect to frequency *s*, the design parameter λ and the cross-terms

in Fig. 4.1 is similar to the algorithm described in [56]-[57], except in this work it is extended to include design parameter variations of arbitrary functions, as well as to implicitly calculate the cross-moments.

The extension of the proposed algorithm to multiple parameters is also provided in Fig. 4.2, where

MULTI-ORDER ARNOLDI

$\left(\boldsymbol{Y}(\lambda_N,\ldots,\lambda_1,\lambda_0), n_{\lambda_N},\ldots,n_{\lambda_1},n_{\lambda_0},n^c_{\lambda_N},\ldots,n^c_{\lambda_1},n^c_{\lambda_0}\right)$

$\boldsymbol{Q}^{Total} \leftarrow \phi$ *// Initialize* $\boldsymbol{Q}^{Total}$ *to an empty set*

$\boldsymbol{q}_{0\cdots 0} = \boldsymbol{M}_{0\cdots 0} / \left\|\boldsymbol{M}_{0\cdots 0}\right\|$

for $i^c_{\lambda_N} \leftarrow 0$ to $n^c_{\lambda_N}$

$\ddots$

for $i^c_{\lambda_0} \leftarrow 0$ to $n^c_{\lambda_0}$

if (more than one $i^c_{\lambda_k}$'s are $\neq 0$)

$$\boldsymbol{z} = \sum_{i_N}^{i^c_{\lambda_N}} \sum_{i_{N-1}}^{i^c_{\lambda_{N-1}}} \cdots \sum_{i_1}^{i^c_{\lambda_1}} \sum_{i_0}^{i^c_{\lambda_0}} \boldsymbol{A}_{i_N,i_{N-1},\ldots,i_0} \boldsymbol{q}_{i^c_{\lambda_N}-i_N, i^c_{\lambda_{N-1}}-i_{N-1},\ldots,i^c_{\lambda_0}-i_0} + \boldsymbol{B}_{i_N,i_{N-1},\ldots,i_0}$$

for $i_N \leftarrow 0$ to $i^c_{\lambda_N}$

$\ddots$

for $i_0 \leftarrow 0$ to $i^c_{\lambda_0}$

if $(i_N < i^c_{\lambda_N}) \,\&\, (i_{N-1} < i^c_{\lambda_{N-1}}) \,\&\, \cdots \,\&\, (i_0 < i^c_s)$

$\boldsymbol{h} = (\boldsymbol{q}_{i_N,i_{N-1},\ldots,i_0})^T \boldsymbol{z}$

$\boldsymbol{z} = \boldsymbol{z} - \boldsymbol{h}\boldsymbol{q}_{i_N,i_{N-1},\ldots,i_0}$

end if

end for

$\ddots$

end for

$\vdots$

$\boldsymbol{q}_{i_N,i_{N-1},\ldots,i_0} \leftarrow orthogonalize(\boldsymbol{z})$

end if

end for

$\ddots$

end for

$\boldsymbol{Q}^{Total} = [\boldsymbol{Q}^{Total}\ \boldsymbol{q}_{i_N,i_{N-1},\ldots,i_0}]$

for $k \leftarrow 1$ to N

for $i \leftarrow n^c_{\lambda_k} + 1$ to n_{λ_k}

$$\boldsymbol{z} = \sum_{j=1}^{j=i} \boldsymbol{A}^{\lambda_k}_j \boldsymbol{q}^{\lambda_k}_{0\cdots(i-j)_k\cdots 0} + \boldsymbol{B}_i$$

for $j \leftarrow 0$ to $i-1$

$\boldsymbol{h} = (\boldsymbol{q}^{\lambda_k}_{0\cdots j_k\cdots 0})^T \boldsymbol{z}$

$\boldsymbol{z} = \boldsymbol{z} - \boldsymbol{h}\boldsymbol{q}^{\lambda_k}_{0\cdots j_k\cdots 0}$

end for

$\boldsymbol{q}^{\lambda}_{0\cdots i_k\cdots 0} \leftarrow orthogonalize(\boldsymbol{z})$

end for

$\boldsymbol{Q}^{\lambda_k} = [\boldsymbol{q}^{\lambda_k}_{0\cdots I_k\cdots 0}, \boldsymbol{q}^{\lambda_k}_2, \ldots, \boldsymbol{q}^{\lambda_k}_{n_{\lambda_k}}]$

$\boldsymbol{Q}^{Total} = [\boldsymbol{Q}^{Total}\ \boldsymbol{Q}^{\lambda_k}]$

end for

return($\boldsymbol{Q}^{Total}$)

Fig 4.2. Multi-Order Block Arnoldi Procedure including self-terms; with respect to design parameters $\lambda_N,\ldots,\lambda_0$ and the cross-terms.

$$\boldsymbol{A}_{i_N,\ldots,i_0} = -\left(\boldsymbol{Y}(h_{N_0},\ldots,h_{0_0})\right)^{-1} \frac{1}{i_N!} \cdots \frac{1}{i_0!} \frac{\partial^{i_N}}{\partial h_N^{i_N}} \cdots \frac{\partial^{i_0}}{\partial h_0^{i_0}} \boldsymbol{Y}(h_N,\ldots,h_N)\Big|_{h_{N_0},\ldots,h_{0_0}} \tag{4.16}$$

$$\boldsymbol{B}_{i_N,\ldots,i_0} = \left(\boldsymbol{Y}(h_{N_0},\ldots,h_{0_0})\right)^{-1} \frac{\partial^{i_N}}{\partial h_N^{i_N}} \cdots \frac{\partial^{i_0}}{\partial h_0^{i_0}} \boldsymbol{b}(h_N,\ldots,h_N)\Big|_{h_{N_0},\ldots,h_{0_0}} \tag{4.17}$$

The values $h_{N_0},...,h_{0_0}$ are the expansion points of the Taylor series and $n_{h_i}^c$ determines the number of cross-moments with respect to i^{th} parameter h_i for the reduced order system. Using the procedure of Fig. 4.1 or Fig. 4.2 to calculate $\boldsymbol{Q}$ will result in a more accurate reduced order model when compared to directly converting (4.8) and (4.9) to an orthonormal matrix, since implicitly calculating the moments leads to fewer numerical difficulties in the inclusion of higher order moments. This is due to the fact that the higher order moments of (4.8) and (4.9) converge to the largest eigenvalue of the system and are almost identical or parallel to each other causing the matrix $\boldsymbol{K}$ to be ill-conditioned [43], [71].

Using the orthonormal matrix $\boldsymbol{Q}$ derived from Fig. 4.1 or Fig. 4.2, the parametric reduced order model is obtained by a change of variables as

$$\boldsymbol{X}(s,\overline{h}) = \boldsymbol{Q}\hat{\boldsymbol{X}}(s,\overline{h}) \tag{4.18}$$

where $\hat{\boldsymbol{X}}(s,\overline{h}) \in C^q$ and q corresponds to the number of columns in the orthonormal moment matrix $\boldsymbol{Q}$. Substituting (4.18) into (4.4) and pre-multiplying by $\boldsymbol{Q}^T$ yields

$$\hat{\boldsymbol{Y}}(s,\overline{h}) \cdot \hat{\boldsymbol{X}}(s,\overline{h}) = \hat{\boldsymbol{b}}(\mathrm{s}) \tag{4.19}$$

where

$$\hat{\boldsymbol{Y}}(s,\overline{h}) = \boldsymbol{Q}^T\boldsymbol{Y}(s,\overline{h})\boldsymbol{Q} \tag{4.20}$$

$$\hat{\boldsymbol{b}}(\mathrm{s}) = \boldsymbol{Q}^{\mathrm{T}}\boldsymbol{b}(\mathrm{s}) \tag{4.21}$$

and the size of the reduced order matrices are $\hat{\boldsymbol{Y}}(s,\overline{h}) \in C^{q\times q}$; $\hat{\boldsymbol{b}}(s,\overline{h}) \in C^q$. It can be

shown that the reduced system of (4.19) preserves the moments of the original system as presented in [23], [56] and [60].

Note that the size of the reduced order model depends on the number of columns in $\boldsymbol{Q}$. As the variance of the parameters increase or extra design parameters are required the size of the reduced order system will increase since additional moments are required. As a result a trade-off between efficiency and the range of accuracy has to be made for the reduced order model.

4.2.2. Selecting the Order of the Reduced Order Model

To select the appropriate order, error bounds are required to estimate the accuracy of the reduced order model with respect to the original system. Some interesting error bounds in [72]-[74] could be applied to automatically select the order of the reduced model. However, the implementation of these methods requires extra memory resources. In this work the accuracy of the reduced order model is verified by examining the residual error which is defined as [28]-[30],

$$\varepsilon = \frac{\left\| \boldsymbol{Y}(s,\bar{h}) \cdot \boldsymbol{X}(s,\bar{h}) - \boldsymbol{b}(s,\bar{h}) \right\|}{\left\| \boldsymbol{X}(s,\bar{h}) \right\|} \tag{4.22}$$

where $\boldsymbol{X}(s,\bar{h})$ is the approximate solutions derived by (4.18). If the residual error is below a given tolerance for the specified ranges of design parameters and frequency, then the reduced order model is assumed to be accurate and the reduction process is terminated. Otherwise additional moment coefficients or multiple expansion points [43], [72]-[74] can be used in (4.9) to improve the accuracy of the reduced order system.

4.3. Problem Formulation and Numerical Examples

In this section, two numerical examples are presented. The first example is a distributed interconnect network modeled as delay lines using the method of characteristics. The second is a two cascaded inductive irises in a dielectric loaded WR90 waveguide. All computations are performed on a Pentium 4 (2.80 GHz) PC with 2048 MB memory. The developed algorithms are programmed in MATLAB [49].

4.3.1. Example I: RLC Network with Delay Elements

In this example, the distributed network of Fig. 4.3 is analyzed at different temperatures. The dependency of electrical parameters on temperature T is modeled as

$$\begin{aligned} R(T) &= R(T_0)\left(1+\alpha_1^R (T-T_0)+\alpha_2^R (T-T_0)^2\right) \\ L(T) &= L(T_0)\left(1+\alpha_1^L (T-T_0)+\alpha_2^L (T-T_0)^2\right) \\ C(T) &= C(T_0)\left(1+\alpha_1^C (T-T_0)+\alpha_2^C (T-T_0)^2\right) \end{aligned} \tag{4.23}$$

where $(\alpha_1^R, \alpha_2^R), (\alpha_1^L, \alpha_2^L)$ and (α_1^C, α_2^C) are the first and second order temperature coefficients of the resistance *R*, inductance *L* and capacitance *C*, respectively. For the three-coupled interconnect networks, the temperature coefficients of the electrical parameters for $T_0 = 25^\circ$C are

$$(\alpha_1^R, \alpha_2^R) = (0.00404, 15\times10^{-6})$$

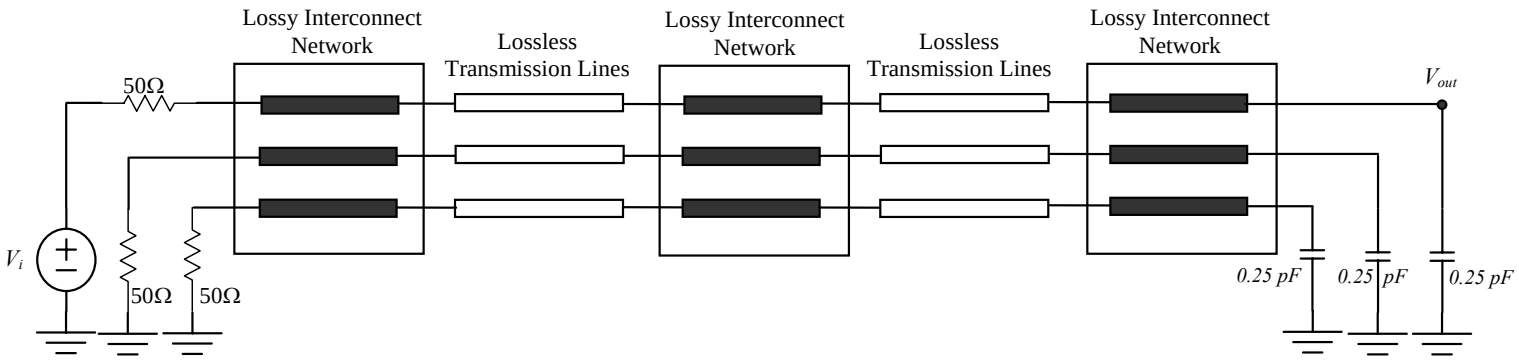

Fig. 4.3. RLC network including delay elements

$$(\alpha_1^L, \alpha_2^L) = (17\times10^{-6}, -18\times10^{-6})$$

$$(\alpha_1^C, \alpha_2^C) = (5.75\times10^{-5}, -1.285\times10^{-5})$$

The per-unit-length parameters of the lossy coupled interconnect network at $T_0 = 25^\circ\text{C}$ are

$$\boldsymbol{R} = \begin{bmatrix} 16 & 0 & 0 \\ 0 & 16 & 0 \\ 0 & 0 & 16 \end{bmatrix} \quad \Omega/cm$$

$$\boldsymbol{L} = \begin{bmatrix} 7.3 & 5.1 & 3.3 \\ 5.1 & 7.3 & 5.1 \\ 3.3 & 5.1 & 7.3 \end{bmatrix} \quad nH/cm \tag{4.24}$$

$$\boldsymbol{C} = \begin{bmatrix} 2.4 & -0.5 & -0.03 \\ -0.5 & 2.4 & -0.5 \\ -0.03 & -0.5 & 2.4 \end{bmatrix} \quad pF/cm$$

and the length of each line is *l*=5cm. The temperature variations of the lossless lines for

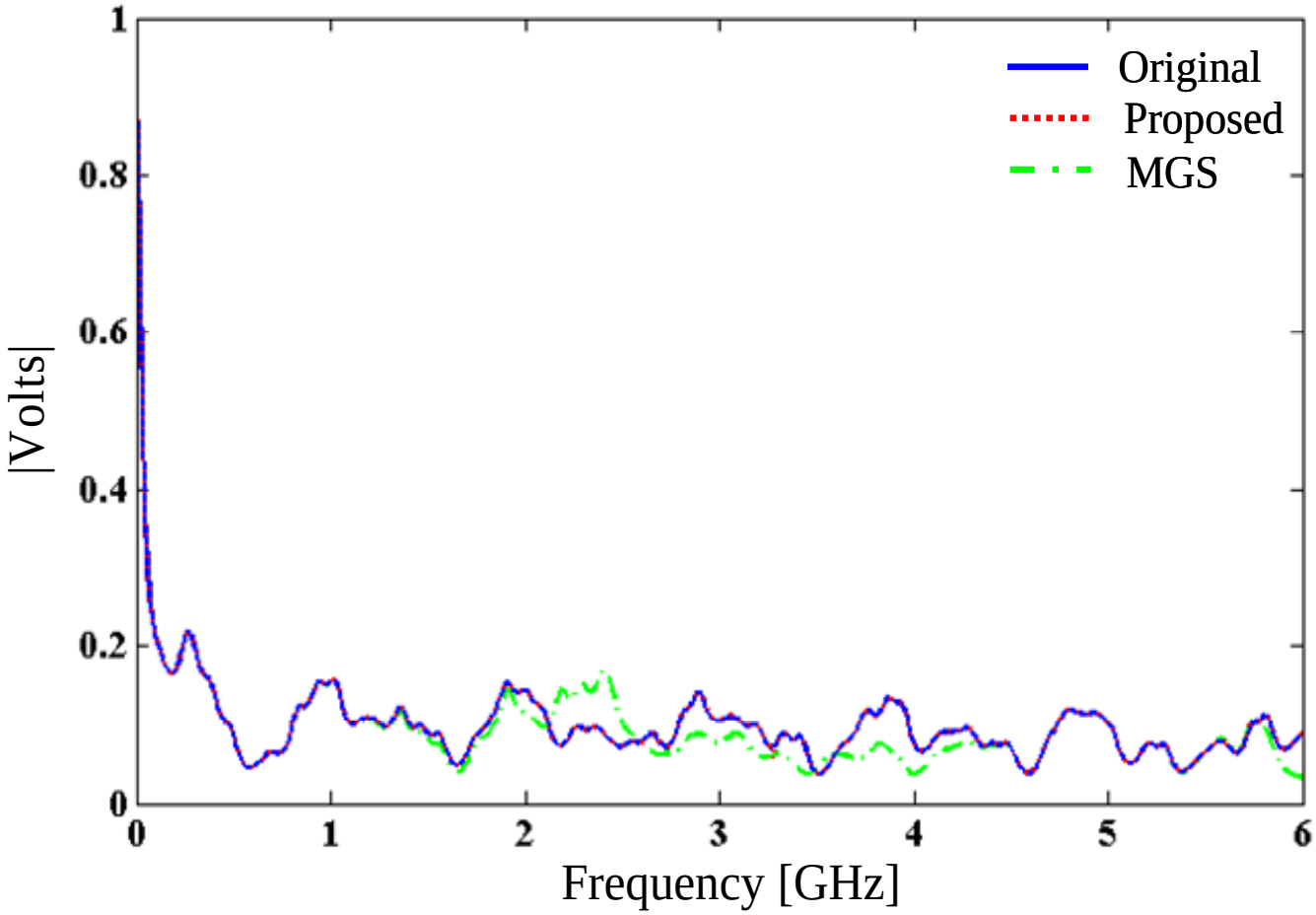

Fig. 4.4. Frequency responses of the system of example 1 at the far end point at the expansion point at T = 5°C.

$T_0 = 25^{\circ}$C are

$$(\alpha_1^L, \alpha_2^L) = (3.02\times10^{-4}, -1.52\times10^{-5})$$

$$(\alpha_1^C, \alpha_2^C) = (2.83\times10^{-4}, -1.48\times10^{-5})$$

The per-unit-length parameters of the lossless lines at $T_0 = 25^{\circ}$C are $L=3.5\,nH/cm$, $C=1.4\,pF/cm$ and the length of each line is l=15cm. The near end resistances R_i and far

end load capacitances C_i are also modeled as functions of temperature as

$$(\alpha_1^R, \alpha_2^R) = (0.00404, 15\times10^{-6})$$

$$(\alpha_1^C, \alpha_2^C) = (5.75\times10^{-5}, -1.285\times10^{-5})$$

for $T_0 = 25^\circ$C, where $R_i(T_0) = 50\Omega$ and $C_i(T_0) = 0.25pF$.

For the system of Fig. 4.3, the lossy coupled interconnect lines are modeled using the conventional lumped model [75] while the lossless lines are modeled using the Method of Characteristics (MoC) [76]. The general form of the Modified Nodal Analysis (MNA) matrices using the MoC and lumped elements can be expressed as [58]

$$\left(\boldsymbol{G}(T) + s\boldsymbol{C}(T) + \sum_i e^{-s\tau_i(T)} \cdot \boldsymbol{A}_i(T)\right)\boldsymbol{X} = \boldsymbol{B}\boldsymbol{V}(s)$$

$$\boldsymbol{I} = \boldsymbol{L}^T \boldsymbol{X} \tag{4.25}$$

where $\boldsymbol{G}(T)$ and $\boldsymbol{C}(T) \in \Re^{\varphi\times\varphi}$ are matrices describing the lumped memoryless and memory elements of the network, respectively. $\boldsymbol{X} \in C^{\varphi}$ is a vector of the unknown voltage and current variables; $\boldsymbol{A}_i(T) \in \Re^{\varphi\times\varphi}$ is the matrix derived from the MoC macromodel and is multiplied by the extracted delay of the lossless $\tau_i = l\sqrt{LC}$ (the description of $\boldsymbol{A}_i$ matrices can be found in [58] to obtain a passive reduced order model); $\boldsymbol{B} \in \Re^{\varphi\times k}$ is a selector matrix that maps the port voltages $\boldsymbol{V}$ into the network; $\boldsymbol{L} \in \Re^{\varphi\times k}$ selects the port current variables $\boldsymbol{I}$ of the network. The original network using the conventional lumped model and MoC consists of 2733 unknown variables.

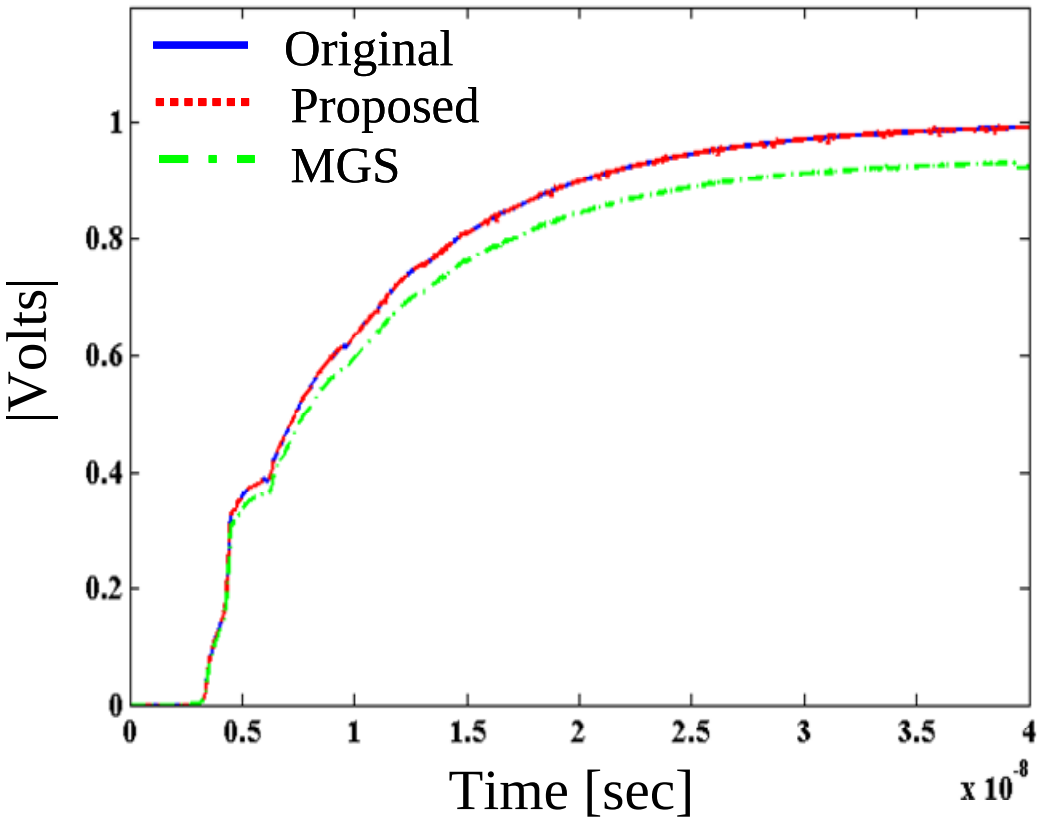

(a)

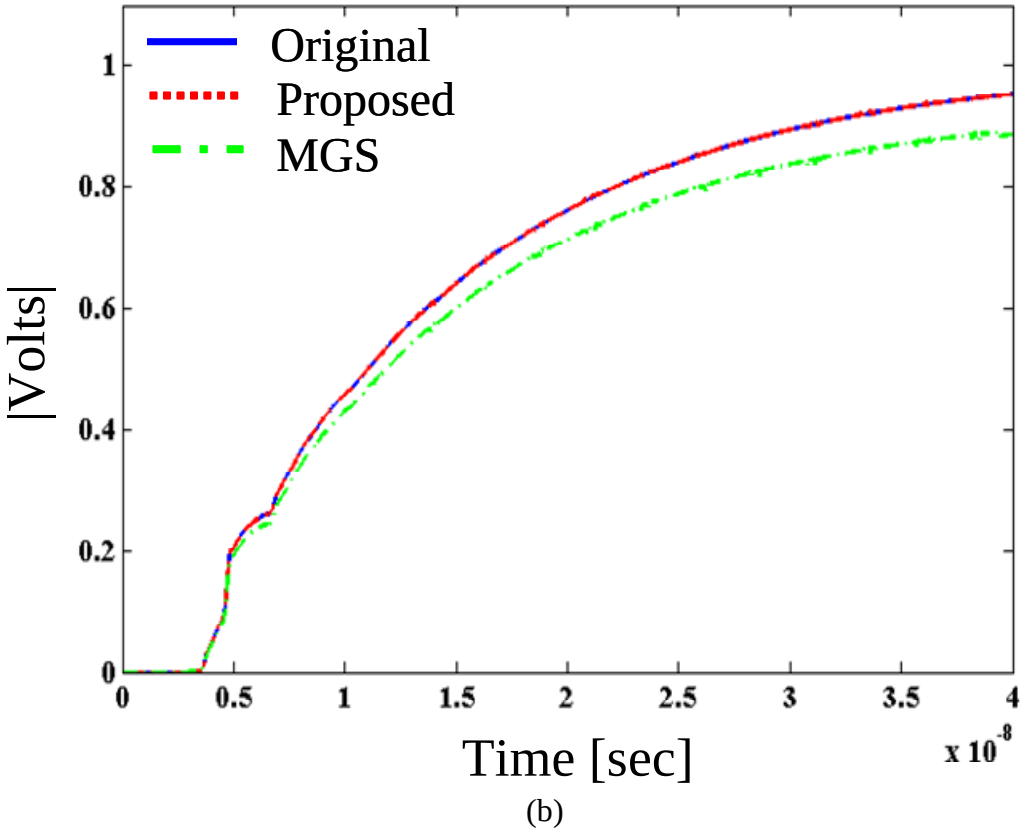

(b)

Fig. 4.5 Time domain response of the system of example 1 at the far end point, at (a) T = -40° C and (b) T = 50° C.

TABLE 4.1
COMPUTATIONAL INFORMATION OF TIME DOMAIN RESPONSE

Solution Method	Size	CPU Time to generate reduced model	Simulation Time	Savings in Size	Speed Up Factor
Original System	2733	-	5085 sec	-	-
Proposed	236	763 sec	297.4 sec	91%	17

4000 simulations corresponding to 400 different time points and 10 different temperature values.

The proposed parameterized model order reduction technique is applied to model variations with respect to frequency and temperature. The frequency bandwidth of interest for this problem ranges from 0 to 6GHz while the temperature variation ranges from -40°C to 50°C. To derive a compact parametric reduced order model two expansion points are selected at frequency = 0.5 GHz, T=5°C and at frequency = 5 GHz, T=5°C. To achieve a residual error of less than $\varepsilon < 10^{-5}$ for (4.25), the reduced order model required 30 moments for frequency, 22 moments for temperature and 7 cross moments for each expansion point. The size of the reduced order model consists of 236 variables.

Fig. 4.4 shows the unit impulse frequency response of node *Vout* at the expansion temperatures of T = 5°C. The results of the proposed model are also compared with Modified Gram Schmidt (MGS). Within the context of this section, MGS refers to parameterized reduction technique that explicitly matches the moments of (4.8) using MGS [44] to construct the orthonormal matrix of $\boldsymbol{Q}$. Both the proposed and MGS are accurate near the expansion points of 0.5 GHz and 5 GHz. However, the proposed

algorithm is able to achieve better accuracy and match the entire frequency range since it takes advantage of the Arnoldi algorithm to implicitly calculate the moments. Fig. 4.5 shows the transient response at node *Vout*, corresponding to a unit step input voltage with a rise time of 0.2 ns at the two extreme temperatures of T = -40°C and T = 50°C. For both simulations, the time domain responses of the reduced order model are in agreement when compared to the original solution. Table 4.1 compares the total size and simulation times of the original and proposed algorithm. For this example, the simulation time of the parameterized reduced order model is about 17 times faster when compared to the original system.

4.3.2. Example II: Cascade Inductive Irises

A four cascaded inductive irises in WR90 waveguide (a=22.86mm, b=10.16mm) is shown in Fig. 4.6. Each of the irises consists of two symmetric H-planes, separated by distance 20 millimeters for the outer cavities and 16.8 millimeters in the middle cavity. The Finite Element Method (FEM) discretization of the electric field vector wave equation [27] for a *k* port device with surface impedance losses of the conductor can be expressed as [57]

$$\begin{aligned} (\boldsymbol{A}_0(\varepsilon_r) + s\boldsymbol{A}_1(\varepsilon_r,\sigma) + s^2\boldsymbol{A}_2(\varepsilon_r) + F(s,\sigma)\boldsymbol{H})\boldsymbol{X} &= s\boldsymbol{B}\boldsymbol{u} \\ \boldsymbol{y} &= \boldsymbol{L}^T\boldsymbol{X} \end{aligned} \tag{4.26}$$

where $\boldsymbol{A}_0, \boldsymbol{A}_1, \boldsymbol{A}_2$ and $\boldsymbol{H} \in \Re^{\varphi\times\varphi}$ are matrices obtained from the FEM approximation; $\boldsymbol{X} \in C^{\varphi}$ is the vector of unknown variables in the approximation of the electric field; $\boldsymbol{B} \in \Re^{\varphi\times k}$ is a selector matrix that maps the excitation input $\boldsymbol{u}$ into the system; $\boldsymbol{L} \in \Re^{\varphi\times k}$

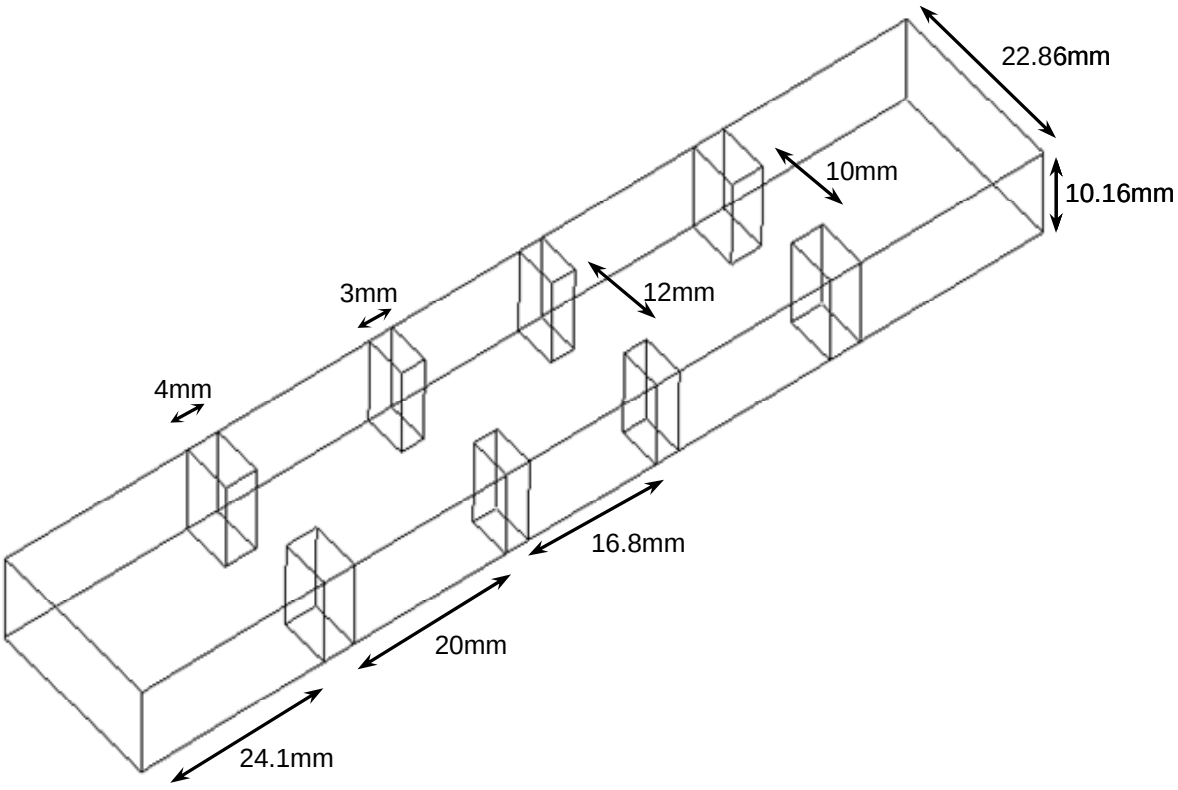

Fig. 4.6. Geometry of the dual inductive iris filter.

selects the output variables of interest and maps them to the output vector $\boldsymbol{y}$ of the electric field used to calculate the *S*-parameters of the system. The scalar function $F(s,\sigma)$ represents the skin effect losses in a non-perfect conductor modeled as [57],

$$F(s,\sigma)=\frac{1}{1+j\sqrt{\frac{2s\sigma}{\mu}}} \tag{4.27}$$

where μ is the magnetic permeability of the material and σ is the conductivity.

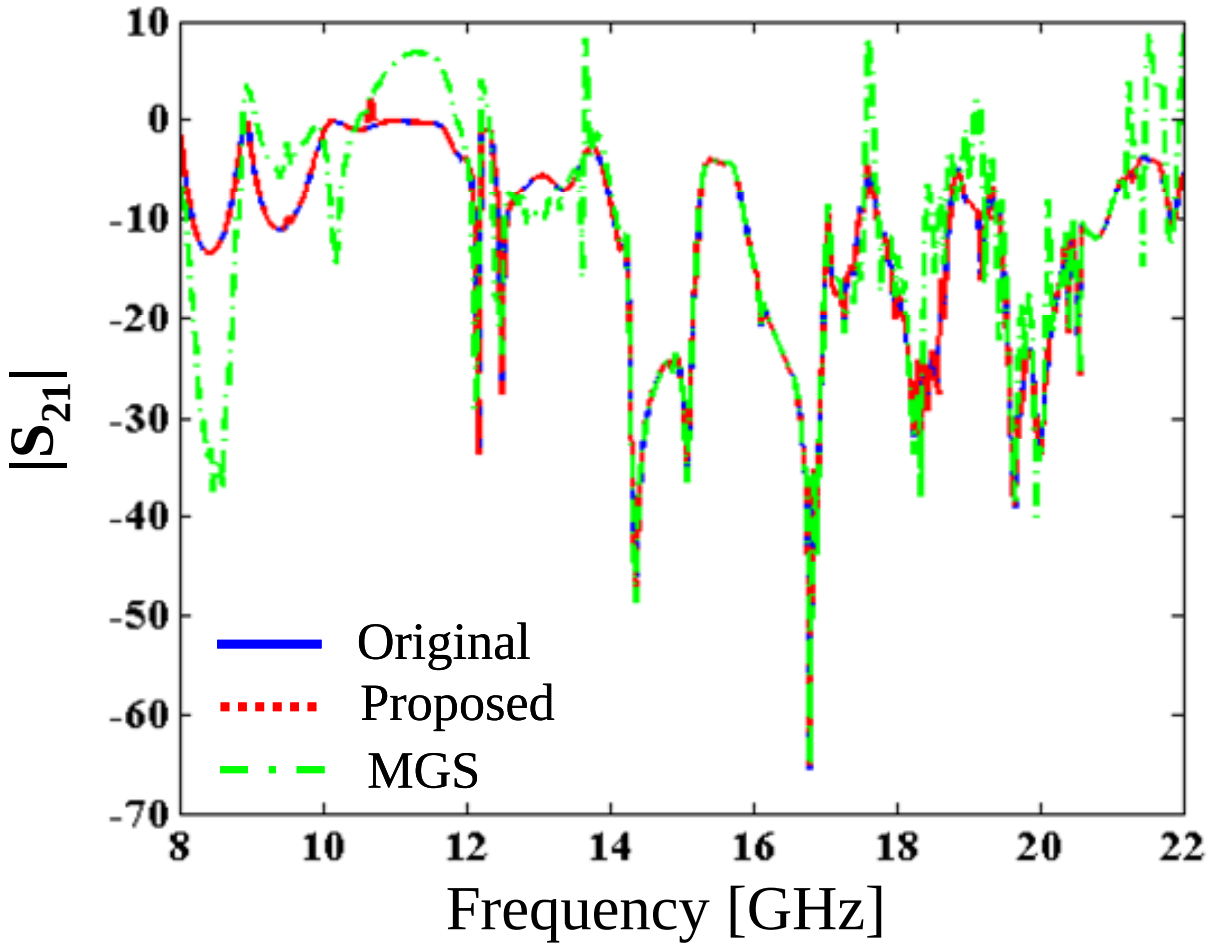

Fig. 4.7. The magnitude of S_{21} as a function of frequency at the expansion point at the mid-range of design parameters ε_r and σ .

The structure is discretized using Lagrange-quadratic elements and the total number of degrees of freedom in the original system is equal to 52746. The bandwidth of interest for this problem ranges from 8GHz to 21GHz. The design parameters of interest are the dielectric permittivity which ranges from ε_r =1 to 5 which loads the waveguide and the conductivity of non-perfect metallic walls of the irises σ which ranges from 3.78e7 [S/m] for aluminum to 6.301e7 for silver. The proposed multi-order Arnoldi algorithm is implemented to obtain a parameterized reduced order system of size 296.

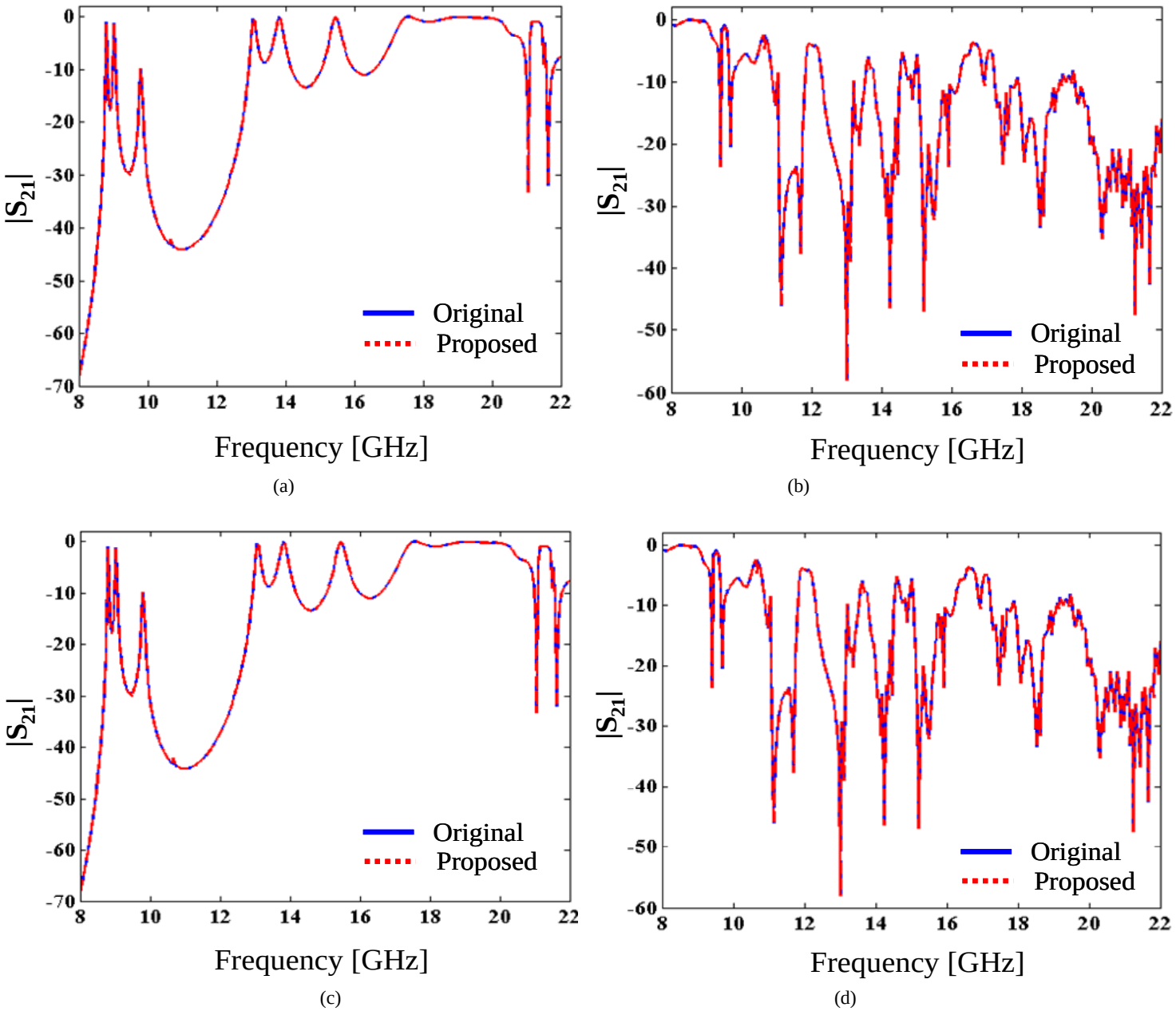

Fig. 4.8. The magnitude of S_{21} as a function of frequency for different parameter values at the corner of design parameters; (a) ε_r =1 and σ =3.78e7 [S/m], (b) ε_r =5 and σ =3.78e7 [S/m], (c) ε_r =1 and σ =6.301e7 [S/m] and (d) ε_r =5 and σ =6.301e7 [S/m].

For this example, two expansion points are selected at frequency=12GHz, ε_r =3, σ =5.8e7 [S/m] and at frequency=16GHz, ε_r =3, σ = 5.8e7[S/m]. To achieve a residual

error of less than $\varepsilon < 10^{-5}$ for (26), each expansion point uses 32 moments for frequency, 26 moments for ε_r, 9 moments for σ and 7 cross moments.

Fig. 4.7 shows the magnitude of S_{21} as a function of frequency at the expansion point at ε_r =3 and σ = 5.8e7, calculated by the proposed method and compared to MGS. As expected, the proposed approach is able to achieve better accuracy than MGS since it uses the Arnoldi algorithm to implicitly calculate the moments. Fig. 4.8 shows the magnitude of S_{21} as a function of frequency at the four extreme corners of parameter ranges for ε_r and σ. Table 4.2 compares the total size and simulation times of the original and proposed reduced order model. For this example, a speed up of 137 was achieved using the proposed approach when compared to the original simulation time.

TABLE 4.2
COMPUTATIONAL INFORMATION

Solution Method	Size	CPU Time to generate reduced model	Simulation Time	Savings in Size	Speed Up Factor
Original System	52572	-	44 hours & 34 min	-	-
Proposed	296	34 min & 22 sec	19 min & 33 sec	99.4%	137

1875 simulations corresponding to 125 different frequency points, 5 different values of ε_r and 3 different values of σ.

Chapter 5

5. Sensitivity Analysis of Microwave Circuits using Parameterized Model Order Reduction Techniques

5.1. Introduction

In this chapter, a parameterized model order reduction technique is used to efficiently solve the original FEM network and to calculate sensitivities of microwave circuits. The proposed methodology uses a multi-order Arnoldi method to calculate the moments with respect to arbitrary functions of frequency and design parameters, as well as the cross-moments. This procedure results in a parameterized reduced order model that is valid over a user defined range of design parameter values (such as material properties, geometrical parameters) and can be used to calculate sensitivities using an adjoint variable method. Such an approach is significantly more CPU efficient in optimization since a new reduced model is not required each time a design parameter is modified. Furthermore, the solution of the original FEM network, as well as the sensitivities with respect to any network parameter is obtained from the solution of the reduced order model.

This chapter is organized as follows. Section 5.1 describes the adjoint variable method using parameterized MOR. A numerical example is provided is Section 5.2 to illustrate the validity of the proposed algorithm.

5.2. Sensitivity Analysis using Parameterized MOR

This section describes how to determine the sensitivities of electromagnetic structures using the adjoint variable method and the reduced order model of (4.19).

5.2.1. Adjoint Variable Method using MOR

Let the objective function of interest be defined as $F(\bar{h}, \boldsymbol{X}(s,\bar{h}))$. The goal is to find the sensitivity of the objective function with respect to a network parameter h_k, as

$$\frac{\partial}{\partial \lambda_k}\left(F(\bar{h}, \boldsymbol{X}(s,\bar{h}))\right) = \frac{\partial F(\bar{h}, \boldsymbol{X}(s,\bar{h}))}{\partial h_k} + \frac{\partial F(\bar{h}, \boldsymbol{X}(s,\bar{h}))}{\partial \boldsymbol{X}(s,\bar{h})}\frac{\partial \boldsymbol{X}(s,\bar{h})}{\partial h_k} \tag{5.1}$$

In the proposed scheme, the solution of the original network is obtained by solving (4.19) and using (4.18) to calculate $\boldsymbol{X}(s,\bar{h})$. Thus to calculate (5.1) using the reduced order model requires differentiating (4.18) with respect to h_k as

$$\frac{\partial \boldsymbol{X}(s,\bar{h})}{\partial h_k} = \boldsymbol{Q}\frac{\partial \hat{\boldsymbol{X}}(s,\bar{h})}{\partial h_k} + \frac{\partial \boldsymbol{Q}}{\partial h_k}\hat{\boldsymbol{X}}(s,\bar{h}) \tag{5.2}$$

Note that if the moments of $\boldsymbol{Q}$ are only with respect to frequency, then $\partial \boldsymbol{Q}/\partial h_k$ needs to be evaluated since the frequency moments change and a new reduced order model is required each time a design parameter is changed [80], [89]-[90]. In the proposed scheme, the moments of $\boldsymbol{Q}$ are with respect to frequency and the design parameters. As a result, the reduced order model of (4.19) is able to capture the variance with respect to

frequency and design parameter variables without the need to recalculate $\boldsymbol{Q}$. Thus $\partial \boldsymbol{Q} / \partial h_k = \boldsymbol{0}$ and (5.2) reduces to

$$\frac{\partial \boldsymbol{X}(s,\bar{h})}{\partial h_k} = \boldsymbol{Q} \frac{\partial \hat{\boldsymbol{X}}(s,\bar{h})}{\partial h_k} \tag{5.3}$$

This approach is significantly more efficient in optimization since $\partial \boldsymbol{Q} / \partial \lambda_k$ does not have to be evaluated and a new reduced model is not required each time a design parameter is modified.

Next, the sensitivity of the reduced order model is obtained by differentiating (4.19) by h_k

$$\frac{\partial \hat{\boldsymbol{X}}(s,\bar{h})}{\partial h_k} = \hat{\boldsymbol{Y}}^{-1}(s,\bar{h}) \left(\frac{\partial \hat{\boldsymbol{b}}(s,\bar{h})}{\partial h_k} - \frac{\partial \hat{\boldsymbol{Y}}(s,\bar{h})}{\partial h_k} \hat{\boldsymbol{X}}(s,\bar{h}) \right) \tag{5.4}$$

Using (4.20), (4.21) and (5.3), the derivatives of $\hat{\boldsymbol{Y}}(s,\bar{h})$ and $\hat{\boldsymbol{b}}(s,\bar{h})$ with respect to h_k are

$$\frac{\partial \hat{\boldsymbol{Y}}(s,\bar{h})}{\partial h_k} = \boldsymbol{Q}^T \frac{\partial \boldsymbol{Y}(s,\bar{h})}{\partial h_k} \boldsymbol{Q} \tag{5.5}$$

$$\frac{\partial \hat{\boldsymbol{b}}(s,\bar{h})}{\partial h_k} = \boldsymbol{Q}^{\mathrm{T}} \frac{\partial \boldsymbol{b}(s,\bar{h})}{\partial h_k} \tag{5.6}$$

The sensitivity of the objective function using the reduced order model can be calculated by substituting (4.18), (5.3) and (5.4) into (5.1) to obtain

$$\frac{\partial}{\partial h_k}\left(F(\bar{h}, \boldsymbol{X}(s,\bar{h}))\right) = \frac{\partial F(\bar{h}, \boldsymbol{Q}\hat{\boldsymbol{X}}(s,\bar{h}))}{\partial h_k} + \hat{\boldsymbol{X}}_a^{\,T}(s,\bar{h})\left(\frac{\partial \hat{\boldsymbol{b}}(s,\bar{h})}{\partial h_k} - \frac{\partial \hat{\boldsymbol{Y}}(s,\bar{h})}{\partial h_k}\hat{\boldsymbol{X}}(s,\bar{h})\right) \tag{5.7}$$

where $\hat{\boldsymbol{X}}_a(s,\bar{h})$ is the solution of the adjoint variable network defined as

$$\hat{\boldsymbol{Y}}^{\boldsymbol{T}}(s,\bar{h})\hat{\boldsymbol{X}}_a(s,\bar{h}) = \left[\frac{\partial F(\bar{h}, \boldsymbol{Q}\hat{\boldsymbol{X}}(s,\bar{h}))}{\partial \hat{\boldsymbol{X}}(s,\bar{h})}\right]^T \tag{5.8}$$

The solution of the adjoint variable network does not require additional lower-upper decompositions to invert $\hat{\boldsymbol{Y}}^{\boldsymbol{T}}(s,\bar{h})$ since the lower-upper matrices are known from the solution of (4.19). This leads to significant computational savings, since the sensitivities with respect to all design parameters can be obtained with only one forward-backward substitution to solve (5.8). In addition, (5.9) has fewer variables when compared to the adjoint variable network derived from the original network of (4.1).

5.2.2. Sensitivity Analysis of S-Parameters

Typical objective functions in analyzing microwave devices are the scattering parameters (*S*-parameters), electromagnetic fields and potentials, dispersion curves and current densities. This section briefly describes how to calculate the sensitivities of the *S*-parameters using the proposed model order reduction algorithm. From the solution of the FEM equations, the scattering parameters S_{ij} $(i = 1, \ldots, N)$ can be calculated as [78]-[81]

$$S_{ij} = -\frac{1}{2} \boldsymbol{X}^{(i)T} \boldsymbol{Y} \boldsymbol{X}^{(j)} \tag{5.9}$$

where $\boldsymbol{X}^{(i)}$ and $\boldsymbol{X}^{(j)}$ are the vectors containing the E-field solution at ports *i* and *j*, respectively, and the superscript *T* denotes the transpose of a matrix. The derivate of the scattering parameters with respect to a network parameter h_k is obtained as [78]-[81]

$$\frac{\partial S_{ij}}{\partial h_k} = -\frac{1}{2} \boldsymbol{X}^{(i)T} \frac{\partial \boldsymbol{Y}}{\partial h_k} \boldsymbol{X}^{(j)} \tag{5.10}$$

The sensitivity of the *S*-parameters using (5.10) is valid provided the geometries of port *i* and *j* do not change as h_k varies [78]-[81], [85]. Note that (5.10) does not require an adjoint-system analysis since the derivatives of the electric field with respect to h_k are not used. For this scenario, even though adjoint-variable solution of (5.8) is not required, the parameterized reduced order model can still be used to efficiently calculate sensitivities of the *S*-parameters by substituting (4.18) into (5.9), as

$$\frac{\partial S_{ij}}{\partial h_k} = -\frac{1}{2} \hat{\boldsymbol{X}}^{(i)T} \frac{\partial \hat{\boldsymbol{Y}}}{\partial h_k} \hat{\boldsymbol{X}}^{(j)} \tag{5.11}$$

where $\hat{\boldsymbol{X}}^{(i)}$ and $\hat{\boldsymbol{X}}^{(j)}$ are obtained by solving (4.19). Note that in comparison to using Padé rational function to calculate the sensitivities of the *S*-parameters [80], the proposed approach does not have to recalculate the system moments each time a design parameter is changed, leading to significant computational savings.

For the case when the geometries of port *i* and *j* change as h_k varies, the sensitivities of the *S*-parameters require an adjoint-system analysis which can be evaluated using

(4.19), (5.7) and (5.8). How to define the objective function to calculate the sensitivities of the *S*-parameters from the solution of the original and adjoint-variable networks is described in [11]-[12].

5.3. Numerical Example

An H-plane WR90 waveguide (a=22.86mm, b=10.16mm) loaded with dielectric is shown in Fig. 5.1. The input port consists of two symmetric H-planes that control the size of the port by changing the spacing between the planes of the thick iris. The structure is discretized using Lagrange-quadratic elements and the total number of degrees of freedom in the original FEM system is equal to 13625. The bandwidth of interest is from 50GHz to 75GHz. The design parameters of interest in this example are the dielectric permittivity which ranges from ε_r =1 to 5 and the spacing between the planes of the input iris *w*, which ranges from 0.00386m to 0.00586m.

For this example, the FEM discretization of the electric field vector wave equation has the following dependency of frequency

$$(\boldsymbol{Y}_0(\varepsilon_r, w) + s\boldsymbol{Y}_1(\varepsilon_r, w) + s^2\boldsymbol{Y}_2(\varepsilon_r, w) + F(s)\boldsymbol{H})\boldsymbol{X} = s\boldsymbol{b}(\varepsilon_r, w)\boldsymbol{u} \tag{5.12}$$

where $\boldsymbol{Y}_0, \boldsymbol{Y}_1, \boldsymbol{Y}_2$ and $\boldsymbol{H} \in \Re^{\varphi\times\varphi}$ are matrices obtained from the FEM approximation [27], [57]; $\boldsymbol{X} \in C^{\varphi}$ is the vector of unknown variables in the approximation of the electric field; $\boldsymbol{b} \in \Re^{\varphi\times k}$ is a selector matrix that maps the excitation input $\boldsymbol{u}$ into the system. The scalar function *F(s)* represents the skin effect losses in a non-perfect conductor modeled as

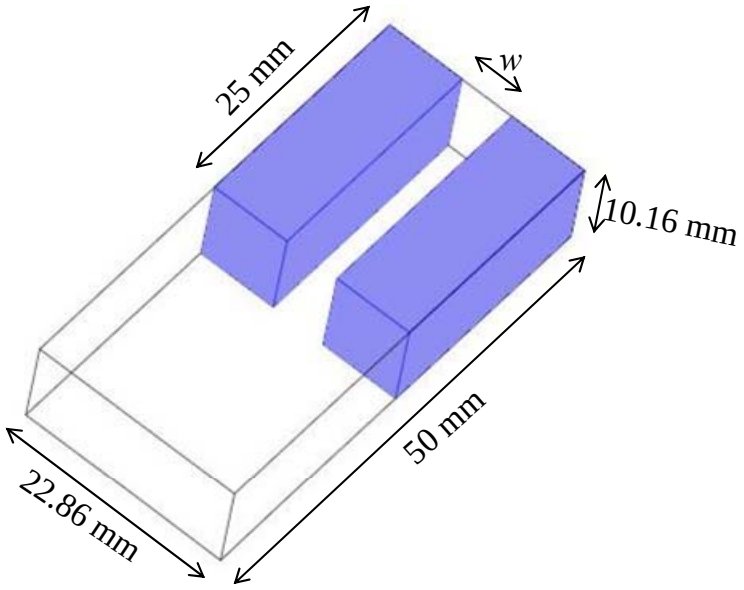

Fig. 5.1. WR90 waveguide with metallic iris at the input port. The rest of the waveguide is filled with dielectric material.

$$F(s) = \frac{1}{1 + j\sqrt{\frac{2s\sigma}{\mu}}} \tag{5.13}$$

where $\mu = \mu_0 \mu_r$. The matrices $\boldsymbol{Y}_0, \boldsymbol{Y}_1, \boldsymbol{Y}_2$ and $\boldsymbol{b}$ have a linear dependency with respect to ε_r and can be expressed as

$$\begin{aligned} \boldsymbol{Y}_i(\varepsilon_r, w) &= \boldsymbol{Y}_{i0}(w) + \varepsilon_r \boldsymbol{Y}_{i1}(w) \\ \boldsymbol{b}(\varepsilon_r, w) &= \boldsymbol{b}_0(w) + \varepsilon_r \boldsymbol{b}_1(w) \end{aligned} \tag{5.14}$$

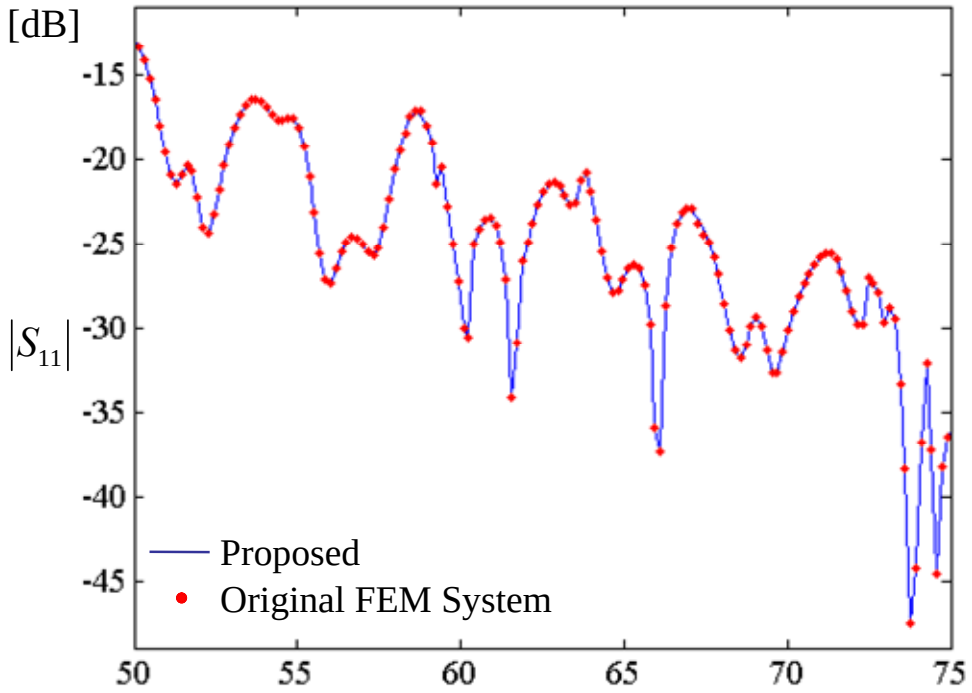

(a)

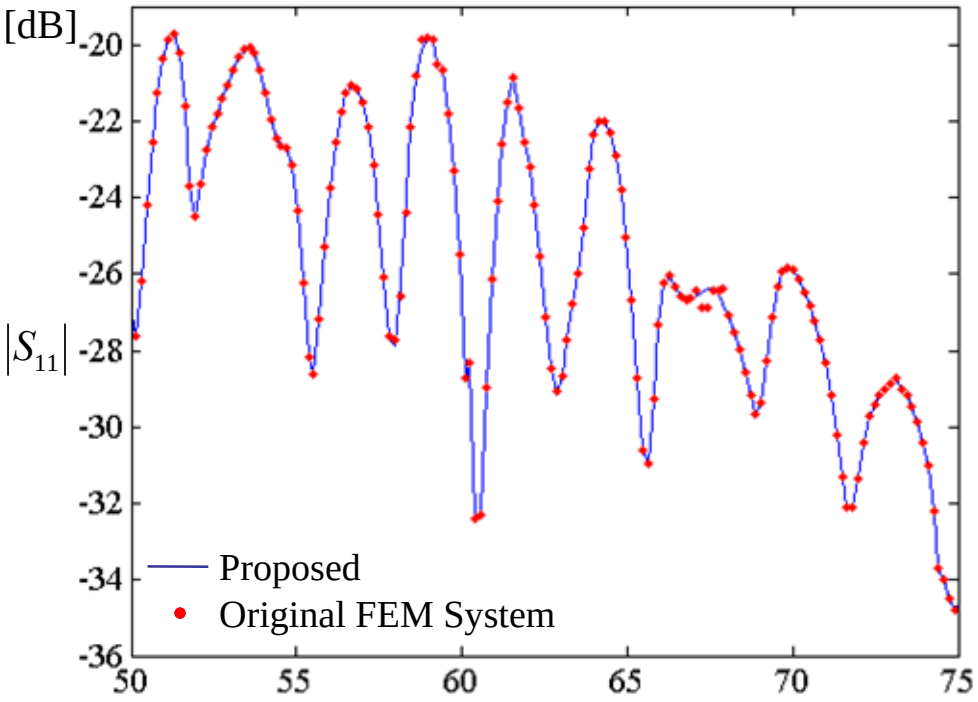

(b)

Fig. 5.2a. S_{11} of the waveguiding structure at extreme corners of parameter ranges for ε_r and w (a) ε_r =1 and w=0.00386, (b) ε_r =1 and w=0.00586.

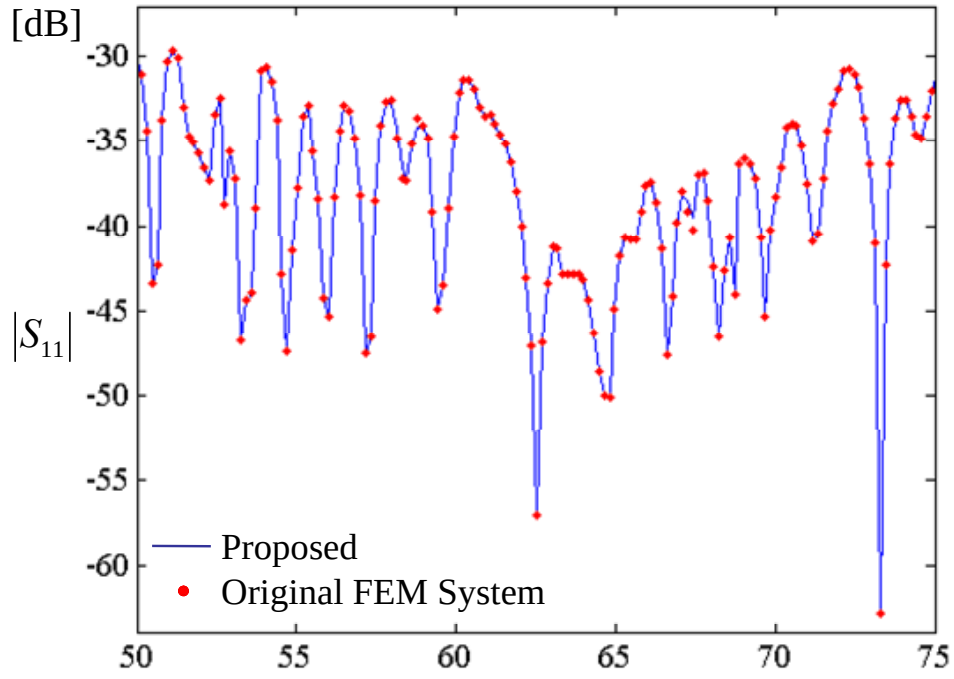

(a)

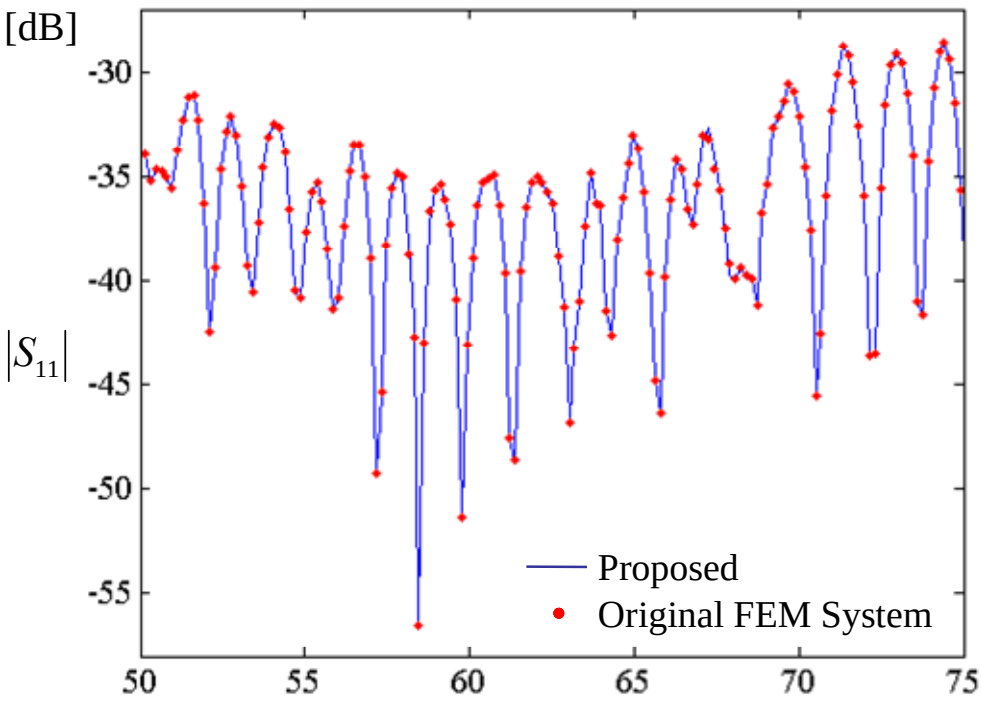

(b)

Fig. 5.2b. $|S_{11}|$ of the waveguiding structure at extreme corners of parameter ranges for ε_r and w (a) ε_r =5 and w=0.00386 and (b) ε_r =5 and w=0.00586.

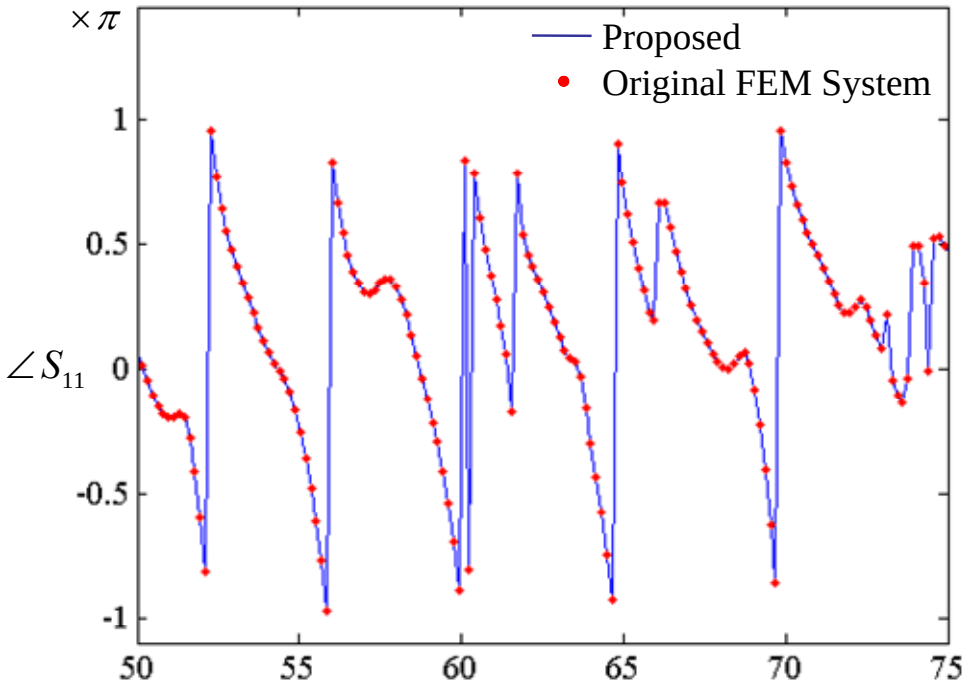

(a)

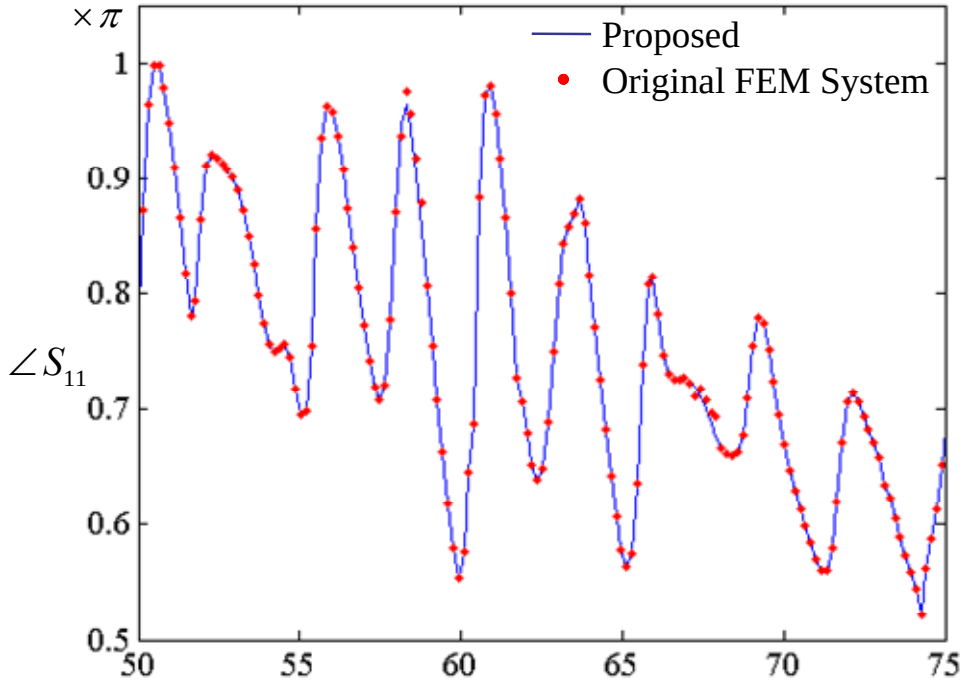

(b)

Fig. 5.3a. $\angle S_{11}$ of the waveguiding structure at extreme corners of parameter ranges for ε_r and w (a) ε_r =1 and w=0.00386, (b) ε_r =1 and w=0.00586.

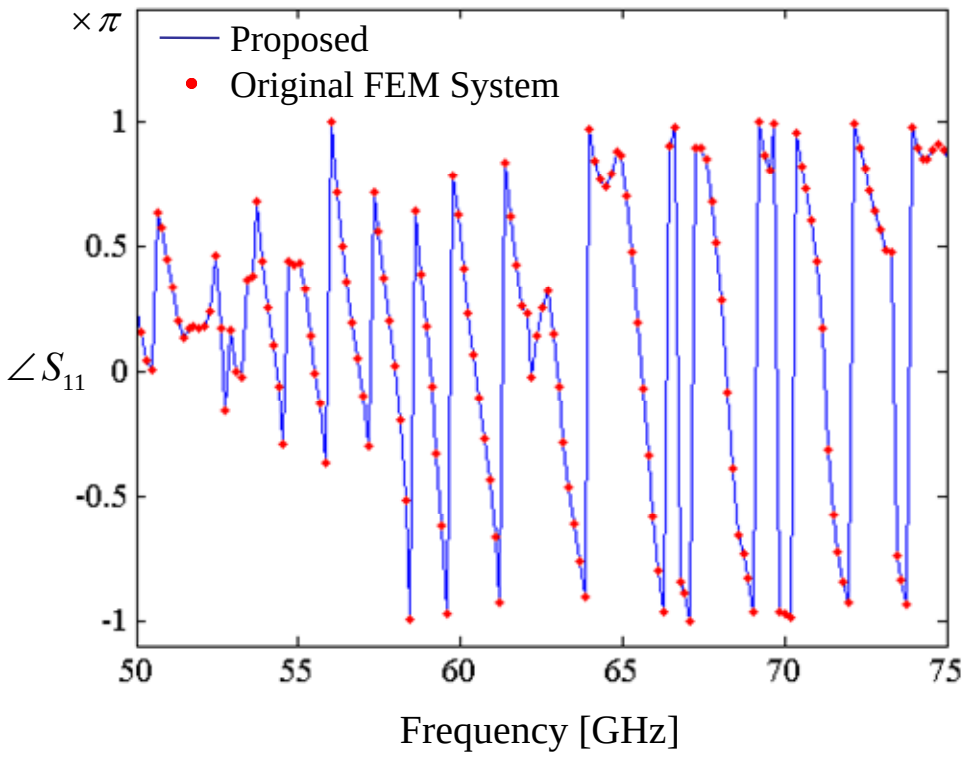

(a)

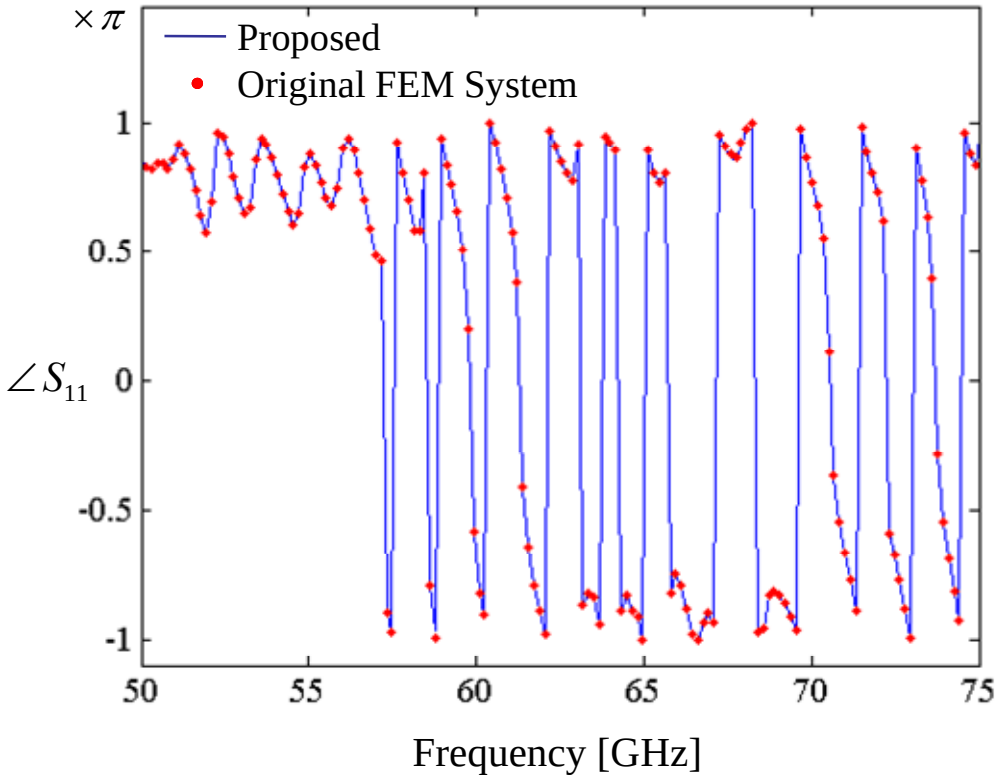

(b)

Fig. 5.3b. $\angle S_{11}$ of the waveguiding structure at extreme corners of parameter ranges for ε_r and w (a) ε_r =5 and w=0.00386 and (b) ε_r =5 and w=0.00586.

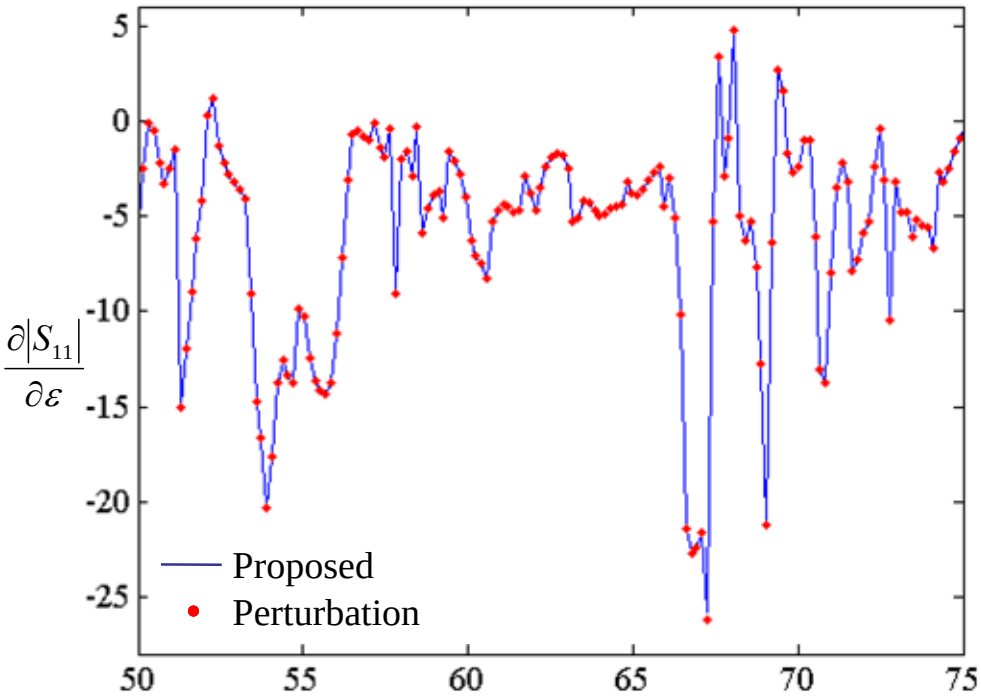

(a)

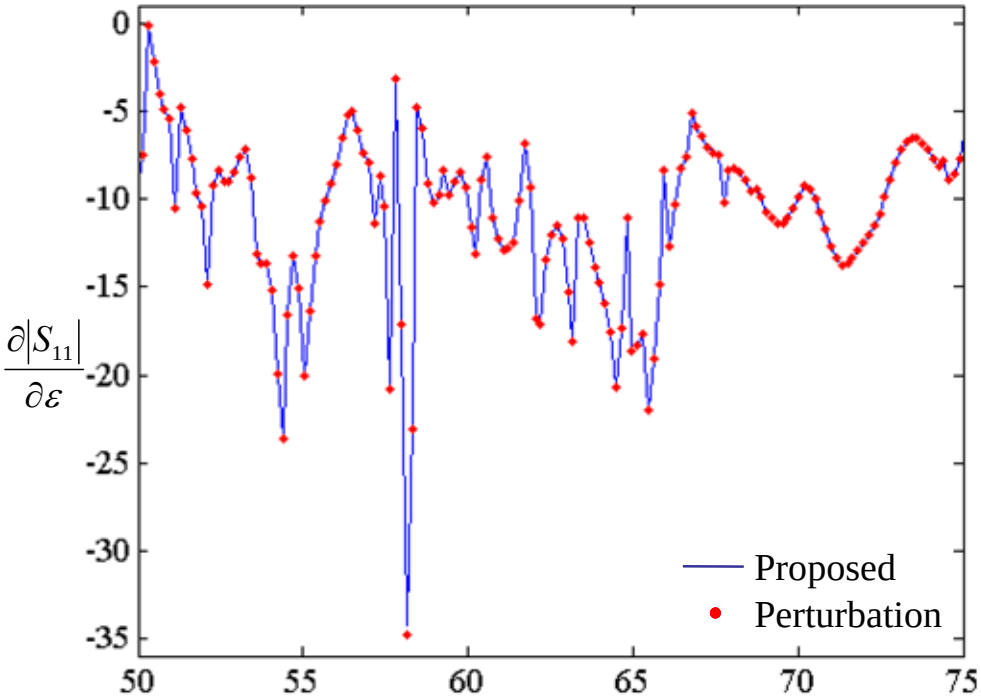

(b)

Fig. 5.4a. Sensitivities of $|S_{11}|$ of the waveguiding structure with respect to ε_r at (a) ε_r =3, w=0.00386, (b) ε_r =3, w=0.00586.

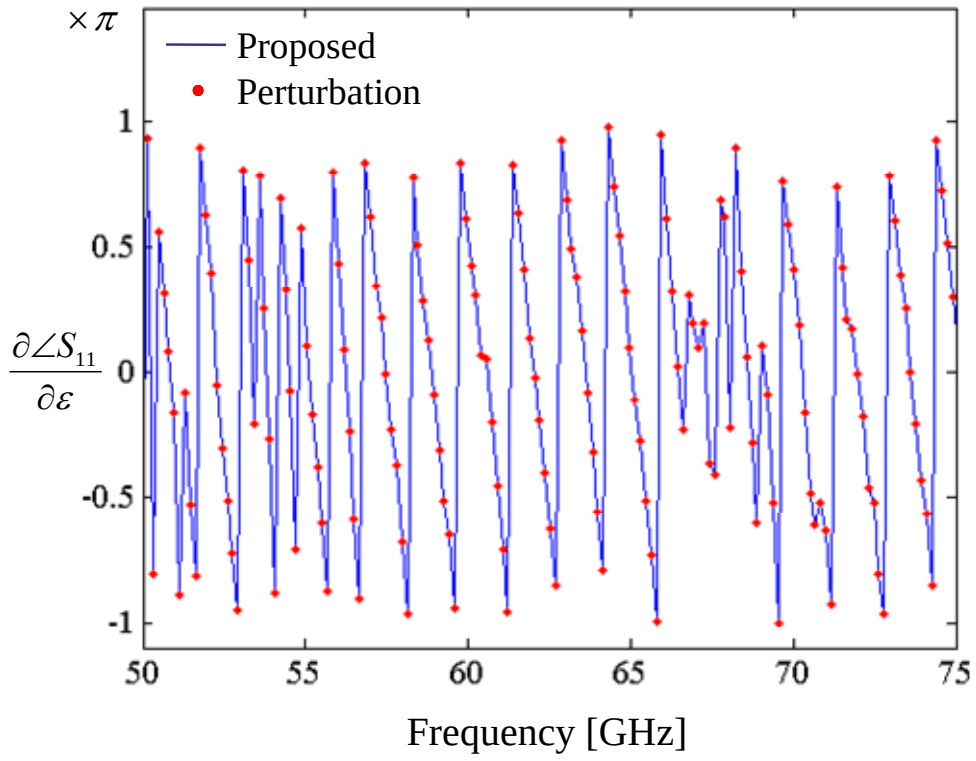

(a)

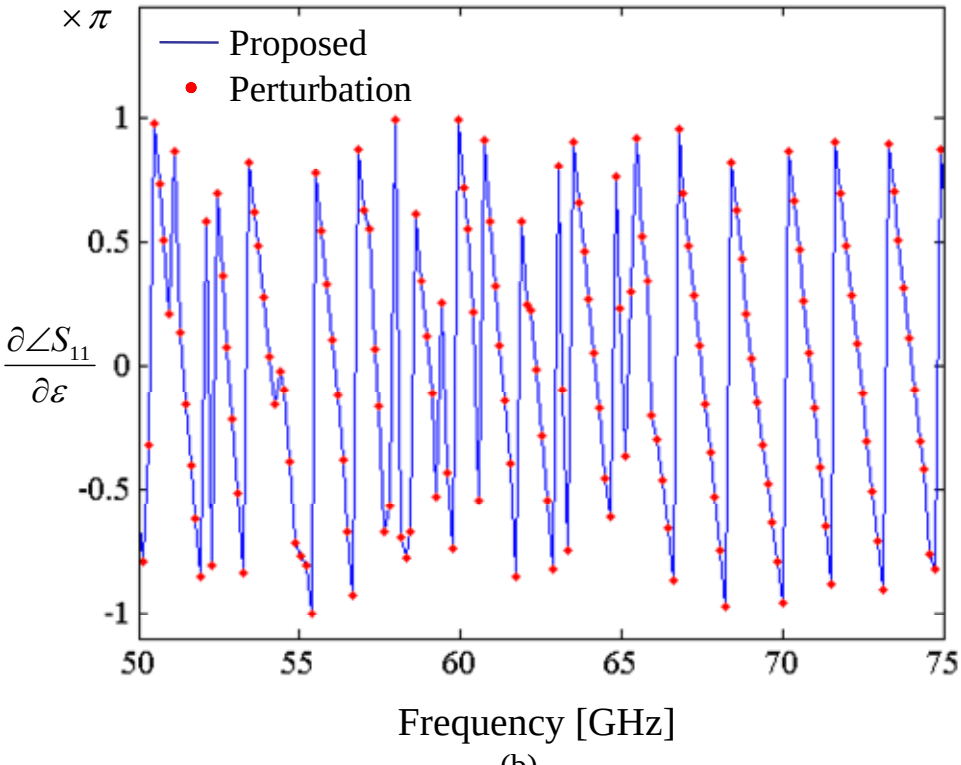

(b)

Fig. 5.4b. Sensitivities of $\angle S_{11}$ of the waveguiding structure with respect to ε_r at (a) ε_r =3, w=0.00386, (b) ε_r =3, w=0.00586.

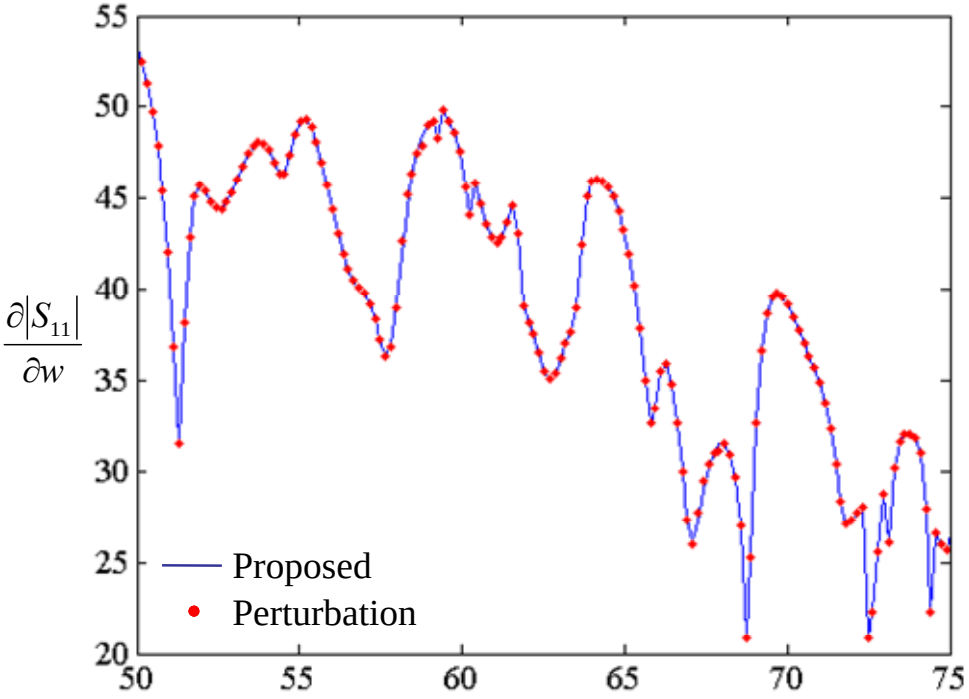

(a)

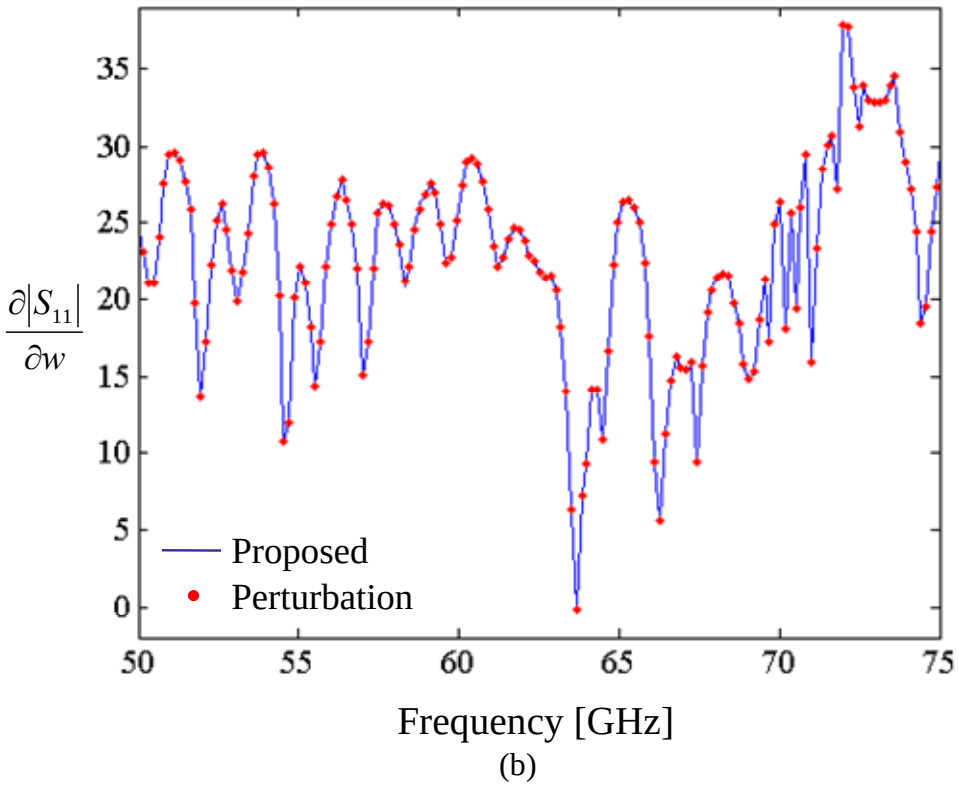

(b)

Fig. 5.5a. Sensitivities of $|S_{11}|$ of the waveguiding structure with respect to w at (a) ε_r =1, w=0.00486, (b) ε_r =5, w=0.00486.

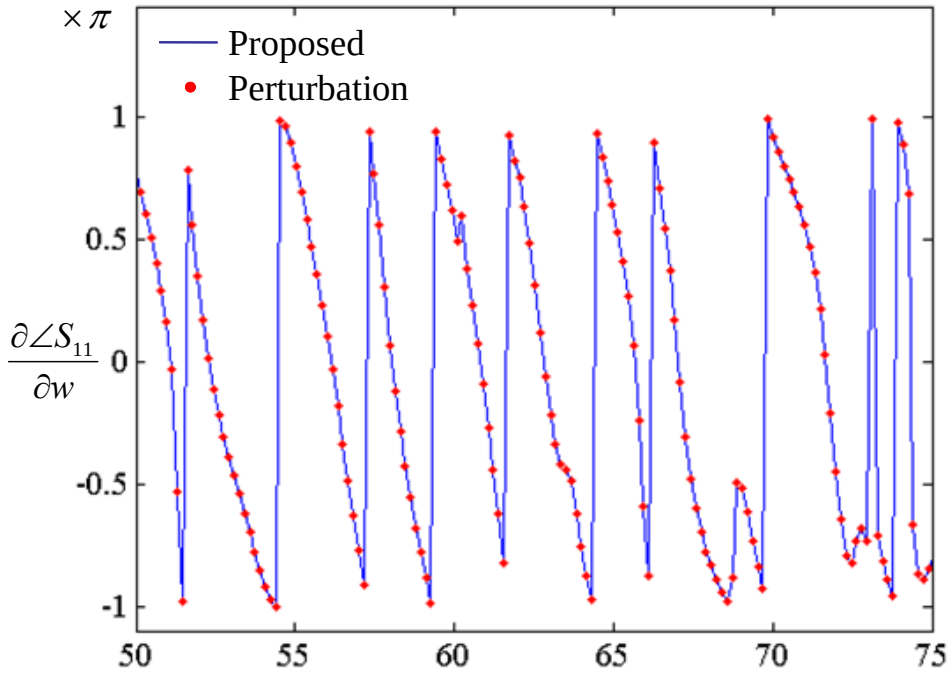

(a)

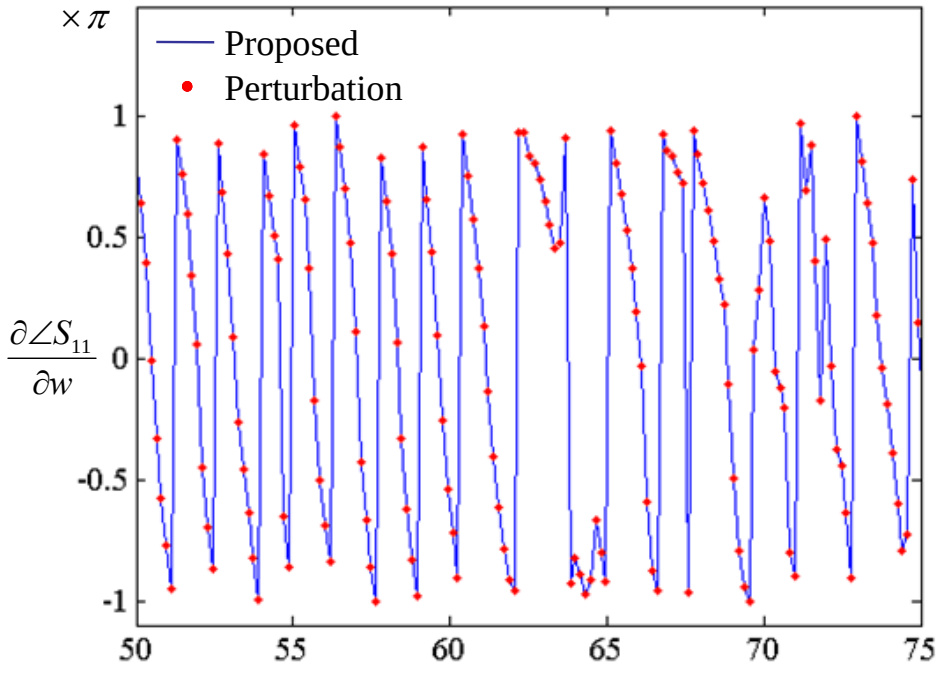

(b)

Fig. 5.5b. Sensitivities of $\angle S_{11}$ of the waveguiding structure with respect to w at (a) ε_r =1, w=0.00486, (b) ε_r =5, w=0.00486.

To obtain a parameterized reduced order model that includes the spacing between the planes of the input iris *w*, the following procedure is followed based on a polynomial fitting approach [47], [92]-[95].

1. First, a number of evaluation points of the design parameter *w* are chosen. Here we considered 10 test points (w_i , i = 1,….10) between *w*=0.00386m and 0.00586m.
2. The matrices $\boldsymbol{Y}_{i0}, \boldsymbol{Y}_{i1}$, $\boldsymbol{b}_0$ and $\boldsymbol{b}_1$ of (5.14) depends on '*w*'. At each test point w_i, the matrices $\boldsymbol{Y}_{i0}, \boldsymbol{Y}_{i1}, \boldsymbol{b}_0$ and $\boldsymbol{b}_1$ are determined. The crucial point in this technique is that the finite element mesh for all the test points is identical (i.e., they have the same number of degrees of freedom and their corresponding locations in the system matrices are same). For each of the test points, the mesh was adjusted in the areas close to where the geometry has been perturbed.
3. The elements of the matrices $\boldsymbol{Y}_{i0}, \boldsymbol{Y}_{i1}, \boldsymbol{b}_0$ and $\boldsymbol{b}_1$ which are affected by the mesh adjustments at each test point w_i are then fitted to a low order polynomial. This example requires a quadratic fit for the matrices since Lagrange-quadratic elements are used, where $\boldsymbol{b}_{i0}(w)$ is expressed as

$$\boldsymbol{Y}_{i0}(w) = \boldsymbol{Y}_{i00} + w\boldsymbol{Y}_{i01} + w^2\boldsymbol{Y}_{i02} \tag{5.15}$$

The matrices $\boldsymbol{Y}_{i1}, \boldsymbol{b}_0$ and $\boldsymbol{b}_1$ are also expressed as quadratic polynomials as in (5.15).

4. In order to find an accurate fit for $\boldsymbol{Y}_{i0}$, a least squares method is used to calculate the three coefficients $\boldsymbol{Y}_{i00}, \boldsymbol{Y}_{i01}$ and $\boldsymbol{Y}_{i02}$ of the second order polynomial matching the 10 test points as

$$\begin{bmatrix} 1 & w_1 & w_1^2 \\ 1 & w_2 & w_2^2 \\ \vdots & \vdots & \vdots \\ 1 & w_{10} & w_{10}^2 \end{bmatrix} \begin{bmatrix} Y_{i00}^{j,k} \\ Y_{i01}^{j,k} \\ Y_{i02}^{j,k} \end{bmatrix} = \begin{bmatrix} Y_{i0}^{j,k} \big| w = w_1 \\ Y_{i0}^{j,k} \big| w = w_2 \\ \vdots \\ Y_{i0}^{j,k} \big| w = w_{10} \end{bmatrix}$$

where *j*, *k* denotes the element indices of the matrix. A similar procedure is used to fit the elements of the other matrices.

5. Once the matrices of (5.12) are determined from (5.14) and (5.15), the technique proposed in section 4.2 is used to generate a parameterized reduced order system as a function of frequency, ε_r and *w*.

To select the appropriate size of the reduced order model the residual error of (4.22) is examined. For this example, four expansion points were selected at frequency = 50GHz, ε_r =3, *w*=0.00486, at frequency = 55GHz, ε_r =3, *w*=0.00486, at frequency = 60GHz, ε_r =3, *w*=0.00486 and at frequency = 70GHz, ε_r =3, *w*=0.00486 to derive a parametric reduced order model with residual error of less than 10^{-5}. Each expansion point used 12 moments for frequency, 11 moments for ε_r, 11 moments for *w* and 4 cross moments. Fig. 5.2a and 5.2b show the amplitude and Fig. 5.3a and 5.3b show the phase of scattering parameter, S_{11}, respectively, as a function of frequency at the four extreme corners of parameter ranges for ε_r and *w*. The reduced order model obtained using the proposed approach shows good agreement with the results of the original FEM model. Sample sensitivities of the amplitude and phase of S_{11} each with respect to ε_r and *w* using equations (2.49) and (2.50) and the proposed reduced order model are shown in Fig. 5.4a, 5.4b and Fig. 5.5a and 5.5b, respectively. To calculate the sensitivities with

respect to ε_r, (5.11) is used since the port geometries do not change as ε_r varies and to calculate the sensitivities with respect to *w*, (5.7)-(5.8) are used since the port geometries change as *w* varies. The results of the proposed method are compared with the perturbation of the original FEM network. Both the proposed method and the perturbation results are in good agreement.

It is to be noted that using the proposed parameterized reduced order model to calculate sensitivities provides the following advantages:

1. Using the parameterized reduced order model provides significant CPU advantage compared to the solution of the original FEM network. Table I compares the total size, CPU times to generate the parametric reduced order model, and simulation times of the proposed method and original FEM network.
2. Perturbation based techniques can lead to inaccurate results depending on the magnitude of the perturbation.
3. In addition, the perturbed network must be solved separately for every parameter of interest.

TABLE 5.1
COMPUTATIONAL INFORMATION

Solution Method	Size	CPU Time to generate reduced model	Simulation Time	Savings in Size	Speed Up Factor
Original System	13625	-	5 hours & 53 min	-	-
Proposed	304	12 min & 17 sec	8 min & 11 sec	98%	43

3600 simulations corresponding to 200 different frequency points, 6 different values of ε_r and 3 different values of *w*. All computations are performed on a Pentium 4 (2.8GHZ) PC with 2048 MB memory.

However, in the proposed approach, the sensitivity information with respect to all the parameters can be essentially obtained from the solution of the reduced order model using (5.7)-(5.8) or (5.11). For the case when (5.7)-(5.8) is used, the additional cost to calculate the sensitivities is only one forward-backward substitution of the reduced order model equations.

Chapter 6

6. Conclusion and Future Research

6.1. Conclusion

In this thesis, three major contributions have been made to address the computational complexities involved in the simulation of high frequency EM structures. Firstly, a parameterized model order reduction technique has been developed to solve eigenvalue equations of electromagnetic structures that are discretized by using FEM. The proposed algorithm uses a multidimensional subspace method based on modified perturbation theory and singular-value decomposition to perform reduction directly on the finite element eigenvalue equations. Applying this procedure parametric reduced order models can be obtained that are valid over the desired parameter range without the need to redo the reduction when design parameters are changed. This leads to significant computational savings since a new reduced order model is not required each time a design parameter is changed.

The second part deals with a multi-order Arnoldi model order reduction algorithm, as the traditional model order reduction techniques using the Arnoldi algorithm are only applicable to first order linear systems and can not directly include arbitrary functions of frequency dependant materials and boundaries. In this part of the thesis, a multi-order Arnoldi model order reduction algorithm is developed to generate efficient reduced order models that include arbitrary functions of frequency and design parameters. This procedure is able to provide more accurate reduced order systems when compared with

traditional approaches such as Modified Gram Schmidt (MGS).

Finally, in the third part of the thesis an efficient technique has been developed to calculate sensitivities of EM structures with respect to network design parameters. The proposed algorithm uses a parametric reduced order model to solve the original network and an adjoint variable method to calculate sensitivities. The main advantage of the proposed method is that the solution of the original network as well as sensitivities with respect to any parameter are obtained from the solution of the reduced order model.

6.2. Suggestions for Future Research

This section provides some suggestions for future research based on the work presented in this thesis.

Nonlinear MOR algorithms have been developed to efficiently model integrated, microwave and micro-electromechanical systems [96]-[98]. However, the nonlinear reduced order models of [96]-[98] do not capture the variances of design parameters and are not valid if design parameters are changed. A suggested future project is to extend the nonlinear MOR algorithms of [96]-[98] to include design parameter variations. This can be achieved by using multi-dimensional Taylor series or Voltera series to obtain a parametric reduced order nonlinear model. The development of such an algorithm can be used to study the properties of nonlinear integrated, microwave and micro-electromechanical systems without the need to solve the original large nonlinear system. In addition, the parametric reduced order nonlinear model algorithm can be combined with the adjoint variable technique to perform sensitivity analysis of nonlinear systems.

References

[1] B.M. Notaros, M. Djordjevic, and M.M Ilic, "High order electromagnetic modeling for wireless technology applications," *IEEE Topical Conference On Wireless Communication Technology*, pp. 229-232, 2003.

[2] P. P. Silvester and R. L. Ferrari, *Finite Elements for Electrical Engineers*, Cambridge University Press, Cambridge, UK, 1996.

[3] J.M. Jin, *The finite element method in electromagnetics*. Wiley, New York, 2002.

[4] M.N.O. Sadiku, Numerical Techniques in Electromagnetics. CRC Press LLC, 2001.

[5] A.F. Peterson, S.L. Ray, and R. Mittra, *Computational Methods for Electromagnetics*. IEEE Press, 1998.

[6] M.N.O Sadiku and A.F Peterson, "A Comparison of numerical methods for computing electromagnetic fields," *Proceedings of IEEE South-east con.*, 1990.

[7] M.A Kolbehdari, M. Srinivasan, M.S. Nakhla, Q.-J. Zhang and R. Achar, "Simultaneous time and frequency domain solutions of EM problems using finite element and CFH techniques," *IEEE Trans. Microwave Theory Tech.*, vol. 44, no. 9, pp. 1526-1534, Sept. 1996.

[8] Jian Gong and J.L. Volakis, "AWE implementation for electromagnetic FEM analysis," *Electronics Letters*, vol. 32, no. 24, pp. 2216-2217, Nov. 1996.

[9] Xiao-Ming Zhang and Jin-Fa Lee, "Application of the AWE method with the 3-D TVFEM to model spectral responses of passive microwave components," *IEEE Trans. Microwave Theory Tech.*, vol. 46, no. 11, pp. 1735-1741, Nov. 1998.

[10] L. Zhao and A.C.Cangellaris, "Reduced-order modeling of electromagnetic field interactions in unbounded domains truncated by perfectly matched layers," *Microwave Opt. Technol. Lett.*, vol. 17, no. 1, pp. 62-66, Jan. 1998.

[11] M.R. Zunoubi, K.C. Donepudi, J.M. Jin and W.C. Chew, "Efficient time-domain and frequency-domain finite-element solution of Maxwell's equations using spectral Lanczos decomposition method," *IEEE Trans. Microwave Theory Tech.*, vol. 46, pp. 1141-1149, Aug. 1998.

[12] A. Cangellaris, M. Celik, S. Pasha and L. Zhao, "Electromagnetic model order reduction for system-level modeling," *IEEE Trans. Microwave Theory Tech.*, vol. 47, pp. 840-849, June 1999.

[13] D. K. Sun, Z. Cendes and J. F. Lee, "ALPS-A new fast frequency-sweep procedure for microwave devices," *IEEE Trans. Microwave Theory Tech.*, vol. 49, pp. 398-402, Feb. 2001.

[14] Y. Zhu and A. C. Cangellaris, "A new finite element model for reduced order electromagnetic modeling," *IEEE Microwave and Wireless Components Letters*, vol. 11, no. 5, May 2001.

[15] Y. Zhu and A. C. Cangellaris, "Finite element-based model order reduction of electromagnetic devices," *Int. J. Numer. Model.*, vol 15, no.1, pp. 73-92, Jan. 2002.

[16] H. Wu and A. C. Cangellaris, "Model-Order reduction of finite-element approximations of passive electromagnetic devices including lumped electrical-circuit models," *IEEE Trans. Microwave Theory Tech.*, vol. 52, no.9, pp.2305-2313, Sept. 2004.

[17] E. B. Rudnyi, and J. G. Korvink, "Review: Automatic model reduction for transient simulation of MEMS-based devices," *Sensors Update*, Feb 2003.

[18] J. V. Clark, N. Zhou, D. Bindel, L. Schenato, W. Wu, J. Demmel and K. S. J. Pister, "3D MEMS simulation modeling using modified nodal analysis," Proc. *of the Microscale Systems: Mechanics and Measurements Symposium*, Portland, OR, Jun. 2001.

[19] M. K Sampath, A. Dounavis, and R. Khazaka, "Parameterized model order reduction techniques for finite element based full wave analysis," *IEEE MTT-S Int. Microwave Symposium Digest*, San Franciso, CA, June 2006.

[20] D. Celo, G. Xiaoming, P. K. Gunupudi, R. Khazaka, D. J. Walkey, T. Smy and M. S. Nakhla, "The creation of compact thermal models of electronic components using model reduction," *IEEE Transactions on Advanced Packaging,* vol. 28, Issue 2, pp. 240 – 251, May 2005.

[21] P. Gunupudi, R. Khazaka, and M. Nakhla, "Analysis of transmission line circuits using multidimensional model reduction techniques," *IEEE Trans. Adv. Packaging*, vol. 25, no. 2, pp. 174-180, May 2002.

[22] P. Gunupudi, R. Khazaka, M. Nakhla, T. Smy , and D. Celo "Passive parameterized time-domain macromodels for high-speed transmission-line networks," *IEEE Trans. Microw. Theory Tech.*, vol. 51, no.12, pp.2347-2354, Dec. 2003.

[23] P. Gunupudi and M. Nakhla, "Multi-dimensional model reduction of VLSI interconnects," *Proc. IEEE Custom Integrated Circuits Conf.*, May 2000, pp. 499–502.

[24] L. Daniel, and J. K. White, “Automatic generation of geometrically parameterized reduced order models for integrated spiral RF-inductors,” *IEEE Behavioral Modeling and Simulation BMAS 2003*, San Jose, CA., 2003.

[25] L. Daniel, O. C. Siong, L. S. Chay, K. H. Lee and J. White, “A Multiparameter moment-matching model-reduction approach for generating geometrically parameterized interconnect performance models,” *IEEE Trans. CAD of Integrated Circuits and Systems.*, vol. 23, no.5 , pp. 678-693, May 2004.

[26] J. H Lee, D. Vasilyev, A. Vithayathil, L. Daniel, and J. White, “Accelerated optical topography inspection using parameterized model order reduction,” *IEEE Int. Microwave Symp.*, Long Beach, CA, 2005, pp. 1771-1774.

[27] M. Salazar-Palma, T. K. Sarkar, L. E. Garcia-Costillo, T. Roy and A. Djordjevic, *Iterative and self-adaptive finite-elements in electromagnetic modeling*, Artech House, 1998.

[28] S. V. Polstyanko, R. Dyczij-Edlinger, and J. F. Lee, “Fast frequency sweep technique for the efficient analysis of dielectric waveguides,” *IEEE Trans. Microw. Theory Tech.*, vol. 45, no. 7, pp. 1118–1126, Jul. 1997.

[29] F. Bertazzi, O. A. Peverini, M. Goano, G. Ghione, R. Orta, and R. Tascone, “A fast reduced-order model for the full-wave EM analysis of lossy inhomogeneous anisotropic waveguides,” *IEEE Trans. Microw. Theory Tech.*, vol. 50, no. 9, pp. 2108–2114, Sep. 2002.

[30] Shih-Hao Lee; Ting-Yi Huang; Ruey-Beei Wu, **“**Fast waveguide Eigenanalysis by wide-band finite-element model-order reduction,“ *IEEE Trans. Microw. Theory Tech.* vol. 53, Issue 8, pp. 2552 – 2558, Aug. 2005.

[31] R. B. Wu, "Finding Taylor expansion of dispersion curve for arbitrarily indexed optical fibers by hyper-perturbation theory," *IEEE Trans. Magn.*, vol. 27, no. 9, pp. 3894–3897, Sep. 1991.

[32] J. E. Bracken, V. Raghvan, and R. A. Rohrer, "Interconnect simulation with asymptotic waveform evaluation," *IEEE Trans. Circuits Syst.*, vol. 39, pp. 869–878, Nov. 1992.

[33] E. Chiprout and M. S. Nakhla, "Analysis of interconnect networks using complex frequency hopping (CFH*)," IEEE Trans. Computer-Aided Design*, vol. 14, pp. 186-200, Feb.1995.

[34] M. Celik, and A. C. Cangellaris, "Efficient transient simulation of lossy packaging interconnects using moment matching techniques," *IEEE Trans. Comp., Packag. Manuf. Technol. B*, vol 19, pp. 64-73, Feb. 1996.

[35] E. Grimme, *Krylov Projection Methods for Model Reduction*, Ph.D. thesis, University of Illinois, Urbana-Champaign, 1997.

[36] I. M. Elfadel and D. D. Ling, "A block rational Arnoldi algorithm for multipoint passive model order reduction for multiport RLC networks," *IEEE/ACM Proc. ICCAD*, pp. 66-71, 1997.

[37] A. Odabasioglu, M. Celik, L. T. Pileggi, "PRIMA: passive reduced-order interconnect macromodeling algorithm," *IEEE Trans. Computer- Aided Design,* vol. 17, pp. 645-654, Aug. 1998.

[38] P. Gunupudi, M. Nakhla and R. Achar, "Efficient simulation of high-speed distributed interconnects using Krylov subspace techniques," *Proc. IEEE EPEP Topical Meeting*, pp. 295-298, Oct. 1998.

[39] Q. Yu, J.M.L. Wang, E.S. Kuh, " Passive multipoint moment matching model order reduction algorithm on multiport distributed interconnect networks," *IEEE Trans. Circuits Syst. I*, vol. 46, Jan. 1999.

[40] P. Gunupudi, R. Khazaka, and M. Nakhla, " Analysis of transmission line circuits using multidimensional model reduction techniques," *IEEE Trans. Advanced Packaging.,* vol. 25, no. 2, pp. 174-180, May. 2002.

[41] L. Daniel and J. K. White, "Automatic generation of geometrically parameterized reduced order models for integrated spiral RF-inductors," *IEEE Behavioral Modeling and Simulation BMAS 2003*, San Jose, CA., Oct. 2003.

[42] P. K. Gunupudi, R. Khazaka, M.S. Nakhla, T. Smy, and D. Celo, "Passive parameterized time-domain macromodels for high-speed transmission-line networks," *IEEE Trans. Microwave Theory Tech.*, vol. 51, no. 12, pp. 2347-2354, Dec. 2003.

[43] R. Achar, M. Nakhla, "Simulation of high-speed Interconnects," *Proceedings of the IEEE*, vol. 49, pp. 693-728, May 2001.

[44] J. W. Demmel, *Applied Numerical Linear Algebra*. Philadelphia, PA: SIAM, 1997.

[45] R. D. Slone, R. Lee, and J. F. Lee, "Broadband model order reduction of polynomial matrix equations using single-point well-conditioned asymptotic waveform evaluation: derivations and theory," *Int. J. Numer. Meth. Engng.,* vol 58, pp. 2325-2342, 2003.

[46] M. K. Sampath, A. Dounavis, and R. Khazaka, "Generation of geometrically parameterized reduced order models for full wave problems," *Proc. Electrical*

Performance for Electronic Packaging, pp. 343-346, Scottsdale, Arizona, Oct. 2006.

[47] M. K. Sampath, A. Dounavis, and R. Khazaka, "Parameterized model order reduction techniques for FEM based full wave analysis," *IEEE Transactions on Advanced Packaging*. vol. 32, no. 1, pp. 2-12, Feb. 2009.

[48] O. Farle, V. Hill, P. Nickel and Romanus Dyczij-Edlinger, "Multivariate finite element model order reduction for permittivity or permeability estimation", *IEEE Trans. On Magnetics*, vol. 42, no. 4, April 2006 pp.623-626.

[49] MATLAB 7.0.0.19920 (R14) *User's Guide 2004*, The Mathworks Inc., Natick, MA.

[50] A. E. Ruehli and A. C. Cangellaris, "Progress in the methodologies for the electrical modeling of interconnect and electronic packages," *Proc. IEEE*, vol. 89, no. 5, pp. 740–771, May 2001.

[51] L. T. Pillage and R. A. Rohrer, "Asymptotic waveform evaluation for timing analysis," *IEEE Trans. Computer-Aided Design*, vol. 9, pp. 352–366, Apr. 1990.

[52] C. Lanczos, "An iteration method for the solution of the Eigenvalue problem of linear differential and integral operators," *J. Res. Nat. Bur. Stand.*, vol. 45, pp. 255–282, Oct. 1950.

[53] P. Feldmann and R. W. Freund, "Efficient linear circuit analysis by pade approximation via the Lanczos process," *IEEE Trans. Computer-Aided Design*, vol. 14, no. 5, pp. 639-649, May 1995.

[54] P. Feldmann and R. W. Freund, "Reduced-order modeling of large linear subcircuits via a block Lanczos algorithm," *Proceedings of the 32nd ACMIIEEE Design Automation Conference,* pp. 474-479, June 1995.

[55] L. M. Silveira, M. Kamon, and J. White, "Efficient reduced order modeling of frequency-dependent coupling inductances associated with 3-D interconnect structures," *Proceedings of the 32nd ACMIIEEE Design Automation Conference,* pp. 376-380, June 1995.

[56] B. Salimbahrami, R. Eid and B. Lohmann, "Model reduction by second order Krylov subspaces: Extensions, stability and proportional damping," *IEEE International Symposium on Intelligent*, pp. 2997-3002, Oct. 2006.

[57] H. Wu and A. Cangellaris, "Krylov model order reduction of finite element models of electromagnetic structures with frequency-dependent material properties," *IEEE MTT-S International Microwave Symposium Digest,* pp. 52-55, June 2006.

[58] W. Tseng, C. Cheng, E. Gad, M. Nakhla and R. Achar, "Passive order reduction for RLC circuits with delay elements," *IEEE Trans. Advanced Packaging*, vol. 30, no. 4, pp. 830–840, Nov. 2007.

[59] Y. Su, J. Wang, X. Zeng, Z. Bai, C. Chiang, and D. Zhou, "SAPOR: Second-order Arnoldi method for passive order reduction of RCS circuits," *IEEE Proc. Int. Conf. Comput.-Aided Design*, pp. 74–79, Nov. 2004.

[60] Z. Bai and Y. Su, "Dimension reduction of second-order dynamical systems via a second-order Arnoldi method," *SIAM J. Sci. Comput.*, vol. 26, no. 5, pp. 1692–1709, 2005.

[61] Z. Bai and Y. Su, “SOAR: A second-order Arnoldi method for the solution of the quadratic Eigenvalue problem,” *SIAM J. Matrix Anal. Appl.*, vol. 26, no. 3, pp. 640–659, 2005.

[62] M. Ahmadloo and A. Dounavis,” Parameterized model-order reduction for efficient Eigenanalysis of dielectric waveguide structures,” *IEEE Trans. Microw. Theory Tech.*, vol. 59, no. 12, pp. 2851-2859, Dec. 2008.

[63] B. Gustavsen, and A. Semlyen, "Rational approximation of frequency domain responses by vector fitting," *IEEE Trans. Power Delivery*, Vol. 14, no. 3, pp. 1052-1061, July 1999.

[64] S. Grivet-Talocia, “Package macromodeling via time-domain vector fitting”, *IEEE Microwave and Wireless Components Letters*, vol. 13, no. 11, pp. 472-474, Nov. 2003.

[65] Y. S. Mekonnen, W. T. Beyene, and J. Schutt-Ainé, “Improved high order rational approximation by combining rational interpolation with the vector fitting method,” *Applied Computational Electromagnetic Society (ACES)*, Syracuse, NY, April 19-23, 2004.

[66] A. Chinea and S. Grivet-Talocia, “A Passivity enforcement scheme for delay-based transmission line macromodels”, *IEEE Microwave and Wireless Components Letters*, vol. 17, no. 8, pp. 562-564, Aug. 2007.

[67] D. D. Zutter and L. Knockaert, "Skin effect modeling based on a differential surface admittance operator," *IEEE Trans. Microwave Theory Tech.*, vol. 53, pp. 2526-2538, Aug. 2005.

[68] A. C. A. Rong and L. Dong, "Comprehensive broadband electromagnetic modeling of on-chip interconnects with a surface discretization based generalized peec model," *IEEE Trans. Adv. Packaging*, vol. 28, pp. 434-444, Aug. 2005.

[69] G. V. Eleftheriades and K. G. Balmain, *Negative refraction metamaterials: fundamental principles and applications*. New York: Wiley-IEEE Press, 2005.

[70] A. Von Hippel (ed.), *Dielectric materials and applications*. Boston, Mass: Artech House, 1995.

[71] E. Gad and M. Nakhla, "Efficient analysis of non-uniform transmission lines via integrated congruent transform," *IEEE Trans. Very Large Scale Integration (VLSI) Systems*, vol. 12, no. 12, pp. 1307–1320, Dec.2004.

[72] C. Prud'homme, D. Rovas, K. Veroy, Y. Maday, A. T. Patera, and G. Turinici, "Reliable real-time solution of parameterized partial differential equations: Reduced-basis output bounds methods," *J. Fluids Eng.*, 2002.

[73] Z. Bai, R. Slone, W. T. Smith and Q. Ye, "Error bound for reduced system model by pade approximation via the lanczos process," *IEEE Trans. Comput. Aided-Design Integrated Circuits Syst.*, vol. 18, no. 2, pp. 133–141, Feb. 1999.

[74] A. Odabasioglu, M. Celik, and L. T. Pileggi, "Practical considerations for RLC circuit reduction," *IEEE/ACM Proc. ICCAD*, San Jose, CA, pp. 214–219, Nov. 1999.

[75] C. R. Paul, *Analysis of multiconductor transmission lines,* second edition. New York, Wiley, 2008.

[76] F. H. Branin Jr., "Transient analysis of lossless transmission lines," *Proc. IEEE*, vol. 55, pp. 2012–2013, Nov. 1967.

[77] P. Garcia and J. P. Webb, "Optimization of planar device by the finite element method," *IEEE Trans. Microwave Theory Tech.*, vol. 38, no. 1, pp. 48-53, Jan. 1990.

[78] H. B. Lee and T. Itoh, "A systematic optimum design of waveguide-to-microstrip transition," *IEEE Trans. Microwave Theory Tech.*, vol. 45, no. 5, pp. 803-809, May 1997.

[79] H. Akel and J. P. Webb, "Design sensitivities for scattering-matrix calculation with tetrahedral edge elements," *IEEE Trans. Magnetics*, vol. 36, no. 4, pp. 1043-1046, July 2000.

[80] J. P. Webb, "Design sensitivities using high-order tetrahedral vector elements," *IEEE Trans. Magnetics*, vol. 37, no. 5, pp. 3600-3603, Sep. 2001.

[81] J. P. Webb, "Design sensitivities of frequency response in 3-D finite element analysis of microwave devicces," *IEEE Trans. Magnetics*, vol. 38, no. 2, pp. 1109-1112, Mar. 2002.

[82] M. M. Gavrilovic and J. P. Webb, "Accuracy control in the optimization of microwave devices by finite element method," *IEEE Trans. Microwave Theory Tech.*, vol. 50, no. 8, pp. 1901-1911, Aug. 2002.

[83] M. M. Gavrilovic and J. P. Webb, "An error estimation for design sensitivities of microwave device parameters," *Electromagnetics,* vol. 22, no. 4, pp. 315-321, 2002.

[84] D. Nair and J. P. Webb, "Optimization of microwave devices using 3-D finite elements and the design sensitivity of the frequency response," *IEEE Trans. Magnetics*, vol. 39, no. 3, pp. 1325-1328, May 2003.

[85] J. P. Webb, "Finite-element analysis of the effect of geometric tolerances on performance over a frequency band," *IEEE Trans. Microwave Theory Tech.*, vol. 52, no. 1, pp. 306-310, Aug. 2004.

[86] N. K. Nikolova, J. W. Bandler and M. H. Bakr, "Adjoint techniques for sensitivity analysis in high-frequency structure CAD," *IEEE Trans. Microwave Theory Tech.,* vol. 52, no. 1, pp. 403-419, Jan. 2004.

[87] N. K. Nikolova, J. Zhu, M. H. Bakr and J. W. Bandler, "Sensitivity analysis of network parameters with electromagnetic frequecy-domain simulators," *IEEE Trans. Microwave Theory Tech.*, vol. 54, no. 2, pp. 670-681, Feb. 2006.

[88] N. K. Nikolova, X. Zhu, Y. Song, A. Hasib and M. H. Bakr, "S-parameters sensitivities for electromagnetic optimization based on volume field solutions," *IEEE Trans. Microwave Theory Tech.,* vol. 57, no. 6, pp. 1526-1538, June. 2009.

[89] R. Khazaka, P. Gunupudi, and M. S. Nakhla, "Efficient sensitivity analysis of transmission-line networks using model reduction techniques," *IEEE Trans. Microw. Theory Tech.,* vol. 48, no. 12, pp. 2345–2351, Dec. 2000.

[90] T. Ahmed, E. Gad and M. C. E. Yagoub, "An adjoint-based approach to computing time-domain sensitivity of multiport systems of described by reduced order models," *IEEE Trans. Microwave Theory Tech*., vol. 53, no. 11, pp. 3538–3547, Nov. 2005.

[91] M. Ahmadloo and A. Dounavis, "Parameterized model order reduction of electromagnetic systems using multiorder Arnoldi," *Available on IEEE Trans. Advanced Packaging*, Early Access, 2010.

[92] S. W. Director and R. A. Roher, "The generalized adjoint network and network sensitivities," *IEEE Trans. Circuits and Systems.*, vol. 16, no. 3 , pp. 318-323, Aug. 1969.

[93] L. Daniel and J. K. White, "Automatic generation of geometrically parameterized reduced order models for integrated spiral RF-inductors," *IEEE Behavioral Modeling and Simulation conf.*, BMAS 2003, Oct. 2003 San Jose, CA.

[94] L. Daniel, O. C. Siong, L. S. Chay, K.H. Lee and J. White, "A multiparameter moment-matching model-reduction approach for generating geometrically parameterized interconnect performance models," *IEEE Trans. CAD of Integrated Circuits and Systems*, vol. 23, no.5 , pp. 678-693, May 2004.

[95] J. H Lee, D. Vasilyev, A. Vithayathil, L. Daniel and J. White, "Accelerated optical topography inspection using parameterized model order reduction," *IEEE Int. Microwave Symp.*, Long Beach, CA, 2005, pp. 1771-1774.

[96] J. Chen and S. M. Kang, "Model order reduction of weakly nonlinear MEMS devices with Taylor series expansion and Arnoldi process", *Circuits and Systems, Proceedings of the 43rd IEEE Midwest Symposium on,* vol. 1, pp. 248 – 251, 2000.

[97] P. Li and L. T. Pileggi, "NORM: compact model order reduction of weakly nonlinear systems", *Design Automation Conference Proceedings*, pp. 472 – 477, 2003.

[98] M. Rewieński and J. White, "Model order reduction for nonlinear dynamical systems based on trajectory piecewise-linear approximations", *Linear Algebra and its Applications*, vol. 415, Issue 2-3, pp. 426-454, June 2006.

Curriculum Vita

Majid Ahmadloo

EDUCATION

- **Ph. D. Electrical Eng**, University of Western Ontario, London, Ontario, Canada. Graduation: August 2010.
- **M. E. Sc., Electrical Eng**, Shiraz University, Shiraz, Iran. June 2006.
- **B. Eng., Electrical Eng**, Khajeh Nasiredin Toosi University of Technology, Tehran, Iran. April 2003.

RESEARCH INTERESTS

Computational electromagnetics, model order reduction techniques and fast numerical methods for electromagnetic-field computations in microwave and optical systems.

AWARDS AND HONOURS

- University of Western Ontario, Award of Outstanding Presentation in Graduate Symposium, Department of Electrical and Computer Engineering, 2009.
- University of Western Ontario, Western Graduate Research Scholarship (WGRS), 2006 – 2010.
- University of Western Ontario Doctoral Fellowship, 2006 – 2010.
- Iranian Ministry of Science and Technology M.E. Sc. fellowship, 2003 – 2006.
- Iranian Ministry of Science and Technology B.Eng. level fellowship, 1998 – 2003.
- Best Student Paper Award, Iranian Petroleum Engineering Conference, Dec. 2002.
- Iranian National Organization for Development of Exceptional Talents (NODET) fellowship, 1994 – 1998.

WORK EXPERIENCE

Research:

- Research assistant, model order reduction in large electromagnetic problems. The University of Western Ontario, London, Ontario, Canada, 2006 – presents.

Teaching:

- Teaching assistant, the University of Western Ontario, London, Ontario, Canada, Fall 2006 – present.

  Conduct tutorials and labratories. Mark assignments, lab reports, midterms and final exams. Develop teaching material in the following courses:

  Advanced Digital Systems (TA-ECE4434), Electronics I (TA-ECE2231), Electronics II (TA-ECE2235), Introductory Design and Innovation Studio (TA-ES1050)

PUBLICATIONS

Journal Papers

- **M. Ahmadloo** and A. Dounavis, "Sensitivity analysis of microwave circuits using parameterized model order reduction techniques", *(submitted to Microwave Theory and Techniques)*.
- **M. Ahmadloo** and A. Dounavis, "Parameterized model order reduction of electromagnetic systems using multi-order Arnoldi", *IEEE Transactions on Advanced Packaging* (Available on IEEE Xplore, Early Access, 2010).
- **M. Ahmadloo** and A. Dounavis, "Parameterized model-order reduction for efficient Eigenanalysis of dielectric waveguide structures", *IEEE Transactions on Microwave Theory and Techniques*, vol. 56, no. 12, pp. 2851-2858, Dec. 2008.
- **M. Ahmadlou**, M. Kamarei and M. H. Sheikhi, "Negative refraction and focusing Analysis in a left-handed material slab and realization with a 3D photonic crystal structure", *J. Opt. A: Pure Appl.* Opt. 8, pp. 199-204, 2006.

Conference Papers

- **M. Ahmadloo**, S. Roy and A. Dounavis, "Parameterized model order reduction of power distribution planes", *14th International Symposium on Antennas and Electromagnetics and The American Electromagnetics Conference ANTEM/AMEREM*, Ottawa, Canada, July 2010.
- **M. Ahmadloo** and A. Dounavis, "A parameterized model order reduction technique for efficient solution of FEM eigenvalue problems", *Electrical Performance of Electronic Packaging, 2008 IEEE-EPEP*, San Jose, USA, Oct. 2008.
- **M. Ahmadlou**, M. Kamarei and M. H. Sheikhi, "Focusing analysis and negative refraction without negative effective index in a three-dimensional photonic crystal Structure", *14th Iranian Conference on electrical Engineering, ICEE2006*, Tehran, Iran, May 2006.
- **M. Ahmadlou**, M. Kamarei and M. H. Sheikhi, "Wave propagation properties of a Left-Handed Metamaterial slab lens Using 3D-FDTD-PML method", *IST2005*, Shiraz, Iran, Sept. 2006.